12-1-1983

Annular Flow in a Low - Pressure Steam - Water System

Arnfinn Borch Lund

Annular Flow in a Low - pressure Steam - water System

by
Arnfinn Borch Lund

Sivilingeniør in Chemical Engineering
Norwegian Institute of Technology, December 1978

A Thesis

Submitted to the Graduate Faculty

of the

University of North Dakota

in partial fulfillment of the requirements

for the degree of

Master of Science

Grand Forks, North Dakota

December
1983

Annular Flow in a Low - pressure, Steam - water System

Arnfinn Borch Lund

The University of North Dakota, 1983

Faculty Advisor: Dr. Abu R. Hasan

Two-phase annular flow is an important aspect of two-phase flow. Three different models - Ghosal, Wallis, and Levy - were used to calculate the pressure drop in annular two-phase flow. The calculated pressure drop was compared with a set of experimental data. The pressure range of the data was 350 to 850 kPa. Steam quality varied from 4.0 to 52.7 percent, while the total mass flux varied from 245.4 to 2303.7 $kg/m^2,s$.

The predictions of the Wallis model were found to agree best with the data. This model appears to be well developed with respect to the hydrodynamic conditions of annular gas-liquid flow. However, it generally underestimates the pressure drop by 17.15 percent on the average. A simple modification was made to the Wallis model to account for this underestimation. The estimates of this modified model had a standard deviation of only 6.7 kPa, and it underpredicted the pressure drop by an average of 1.00 percent.

This thesis submitted by Arnfinn Borch Lund in partial fulfillment of the requirements for the Degree of Master of Science from the University of North Dakota is hereby approved by the Faculty Advisory Committee under whom the work has been done.

A. Hasan.

Thomas C. Owens

Donald E. Porter

This thesis meets the standards for appearance and conforms to the style and format requirements of the Graduate School of the University of North Dakota, and is hereby approved.

Title Annular Flow in a Low - pressure Steam - water System

Department Chemical Engineering

Degree Master of Science

In presenting this thesis in partial fulfillment of the requirements for a graduate degree from the University of North Dakota, I agree that the Library of this University shall make it freely available for inspection. I further agree that permission for extensive copying for scholarly purposes may be granted by the professor who supervised my thesis work or, in his absence, by the Chairman of the Department or the Dean of the Graduate School. It is understood that any copying or publication or other use of this thesis or part thereof for financial gain shall not be allowed without my written permission. It is also understood that due recognition shall be given to me and to the University of North Dakota in any scholarly use which may be made of any material in my thesis.

Signature Jimmie B. Laird

Date October 31, 1983

CONTENTS

FIGURES

LEVY MODEL

MODIFIED WALLIS MODEL

TABLES

ACKNOWLEDGEMENTS

I would like to express gratitude to my committee, Dr. Abu R. Hasan (advisor), Dr. Thomas Owens, and Dr. Donald E. Porter, for their much appreciated help and inspiration on this project.

Special thanks must also go to the Rotary Foundation for monetary aid to enable me to study in the USA.

I would also like to thank a group of people who helped me during my research. This group includes Lorraine Fortin for her help on the Script language used to type this report, and on the SAS programs used for the regression analysis and the graphs included in this thesis. In the programming, I received a lot of help from Mustafizur Rahman.

Finally, I want to give my loving wife Sølvi special thanks for bearing with and supporting me in my studies.

ABSTRACT

Two-phase annular flow is an important aspect of two-phase flow. Three different models, Ghosal, Wallis, and Levy models, were used to calculate the pressure drop in annular two-phase flow. The calculated pressure drop was compared with a set of experimental data. The pressure range of the data was 350 to 850 kPa. Steam quality varied from 4.0 to 52.7 percent, while the total mass flux varied from 245.4 to 2303.7 $kg/m^2,s$.

The predictions of the Wallis model were found to agree best with the data. This model appears to be well developed with respect to the hydrodynamic conditions of annular gas-liquid flow. However, it generally underestimates the pressure drop by 17.15 percent on the average. A simple modification was made to the Wallis model to account for this underestimation. The estimates of this modified model had a standard deviation of only 6.7 kPa, and it underpredicted the pressure drop by an average of 1.00 percent.

Chapter I

INTRODUCTION

Applications of two-phase flow are numerous, and they have economical, as well as technical importance. Some of the most important applications are boilers, evaporators, condensers and flow of oil-gas mixtures in pipelines.

For flow of a single phase in a pipe, such as a gas or a liquid, the pressure drop can be calculated quite accurately. This is not the case with a mixture of gas and liquid. There are a number of variables that may influence the pressure drop for this type of flow, which include: total mass flux, vapor fraction, pressure, compressibility of the phases, pipe roughness, pipe diameter, inclination of the pipe and a number of other variables of secondary importance. With different combinations of these variables, several different flow patterns can be observed. Different methods must be used to calculate frictional pressure drop depending on the flow pattern. For boilers, condensers and flows that are not adiabatic, the flow pattern will often change along the pipe. This is mainly because the vapor fraction will change, and the vapor fraction is one of the most important variables influencing the flow pattern. The flow pattern may also change for adiabatic flow if the pressure drop is

large enough to influence the vapor fraction, and the corresponding void fraction.

The objective of this study was to evaluate available models based on an annular flow pattern. This flow pattern is one of the most important in two-phase flow. In a tube evaporator, for example, as much as 90 percent of the tube length may be in annular flow. Annular flow is also somewhat easier to handle analytically than other flow patterns because of its relatively simple geometric structure.

The amount of experimental work that has been done in the low pressure region is small compared to what has been done in the high pressure region. Hasan (1)[1] has studied pressure drop for two-phase, steam-water flow in a horizontal test section in the pressure range of 350 to 850kPa. His data for adiabatic conditions which are listed in Appendix A were used for this work. Flow patterns at the experimental conditions were determined, and only the data that belonged to the annular flow pattern were used to evaluate the models. The steam quality for the data varied from 4.0 to 52.7 percent, while the total mass flux was varied from 245.4 to 2303.7 $kg/m^2,s$. The test section had pressure taps at intervals of 0.44 m along the pipe.

---

[1] Numbers in parentheses that are underlined refer to items on the List of References at the end of the paper.

The predicted pressure drop from the models was compared with the experimental data. Then, based on the accuracy of the predictions and how complicated it would be to modify the models, one of the models was modified to more closely fit the experimental data.

Chapter II

LITERATURE SURVEY

2.1 FLOW PATTERN

The importance of flow patterns in two-phase flow is widely recognized. When two phases flow together in a transparent pipe, one can visually observe the various patterns of flow that exist. For example in some cases bubbles flow past the liquid, forming what is known as bubbly flow, or slugs of gas may flow past the liquid, forming slug flow. In some cases the gas may form a core in the pipe. In this case the liquid flows along the wall forming the annular flow region. Each type of flow is a result of various hydrodynamic conditions, and must be treated in a different manner. For horizontal flow, Alves (2) has noted the following flow patterns: (1) Bubbly flow, (2) Plug flow, (3) Stratified flow, (4) Wavy flow, (5) Slug flow and (6) Annular flow.

A visual identification by itself may be subjective. In addition, for most industrial purposes, a visual identification is not possible because most pipes are made of opaque material. In order to overcome this problem, several flow pattern maps have been constructed for horizontal flow.

Baker (3) constructed a map that is widely used in the petroleum industry. This map was later simplified by Bell (4). Mandhane (5) also devised a map based on a large number of experimental data for air-water flow. The general trends of this map were confirmed by a map constructed by Taitel and Dukler (6), having a better theoretical foundation.

By using a flow pattern map, the type of flow can be identified by the input data such as mass flux, vapor fraction, density, pressure, viscosity and pipe diameter. Since the available flow pattern maps are not quite identical, the determination of a flow pattern is still somewhat subjective, but it is still a valuable tool.

The map constructed by Taitel and Dukler appears to be quite similar to that of Mandhane. In addition the Taitel and Dukler map takes the pipe diameter into account.It is also the more recent of the two maps. Therefore, it has been used to evaluate the flow pattern for the present work. The map shown in Figure 1 uses as the abcissa the function F which is defined by the following equation:

$$F = \left(\frac{\rho_g}{\rho_f - \rho_g} \right)^{0.5} \frac{j_g}{(D\, g \cos \theta)^{0.5}} \qquad (1)$$

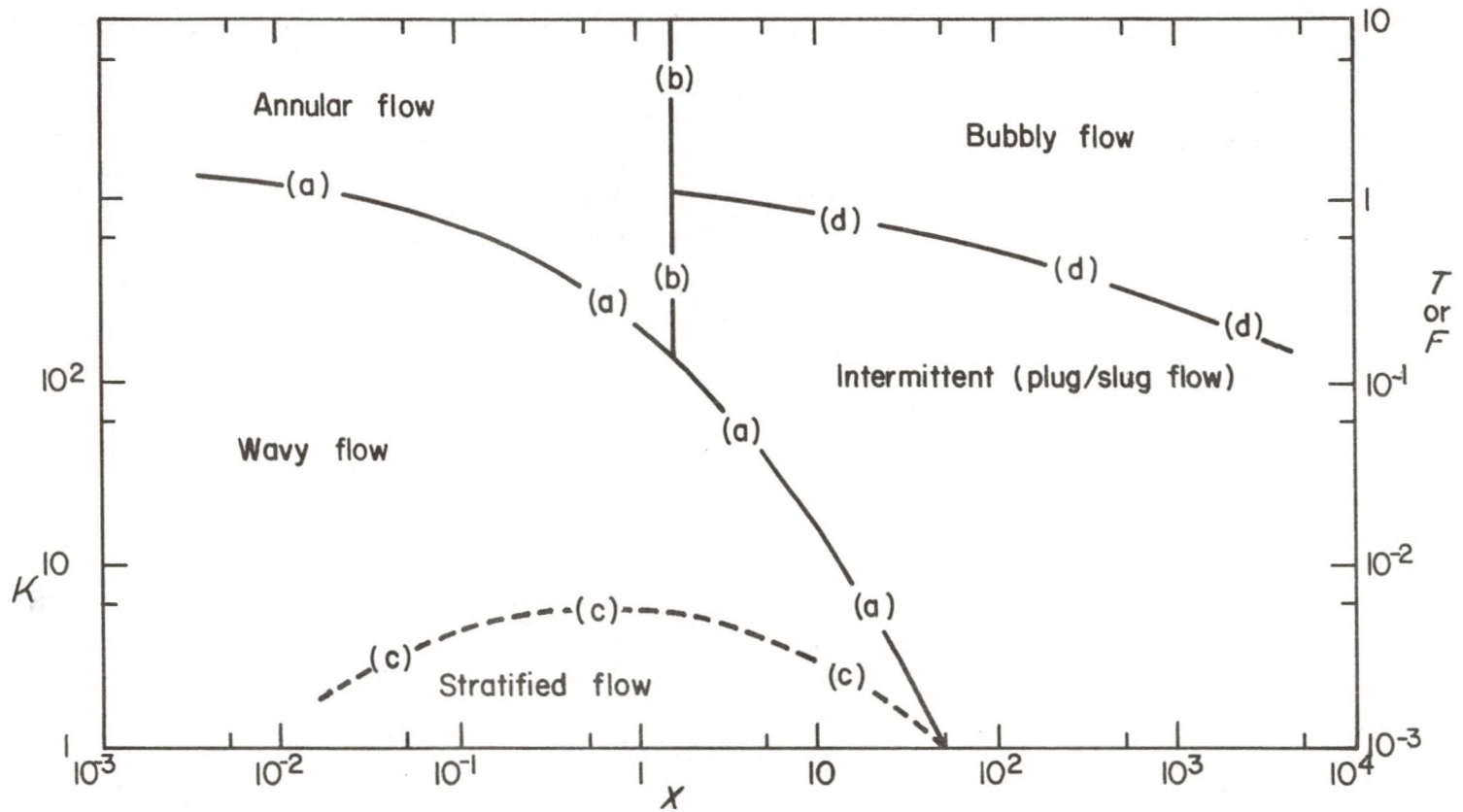

Curve	(a)+(b)	(c)	(d)
Co-ordinate	F vs X	K vs X	T vs X

Figure 1: Flow pattern map for horizontal flow (6).

The ordinate is the Lockhart-Martinelli parameter X, defined by the equation:

$$X = \sqrt{\left(\frac{dp}{dz} F\right)_f \Big/ \left(\frac{dp}{dz} F\right)_g} \qquad (2)$$

The flow pattern map also uses two other parameters for ordinates. For annular flow, however, the only parameters needed are F and X. The transition from annular flow to bubbly flow or plug/slug flow occurs at a constant at value of 1.6 for X. For the transition from annular flow to wavy flow, the flow pattern map must be used with coordinates F and X. The parameter X can also be closely approximated by Equation 3 for turbulent flow.

$$X = \left(\frac{1 - x}{x}\right)^{0.9} \left(\frac{\rho_g}{\rho_f}\right)^{0.5} \left(\frac{\mu_f}{\mu_g}\right)^{0.1} \qquad (3)$$

Equations 1 and 3 were used in the determination for the flow pattern coordinates of the experimental data. With an established flow pattern for each set of data, a comparison between the experimental and predicted pressure drop can be made. Pressure drop can be predicted using several different methods including both general models and models specific to the annular flow pattern.

2.2 GENERAL MODELS

The total pressure gradient during two-phase flow is composed of the frictional, accelerational, and gravitational terms and can be written down as (7):

$$\left(\frac{dp}{dz}\right) = \left(\frac{dp}{dz}\ F\right) + \left(\frac{dp}{dz}\ A\right) + \left(\frac{dp}{dz}\ Z\right) \qquad (4)$$

Because this study deals with horizontal flow only, the gravitational term can be neglected, and Equation 4 can be simplified to:

$$\left(\frac{dp}{dz}\right) = \left(\frac{dp}{dz}\ F\right) + \left(\frac{dp}{dz}\ A\right) \qquad (5)$$

The acceleration component can be expressed by the equation:

$$\left(\frac{dp}{dz}\ A\right) = \frac{1}{A}\ \frac{d}{dz}\left(W_g u_g + W_f u_f\right)$$

$$= G^2\ \frac{d}{dz}\left[\frac{x^2 v_g}{\alpha} + \frac{(1-x)^2\ v_f}{1-\alpha}\right] \qquad (6)$$

Equation 6 reflects the increase or decrease of the volume of the two-phase mixture because of evaporation or condensation.

There are several ways to estimate the frictional component which, for adiabatic conditions, is the more important of the two components. One way to predict the frictional

component is to assume that the gas and the liquid flowing together form a homogenous mixture with average physical properties (8,9,10). The average specific volume can be written as:

$$\bar{v} = x\, v_g + (1-x)\, v_f \qquad (7)$$

From these properties, the friction factor and the frictional pressure gradient can be calculated.

$$-\left(\frac{dp}{dz} F\right) = \frac{2\, f_{TP}\, G^2\, \bar{v}}{D} \qquad (8)$$

The frictional pressure gradient can also be calculated using the separate flow model which assumes that the flow is artificially segregated into two streams, gas and liquid. In this model the two-phase frictional gradient is usually expressed as the pressure gradient for the single phase, (usually the liquid phase) multiplied by a two-phase friction multiplier ϕ_f^2. Thus:

$$-\left(\frac{dp}{dz} F\right) = \frac{2\, f_f\, G^2\, (1-x)^2\, v_f}{D} \phi_f^2 \qquad (9)$$

In order to make an estimate of ϕ_f^2 the Lockhart-Martinelli parameter X, defined by Equation 2, is used. The data gathered for ϕ_f^2 by Lockhart-Martinelli were presented in graphical form (11). Wallis (12) has expressed these data by the following equation:

$$\phi_f^2 = 1 + \frac{C}{X} + \frac{1}{X^2} \qquad (10)$$

The value of C depends on the nature of the flow. For turbulent flow of both the liquid and the gas phase, the value of C is 20.

In most cases, the separated flow model gives a better estimate of the pressure drop than does the homogenous model. As in the homogenous model, knowledge of the flow pattern is not required. However, the error involved in predictions by this, as well as by the homogenous model is usually quite high. Johannessen (13) indicates a standard deviation between the predicted and actual data of about 40 percent. The model does not satisfactorily account for the effect of some of the variables, particularly mass flow rate (14). Several attempts have been made to overcome this source of error (15,16,17,18). Using models specific to the existing flowpatterns usually avoid this problem and allow more accurate predictions of the pressure drop.

2.3 MODELS SPECIFIC TO EXISTING FLOW PATTERNS

Models that are specific to a flow pattern may be almost entirely empirical although most often they have a strong theoretical base. Because these models are often based on particular hydrodynamic features of the flow, they tend to be more accurate. For bubbly flow, the assumption of a ho-

mogenous mixture between the gas and the liquid is good, and the homogenous model works out quite well in this case (19). Usually a factor for slip between the phases is included in the model. This factor indicates the extent to which the gas bubbles are moving faster than the liquid (20). Slug flow is more difficult than bubbly flow to model theoretically. In this flow regime the inclination of the pipe also has a great influence on the theoretical approach of modeling the pressure drop (21). But here also, as in other flow regimes, several models are available (22).

This study, however, is concerned with a detailed look the annular flow regime. In the idealized case, the entire liquid mass flow rate is contained as a symmetrical film on the pipe wall with a smooth interface between the liquid film and the gas core. This, along with the shear stress distribution for horizontal annular flow is illustrated in Figure 2.

The real hydrodynamic behavior is somewhat more complicated. In the general case, a fraction (e) of the liquid will be entrained in the vapor core, and the interface between the gas and the liquid will be highly disturbed. The pressure gradients for the gas phase and the liquid phase have to be equal. This means that the equations for the pressure drop of the gas phase and the liquid phase can be balanced against each other.

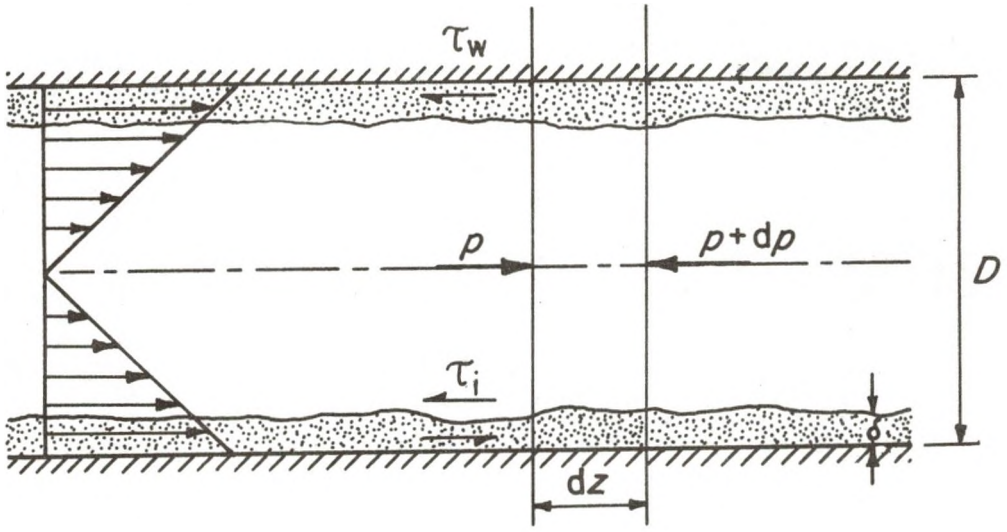

Figure 2: Idealized annular flow

$$-\left(\frac{dp}{dz}F\right) = \frac{4\,\tau_w}{D} \tag{11}$$

$$-\left(\frac{dp}{dz}F\right) = \frac{4\,\tau_i}{D-2\delta} \tag{12}$$

From Equation 11 which is the pressure drop calculated from the liquid phase, an equation for the liquid phase frictional multiplier ϕ_f^2 is derived. Similarly, from Equation 12 which is the pressure drop calculated from the gas phase, an equation for the gas phase frictional multiplier ϕ_g^2 is obtained. Several investigators have attempted to develop realistic models for annular flow. For horizontal annular flow, several measurements have been made to determine the gas flow distribution (23,24). A number of methods have also been developed to determine the interfacial roughness (25,26,27,28).

Ghosal (29) studied annular two-phase cocurrent horizontal flow. Constant wall shear stress in the liquid flow was assumed. The resulting equation for the two-phase frictional multiplier ϕ_f^2 is thus:

$$\phi_f^2 = \frac{3}{4 (1 - 3 a + 2 a^{1.5})} \qquad (13)$$

The two-phase multiplier based on flow of gas alone, can normally be expressed as:

$$\phi_g^2 = \frac{1}{a^{2.5}} \frac{f_i}{f_g} \qquad (14)$$

If the interface between the liquid and gas is smooth, then (f_i / f_g) is close to unity. This, however, is normally not the case. With a wavy interface, the ratio of the interfacial friction factor f_i to the gas-phase friction factor f_g can be expressed by (30):

$$\frac{f_i}{f_g} = (1 + 75 (1 - a)) \qquad (15)$$

The resulting relationshipship between a and ϕ_g^2 is then:

$$\phi_g^2 = \frac{1 + 75 (1 - a)}{a^{2.5}} \qquad (16)$$

From Equation 14 and 16, the Lockhart-Martinelli parameter, X, can be expressed as:

$$X^2 = \frac{4\,(1 + 75(1-\alpha))\,(1 - 3\alpha + 2\alpha^{1.5})}{3\,\alpha^{2.5}} \qquad (17)$$

Equation 17 relates the void fraction α to the Lockhart-Martinelli parameter X. The value of X is calculated from Equation 2, and the void fraction can then be calculated by an iterative procedure from Equation 17. Equation 13 is then utilized to estimate the two-phase friction multiplier and hence (dp/dz F). This model does not take entrainment of liquid into the gas core into account. It also assumes a constant mean velocity within the liquid layer.

Wallis model (31), however, is more developed and takes entrainment into consideration. He starts with the relationship between ϕ_f^2 and the void fraction α :

$$\phi_f^2 = \frac{1}{(\,1 - \alpha\,)^2} \qquad (18)$$

The entrainment of liquid into the gas core makes the average density of the gas core higher. The average density with entrainment can be expressed as:

$$\rho_c = \left[\frac{W_g + e\,W_f}{W_g}\right] \rho_g \qquad (19)$$

This model assumes that the interface velocity of the liquid is twice the mean film velocity. The resulting equation for then is:

$$\phi_g^2 = \left[\frac{1 + 75\ (1 - \alpha)}{\alpha^{2.5}}\right] \left[\frac{W_g + e\ W_f}{W_g}\right] \left[1 - 2\left(\frac{\alpha}{1 - \alpha}\right)\left(\frac{\rho_g}{\rho_f}\right)\left(\frac{W_f\ (1 - e)}{W_g}\right)\right]^2 \qquad (20)$$

Wallis (32) has found a relationship between the entrainment e and dimensionless vapor velocity π defined as:

$$\pi = \frac{G\ x}{\sigma}\ \mu_g (\ v_g\ v_f\ )^{0.5} \qquad (21)$$

The graphical representation of entrainment vs. dimensionless vapor velocity is not suitable for numerical manipulation. Therefore the curve was approximated by the following equations with a standard deviation of 0.0000 for ten data points.

$$e = 0.02271 - 596.6509\ (\pi) + 3223134.0\ (\pi)^2 \qquad (22)$$

for $1.5 < \pi < 4.2$

$$e = -0.4943 + 1049.79\ (\pi) - 330532.9\ (\pi)^2 \qquad (23)$$

for $4.2 < \pi < 14.0$

There are other ways to calculate entrained liquid fraction (33), but this is possibly the easiest for use for numerical manipulation. Calculating the frictional pressure gradient requires an iterative procedure and the void fraction is the critical value because both ϕ_f^2 and ϕ_g^2 have α as a parame-

ter. The iteration continues until one value of a gives the same frictional pressure gradient for both the gas phase and the liquid phase.

Levy (34) used a different approach to calculate the frictional pressure gradient. Instead of using the assumption of one liquid and one gas phase, he divided the flow into three layers.

1. A liquid film of thickness Y_f having a uniform density ρ_f.
2. A transition layer that extends from the edge of the film to the edge of the gas core. The density in the transition layer is assumed to decrease exponentially from the liquid density, ρ_f to the gas core density, ρ_c.
3. A central gas core, extending from the edge of the transition layer to the center of the pipe that has a constant density at ρ_c.

The physical description of this model is illustrated in Figure 3. The dimensionless velocity depends on the radius of the pipe and the distance from the pipe wall. Shear stress is calculated from the dimensionless velocity and pressure drop can be calculated using Equation 24.

$$-\left(\frac{dp}{dz}F\right) = \frac{2\tau_w}{R} \qquad (24)$$

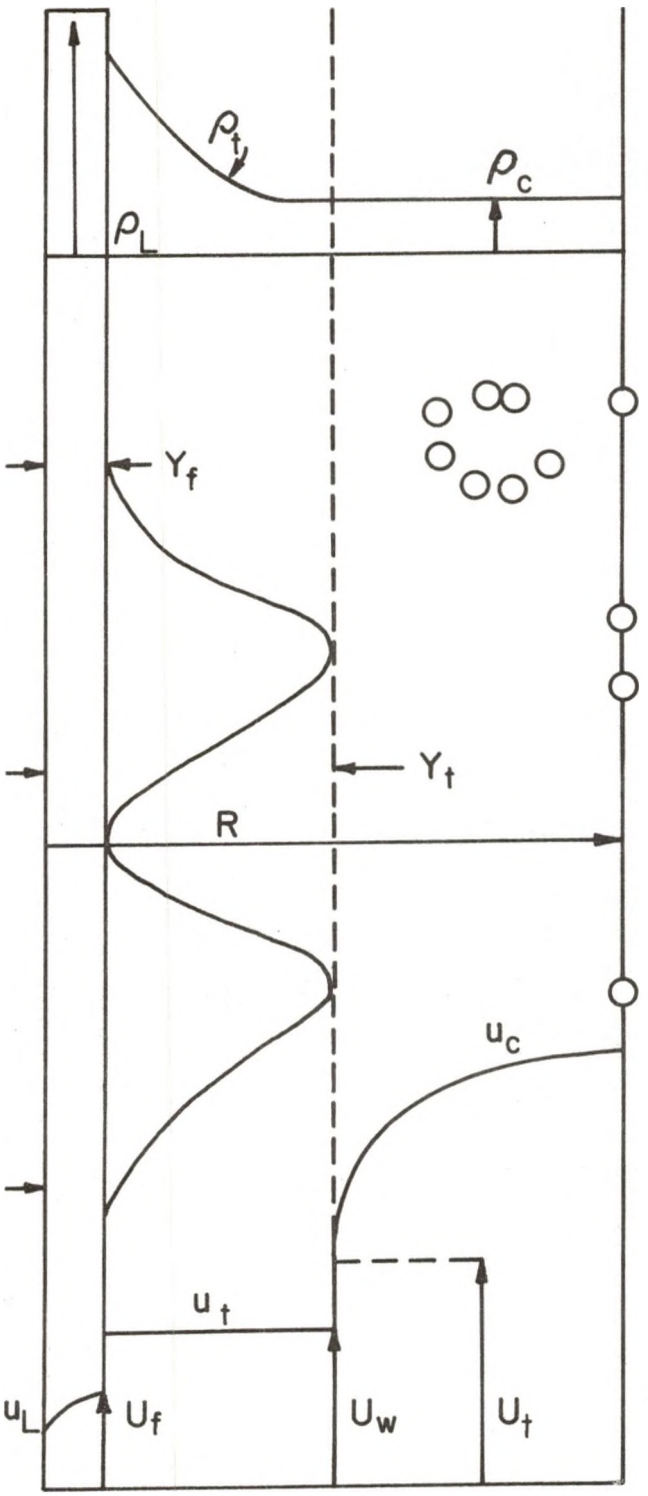

Figure 3: Levy model of annular flow.

Chapter III

COMPUTATIONAL METHODS

A major part of this thesis was to use various models to predict pressure drop for two-phase annular flow. This chapter provides some explanation of the computational procedures and the computer programs used for the calculations.

3.1 PROCEDURES COMMON TO ALL MODELS

The raw data fed into the computer were: Gas load, liquid load, gas enthalpy, liquid enthalpy, inlet pressure and pressure drop for four consecutive pipe sections. The programs to estimate pressure drop using the different models are divided into two parts:

1. The first is the main program which reads the raw data, integrates the calculated pressure gradients into pressure drop, calculates the errror between the estimated and the experimental pressure drops and prints the result.
2. The second is a subroutine that calculates the physical properties of the steam and the water at the existing pressure and temperature. From these properties, the flow pattern map coordinates in Equations 1 and 3 are calculated. The frictional and accelera-

tional pressure gradients are then calculated. This may require calculations that involve additional subroutines for the determination of certain parameters.

3.1.1 The Main Program

The main program begins by reading the raw data. Then it calls up the subroutine PPSSAW in order to get an estimate of the pressure gradient and the flow pattern map coordinates for the inlet conditions. By checking the program output with the flow pattern map, the flow pattern can be quickly identified. The integration of the pressure gradients is then performed using the four point Runge-Kutta method. This method calculates an average pressure gradient for a predetermined pipelength. The length of this pipe section is set equal to the length of the pipe for each pressure drop measurement. For each of these sections, four different pressure gradients are calculated. The pressure gradient is calculated at the beginning and the mid point of the section. With a new and improved estimation of the pressure at the mid point of the section, the pressure gradient is calculated at this point a second time. Then the pressure gradient is calculated at the end of the section. These four pressure gradients are then used to calculate the average pressure gradient for the section.

$$\left(\frac{\overline{dp}}{dz} F\right) = \left(\frac{dp}{dz} F\right)_1 + 2 \left(\frac{dp}{dz} F\right)_2$$

$$+ \quad 2 \left(\frac{dp}{dz} F\right)_3 + \quad \left(\frac{dp}{dz} F\right)_4 \qquad (25)$$

For the calculations of deviation from the experimental data, the following Equations are used:

1. The deviation ϵ_i is defined relative to the experimental pressure drop by the Equation:

$$\epsilon_i = \frac{\Delta P_{i,exp} - \Delta P_{i,calc}}{\Delta P_{i,exp}} (100) \qquad (26)$$

A negative value of ϵ_i indicates that the model overestimates the pressure drop while a positive value indicates that the model underestimates the pressure drop. The average deviation for the four estimated pressure drops in one set of data is then:

$$\bar{\epsilon} = \sum_i \epsilon_i / 4 \qquad (27)$$

2. The absolute average deviation is defined by the Equation:

$$\bar{\epsilon}_A = \sum_i |\epsilon_i| / 4 \qquad (28)$$

This gives the average deviation with no concern whether the model overestimates or underestimates the pressure drop.

The criterion for improving a model is to make the total sum of squares of errors as small as possible. For one experimental run, the sum of squares of errors is calculated from the Equation:

$$SS = \sum_i (\epsilon_i \Delta P_{i,exp})^2 \qquad (29)$$

From the total sum of squares of errors a standard deviation may also be calculated.

3.1.2 The Subroutines

As mentioned earlier in this chapter, the subroutine calculates the physical properties for steam and water at the existing pressure. The Equations for the properties can be found in the listing of the subroutines in appendix B. These Equations are only valid in the pressure region of 100 to 1000 kPa. In addition to these Equations, an Equation to calculate surface tension was needed. Tabulated data for the surface tension (35) was fitted to the data and gave the following Equation with a standard deviation of 0.0000 for ten data points.

$$\sigma = 0.076702 - 1.665\ 10\ (T_{sat}) - 1.386\ (T_{sat})^2 \qquad (30)$$

The steam quality can not be estimated from the vapor and the liquid load alone because equlibrium conditions may not exist. It has to be calculated from the inlet enthalpy i_{in} and the enthalpy of saturated liquid i_{sat} thus:

$$i_{in} = \frac{(G_f\ i_f + G_g\ i_g)}{(G_f + G_g)} \qquad (31)$$

then:

$$x = \frac{(i_{in} - i_{sat})}{i_{fg}} \qquad (32)$$

3.1.3 The accelerational pressure gradient

The accelerational pressure gradient is determinded by calculating the expression within the brackets in Equation 6 for each point on the pipe. The differential is then calculated by dividing the increment of the expression by the distance between each point.

3.2 SUBROUTINES FOR THE DIFFERENT MODELS

3.2.1 Ghosal Model

The calculation procedure that is particular for the Ghosal model is as follows:

1. Calculate the Reynolds numbers.

$$Re_f = G\ (1 - x)\ D\ /\ \mu_f \qquad (33)$$

$$Re_g = G \times D / \mu_g \quad (34)$$

2. Calculate the friction factors using the Blasius Equation.

$$f_f = 0.079 \, (Re_f)^{-0.25} \quad (35)$$

$$f_g = 0.079 \, (Re_g)^{-0.25} \quad (36)$$

3. Calculate the Lockhart - Martinelli parameter X from the ratio between $(dp/dz\ F)_f$ and $(dp/dz\ F)_g$.

$$\left(\frac{dz}{dp} F\right)_f = \frac{2 f_f G^2 (1 - x)^2 v_f}{D} \quad (37)$$

$$\left(\frac{dp}{dz} F\right)_g = \frac{2 f_g G^2 x^2 v_g}{D} \quad (38)$$

4. The program then calls up the subroutine NEWRAP to calculate the void fraction from Equation 16 using the Newton-Raphson method. The method requires an initial guess for α that is relatively close to the final solution. The empirical correlation between and X developed by Wallis (36) was used for the initial guess of α .

$$\alpha = (1 + X^{0.8})^{-0.378} \quad (39)$$

5. Then ϕ_f^2 is calculated using Equation 13 and the total frictional pressure gradient is obtained using Equation 9.

3.2.2 Wallis Model

The calculation procedure that is particular for Wallis model is as follows:

1. Make an initial estimate of the frictional pressure gradient.

   a. Calculate Re and Re using the Equations 33 and 34.

   b. Calculate the Lockhart-Martinelli parameter as in the Ghosal model using Equations 37, 38 and 2.

   c. Calculate ϕ_f^2 using Equation 10.

   d. Estimate the total frictional gradient using Equation 9.

2. a. Calculate the entrainment using Equations 21 and 22 or 23.

   b. Calculate Reynolds number for the liquid film when entrainment is accounted for.

$$Re_{fF} = Re_f (1 - e) \qquad (40)$$

   c. Calculate friction factor for the liquid film when entrainment is accounted for.

$$f_{fF} = 0.079 (Re_{fF})^{} \qquad (41)$$

d. Calculate frictional pressure gradient assuming total flow to be liquid and entrainment taken into consideration.

$$\left(\frac{dp}{dz}\ F\right)_{fF} = \frac{2\ f_{fF}\ G_{fF}\ v_f}{D} \tag{42}$$

3. Then an estimate for the liquid frictional multiplier will be:

$$\phi_{fF}^2 = \left(\frac{dp}{dz}\ F\right) \Big/ \left(\frac{dp}{dz}\ F\right)_{fF} \tag{43}$$

The value of the void fraction α is then calculated using the following equation:

$$\alpha = 1 - \frac{1}{(\phi_{fF}^2)^{0.5}} \tag{44}$$

4. With the value of α, calculate ϕ_g^2 from Equation 20. Calculate then the frictional pressure gradient from the Equation:

$$(dp/dz\ F) = (dp/dz\ F)_g\ \phi_g^2 \tag{45}$$

5. Go back to step 3 with these values for (dp/dz F) and iterate until a constant value for α is obtained.
6. When the required accuracy is obtained, calculate the total pressure gradient using Equation 9.

3.2.3 Levy model

The calculation procedure for the Levy model also involves an iterative procedure. This procedure establishes a value for the liquid film thickness, Y_f. From this value, the friction factor and shear stress are calculated and then the frictional pressure gradient can be calculated.

1. Calculate the density exponent β. This parameter is calculated using the subroutine BETAS, and makes use of the Equation:

$$\beta = 1 + \sqrt{\left[(\rho_f / \rho_g)^{1/\beta} - 1 \right] \frac{\sigma}{0.4} \frac{\rho_f}{R \; G_g^2}} \qquad (46)$$

2. Make an initial estimate of the liquid film thickness Y_f.
3. Calculate the corresponding interface friction factor f_i by the Equation:

$$f_i = 0.005 \; (1 + 150 \; Y_f \; / \; R) \qquad (47)$$

4. Calculate the corresponding wall shear stress τ_w.

$$\tau_w = \rho_g \; f_i \; 0.5 \; (G_g \; / \; \rho_g)^2 \qquad (48)$$

5. Calculate the dimensionless film thickness Y_f^+ by Equation:

$$Y_f^+ = \frac{Y_f \sqrt{\tau_w \; / \; \rho_f} \qquad \rho_f}{\mu_f} \qquad (49)$$

6. Check the value of Y_f^+ . If $Y_f^+ < 30$, then calculate a new value for β .

$$\beta' = 1 + \sqrt{2} \ (\beta - 1) \tag{50}$$

7. Calculate the dimensionless pipe radius.

$$R^+ = \frac{R\sqrt{\tau_w / \rho_f} \qquad \rho_f}{\mu_f} \tag{51}$$

8. The dimensionless velocity of the liquid interface is calculated by the subroutine KYRS. The value is calculated from Equations 52, 53 or 54 depending on the value of Y_f^+.

$$K(Y_f^+, R^+) = 0.5(R^+)(Y_f^+) - 0.333\ (Y_f^+) \tag{52}$$

for $Y_f^+ < 5$.

$$K(Y_f^+, R') = 12.51(R^+) - 10.45 - 8.05(R^+)(Y_f^+)$$
$$+ 2.775(Y^+) + 5(R^+)(Y^+)\ \ln(Y^+)$$
$$- 2.5(Y_f^+)\ \ln(Y_f^+) \tag{53}$$

for $5 < Y_f^+ < 30$

$$K(Y_f^+,R^+) = 3(R^+)(Y_f^+) - 63.9(R^+) - 2.125(Y_f^+)$$
$$- 1.25(Y_f^+)\ \ln(Y_f^+) + 2.5(R^+)(Y_f^+)\ \ln(Y_f^+)$$
$$+ 573.21 \qquad (54)$$

for $Y_f^+ > 30$

9. Calculate the liquid film flowrate per unit pipe area G_{fF}.

$$G_{fF} = \frac{2\ K(Y_f^+,R^+)\ \sqrt{\tau_w/\rho_f}\ \rho_f}{(R^+)^2} \qquad (55)$$

10. Calculate the amount of entrained liquid G_e.

$$G_e = G_f\ (\beta)^{-0.5} \qquad (56)$$

11. Compare the values of G_f and the sum of G_e and G_{fF}. If they are close enough, stop the calculation; if not, a new estimate of Y_f is required, and the calculations are repeated.

12. Calculate the frictional pressure gradient from Equation 24.

Chapter IV

RESULTS

4.1 MODELS TESTED

The three models under consideration were used to predict pressure drop under experimental conditions. Then the predictions were compared with the actual pressure drops. The main results from this comparison are shown Table 1. First, the average deviation in percent for each model is listed. The corresponding standard deviation refers to the spread in percent average deviation. Second, the absolute average deviation and its standard deviation, also in percent, is listed. Third, the total sum of squares of errors for each model is listed. The corresponding standard deviation is in kPa. Plots are made for each model, showing the estimated vs. experimental pressure drop in Figures 4 to 7.

Tables 6 through 9 in appendix D show the results in detail. In Figures 8 through 37, the average deviation of the estimates is plotted against various parameters to show possible trends.

From Table 1, it can be seen that the Ghosal model overestimates the pressure drop by more than 50 percent on the average. The accuracy of the predictions of the model also var-

TABLE 1

MAIN RESULTS OF THE MODELS

	Ghosal model	Wallis model	Levy model
Average Error (percent)	-50.14	17.15	8.77
Standard Deviation (percent)	23.15	8.87	21.50
Absolute Average Deviation (percent)	50.14	17.28	18.43
Standard Deviation (percent)	23.15	8.50	13.89
Total Sum of Squares of Errors $(kPa)^2$	65544.38	5553.71	6992.50
Standard Deviation (kPa)	45.257	13.174	14.782

ies widely. The inaccuracy of this model is also reflected in the total sum of squares of errors.

Wallis model, on the other hand, consistently underestimates the pressure drop. On the average, the model underestimates the pressure drop by 17.15 percent with a standard deviation of the error of 8.87 percent. This model has also the lowest total sum of squares of errors.

The Levy model has the lowest average deviation, but it also has a wide spread in deviation. The model both overestimates and underestimates the pressure drop under different

physical conditions. Therefore, the absolute average deviation of the error is also much higher, 18.43 percent. The total sum of squares of errors is, however, not too much above that of Wallis model.

4.2 MODIFIED WALLIS MODEL

The Wallis model appeared to be the best of the three models tried. The model had the lowest total sum of squares of errors, and the errors showed no trend with any of the parameters involved in the calculations. As mentioned, however, the model in general underestimates the pressure drop by about 17 percent.

The Wallis model was modified with a simple correction factor applied as a multiplier to the frictional pressure gradient from the term in the model. The correction factor was obtained by minimizing the total sum of squares of errors. Because of inherent experimental errors the optimization procedure was not carried out to great length. The details are shown in appendix C. The resulting correction factor of 1.18 gives a total sum of squares of errors of only 1432.80 as shown in Table 2. The equation for the frictional pressure gradient is thus:

$$-\left(\frac{dp}{dz}F\right) = 1.18\,\frac{2\,f_{fF}\,G^2\,(1-x)^2\,(1-e)^2\,v_f}{D}\,\phi_{fF}^2 \qquad (57)$$

TABLE 2

RESULTS FOR MODIFIED WALLIS MODEL

Average Deviation (percent)	1.00
Standard Deviation (percent)	10.81
Average Absolute Deviation (percent)	8.96
Standard Deviation (percent)	6.25
Total Sum of Squares of Errors $(kPa)^2$	1432.80
Standard Deviation (kPa)	6.6914

Note that the average deviation at the optimal point is different from zero.

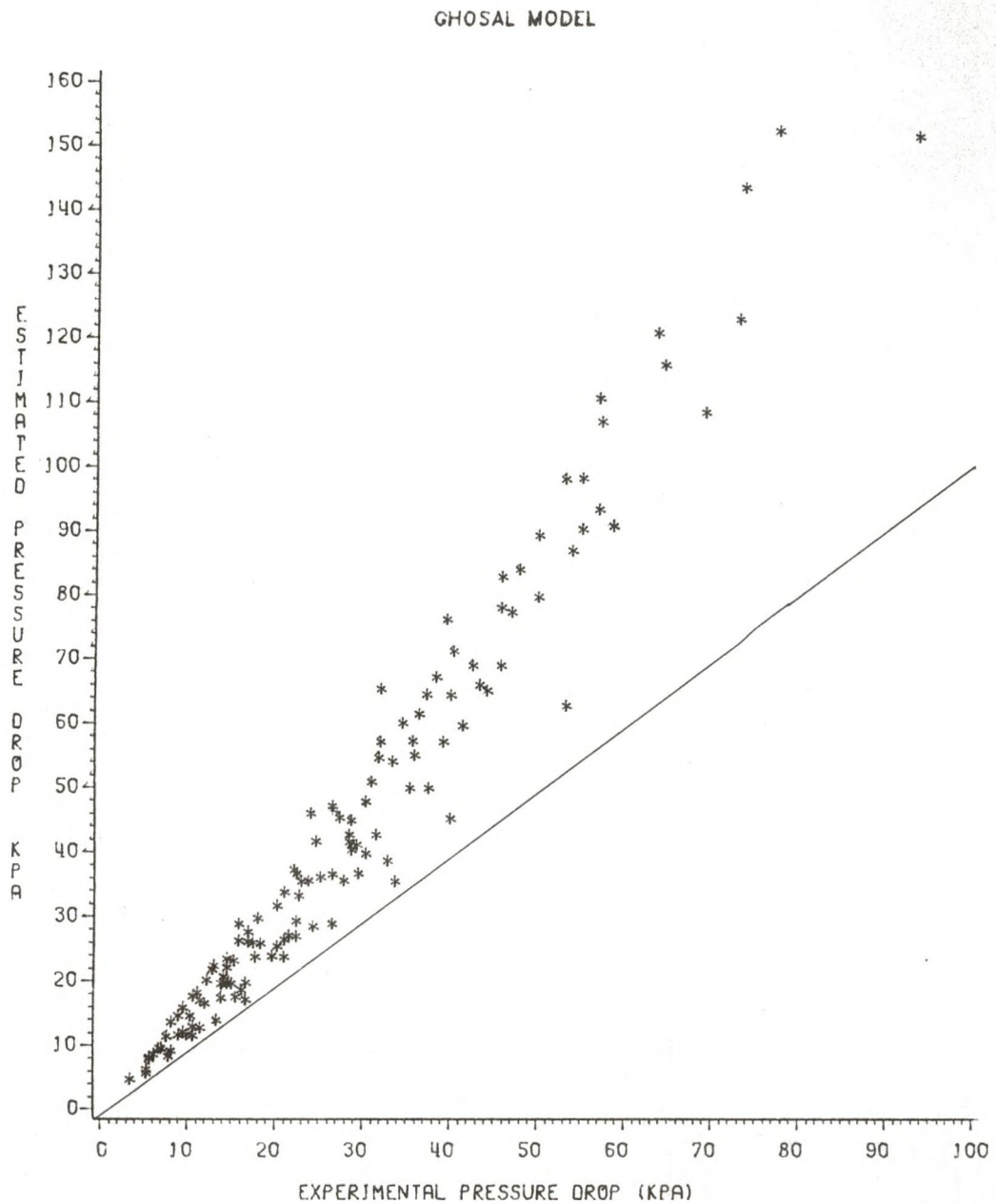

Figure 4: Estimated vs. experimental pressure drop.

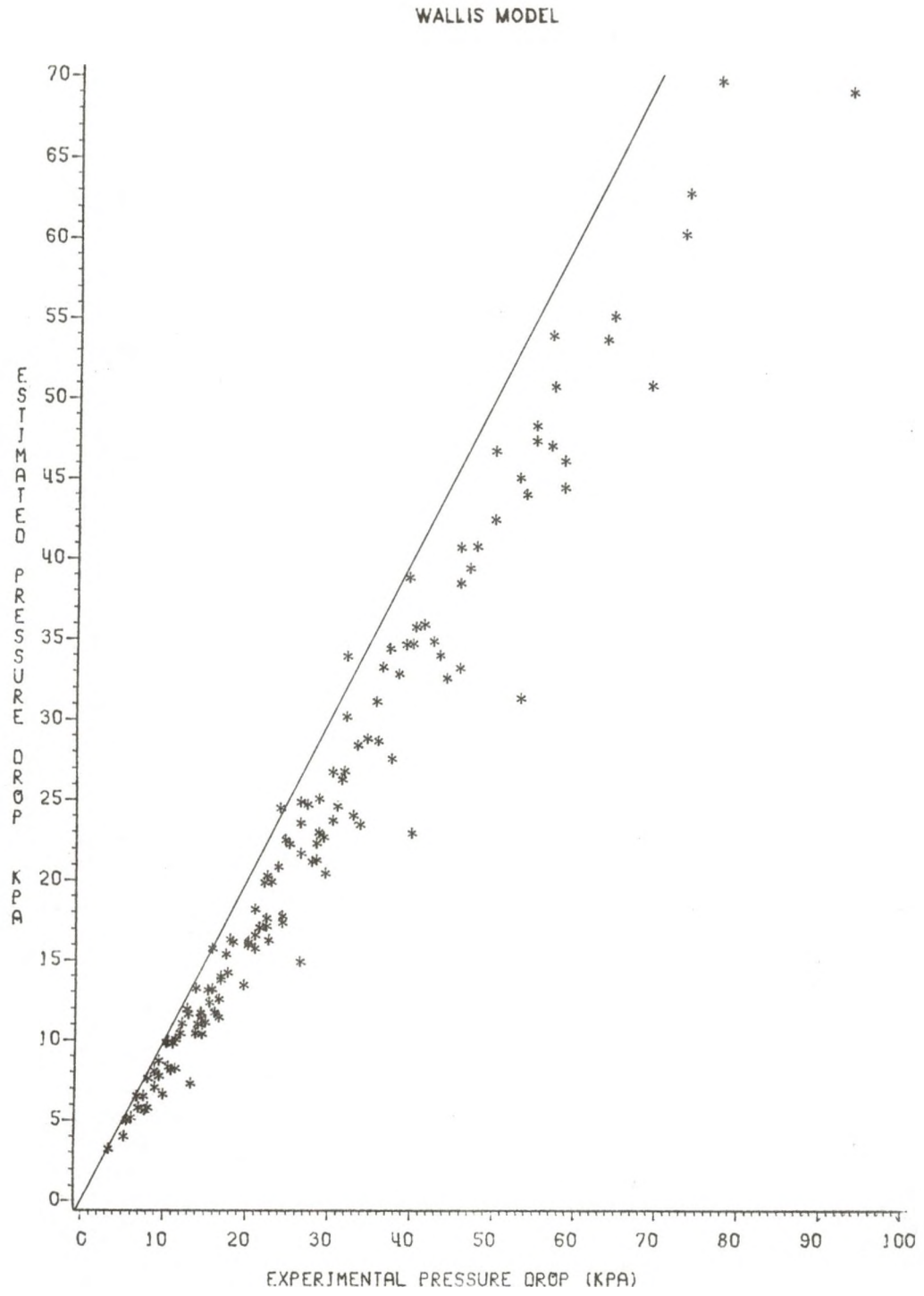

Figure 5: Estimated vs. experimental pressure drop.

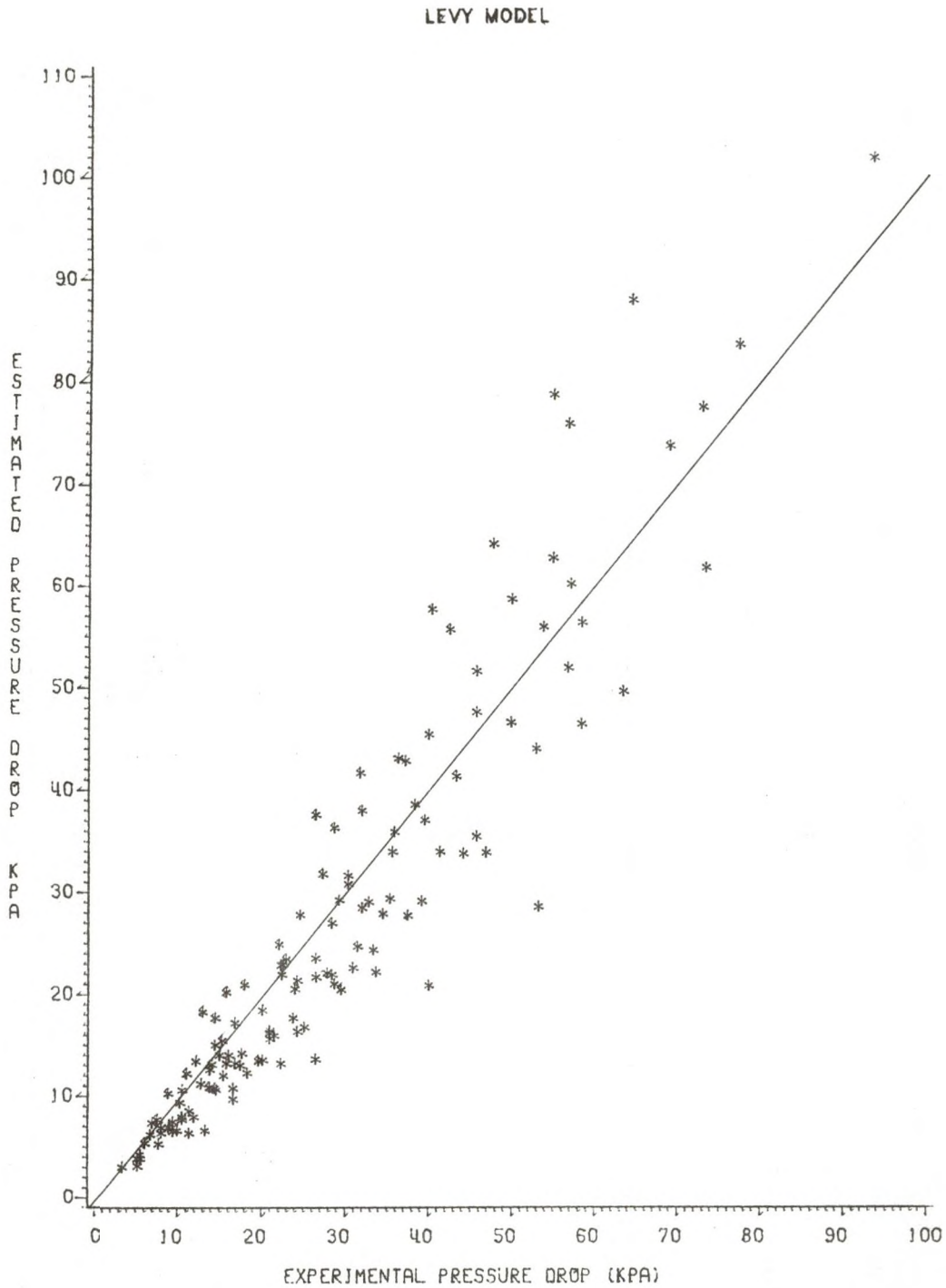

Figure 6: Estimated vs. experimental pressure drop.

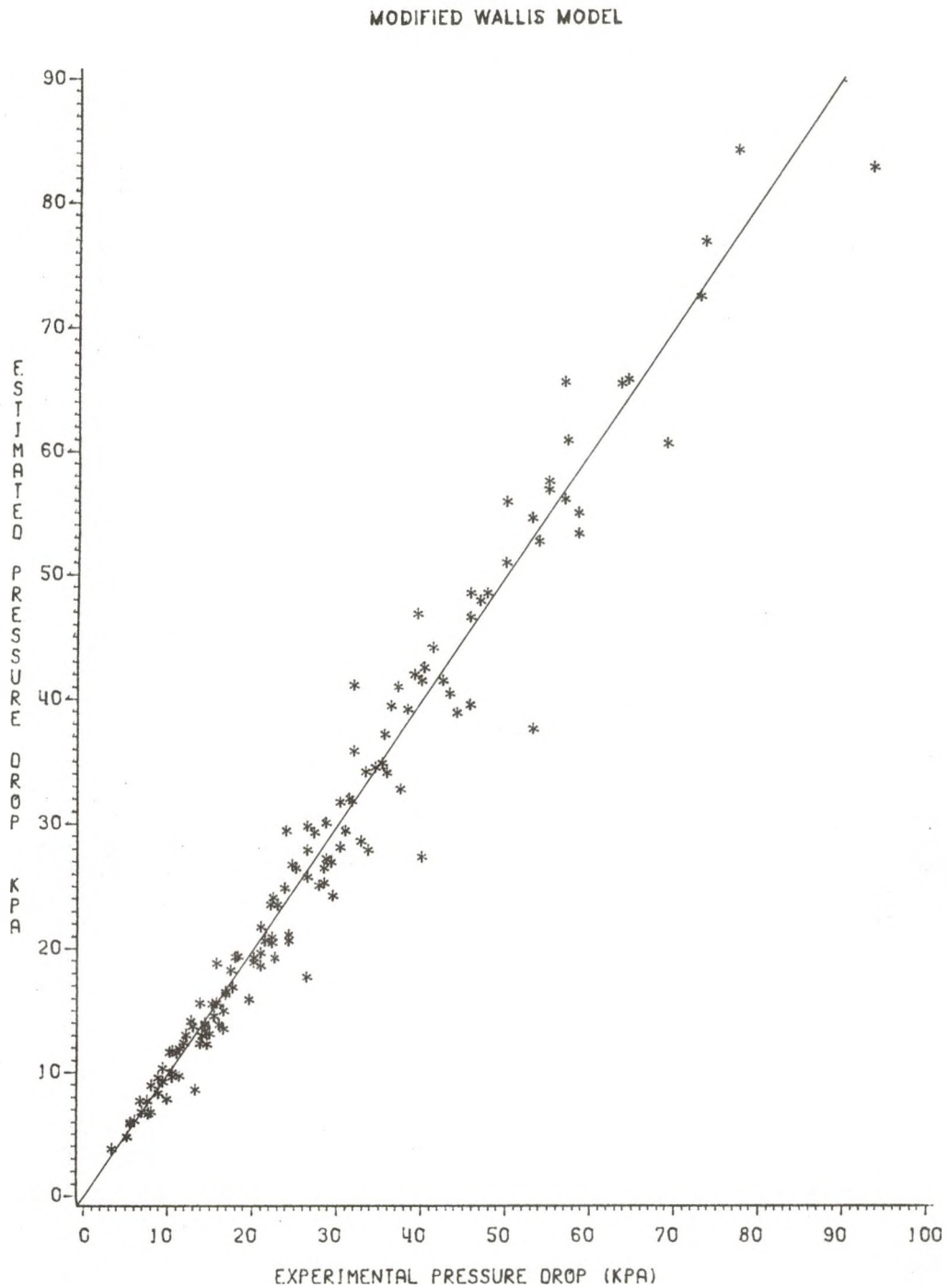

Figure 7: Estimated vs. experimental pressure drop.

Chapter V

DISCUSSION

The Ghosal model is the simplest of the three models. Neither entrainment of liquid into the gas core, nor velocity gradients within the liquid film are taken into account. This may account for the large deviation from the experimental data that the model predicts. There also does not appear to be any trend in the errors when plotted against any of the parameters. It is therefore difficult to see how the model can be modified on the basis of these data. A modification of this model should be based on a more realistic representation of the hydraulic features of annular flow.

Wallis model, on the other hand, is more highly developed and better represents the real behavior of annular flow. Both entrainment and velocity gradients within the liquid film, as well as a wavy interface between the gas and the liquid are taken into account. Therefore, it is not surpriseing that the model's predictions are close to the experimental data. The model also takes care of all the important variables. This is clearly indicated by the random scatter of the error when the error is plotted against various variables. Figures 12 through 15 in appendix F show that the model can not be improved much by including any of

the variables, such as mass flux, steam quality, pressure, etc.

The model underestimates the pressure drop by 17.15 percent on the average. The scatter in the errors are largest at low steam qualities. This may be mainly due to the difficulty in estimating steam quality. Steam quality is measured from the mass flowrates and the enthalpies of steam and water. A small error in these variables can translate into a large error. It is also possible at low steam qualities for the data to be in the transition zone between annular and bubbly flow rather than entirely in the annular flow region. This is probably true for two or three of the data points.

On the whole, however, the predictions of Wallis model are excellent. A simple correction factor can take care of the underestimation of the pressure drop. This correction factor may be needed because the friction factor for this work was calculated using the Blasius equation. Hasan (37) has compared this friction factor with the experimental friction factor obtained for single phase water flow through the equipment. He indicates that at high Reynolds mumbers, the observed friction factor is higher than that estimated from Blasius equation by as much as 15 percent. Most of the data used in this work were at low or moderate Reynolds numbers. The error between the Blasius and experimentaly ob-

tained friction factor is in the neighborhood of 5 to 10 percent.Therefore, the friction factor alone is probably not the entire reason for the underestimation. This argument is reinforced by Figure 21 which shows no trend when the error is plotted against Reynolds number for the liquid film. It seems, however, that modification of the friction factor would improve the predictions based on the Wallis model.

The other assumptions in the model could account for the deviations as well. It is quite likely that the entrainment is not predicted accurately. It is also possible that the model does not take proper account for the wavy nature of the liquid film. The assumption that the liquid film at the interface travels with exactly two times the average film velocity may also be wrong. In addition, the model does not include any effect of gravity on the liquid film. For horizontal flow, the effect of gravity could be significant because it causes the annular film at the bottom of the tube to be thicker than the film at the top. This effect should increase at lower mass velocities, and probably at higher steam qualities. The random nature of the errors when plotted against mass flux and steam quality indicate, however, that the effect of gravity alone will not explain the deviation.

The Levy model is a rather sophisticated development, and would seem to represent the real hydraulic features of annu-

lar flow quite well. Therefore, it was surprising that the model's prediction is not the best of the three. However, the total sum of squares of errors is not much larger than that of the Wallis model. The Levy model was developed for vertical flow, and the data used for this work is from a horizontal pipe. This may explain some of the errors in the predictions of the model. A more sophisticated version of the model where gravity effects are taken into account, has also been developed by Levy (38). The model, however, is even more complicated mathematically and was not considered in this study. It is doubtful, however, that the effects of gravity alone would account for much of the errors in the predictions. Figures 22 through 29 show the trend of errors when plotted against different parameters. Distinct patterns in some of these plots indicate that the model does not properly consider these parameters. This is especially true for steam quality and the density exponent as indicated in Figures 23 and 28, respectively. The Levy model could be modified by including a function of the density exponent or the steam quality in the model. However, there does not seem to be be much physical justification for doing so.

Of the three models, the Wallis model not only performs the best, but also appears to be most suitable for modification. The model is also well developed with respect to the particular hydrodynamic features of annular flow, and the modification can be accomplished using a simple correction factor.

Chapter VI

CONCLUSIONS AND RECOMMENDATIONS

6.1 CONCLUSIONS

1. The Wallis model without any modification appears to be the best among the three models. The standard deviation in the estimation of the pressure drop is 13.174 kPa, and the model underestimates the pressure drop by an average of 17.15 percent. The error appeared to be completely random.
2. The Wallis model was modified by adding the correction factor of 1.18 which gave an improved estimate of the pressure gradient. The standard deviation in the estimated pressure drop was 6.691 kPa. and the model underestimated the pressure drop by an average of 1.00 percent. The error appeared to be completely random.
3. The standard deviation in the estimation of the pressure drop was 14.782 kPa for the Levy model, and the model underestimated the pressure drop by an average of 8.77 percent. The model did not seem to properly account for steam quality.
4. For the Ghosal model, the standard deviation in the estimated of the pressure drop was 45.257 kPa. The

model overestimated the pressure drop by an average of 50.14 percent. The error appeared to be almost random.

6.2 RECOMMENDATIONS

1. The Wallis model should be used with the equation developed by Hasan (37) for the prediction of the friction factor. The equation for the friction factor is:

$$f = 0.00205 + 0.1058\ (Re)^{-0.316} \qquad (58)$$

2. The assumption of the interface velocity between the gas and liquid being twice the mean liquid velocity may not be correct. Therefore, values other than 2 should be used in the optimization procedure.
3. Using the Ghosal correlation for ϕ_f^2 in the Wallis model may yield interesting results.
4. The Levy model should be tried taking the gravitational effects into account.
5. The Wallis model should be evaluated against the data of Hasan (1) where the conditions are not adiabatic.

Appendices

Appendix A

RAW DATA AND INPUT CONDITIONS

TABLE 3

RAW DATA

Run no	Liquid load kg/m^2,s	Vapor load kg/m^2,s	Liquid enthalpy kJ/kg	Gas enthalpy kJ/kg	P kPa	ΔP_1 kPa	ΔP_2 kPa	ΔP_3 kPa	ΔP_4 kPa
1	178.51	66.843	549.0	2739.8	408.14	5.24	10.48	15.44	20.96
2	161.32	98.600	549.8	2739.8	397.78	8.00	16.00	24.27	32.82
11	308.56	76.871	535.1	2743.5	425.38	7.72	16.55	24.27	33.65
18	311.80	167.096	440.5	2752.22	473.68	14.89	29.23	39.99	54.88
20	538.63	98.596	486.7	2742.75	411.58	10.48	21.51	31.44	41.37
21	579.12	50.126	557.4	2739.12	432.26	5.24	11.31	16.55	22.34
28	736.32	50.126	561.6	2738.43	404.68	5.52	11.86	18.20	25.10
29	695.84	93.564	476.8	2738.43	397.78	9.38	20.13	28.68	39.16
36	2179.83	100.265	513.6	2742.8	418.43	2.48	6.07	8.83	12.13
37	2236.88	66.844	533.0	2742.8	437.20	2.34	4.96	7.45	9.93
38	1811.48	98.961	508.1	2744.83	432.22	4.69	11.03	16.82	23.72
39	1896.68	66.844	539.6	2744.83	411.54	2.76	6.89	11.58	16.82
48	159.697	132.354	566.6	2757.85	611.49	6.89	14.34	22.34	30.34
49	223.352	66.844	598.3	2757.85	611.49	3.31	6.62	10.20	13.79
66	520.323	100.265	602.9	2758.35	632.17	8.83	17.65	26.48	35.30
67	459.658	164.630	562.1	2762.00	628.71	12.13	24.55	37.23	49.92
80	587.715	197.217	504.6	2757.38	618.38	16.82	35.85	53.78	72.81
81	645.515	132.354	557.6	2757.38	590.81	10.48	22.39	35.58	49.92
82	700.823	68.513	607.4	2757.38	604.59	5.52	11.31	17.37	23.72
88	1226.88	164.630	530.6	2761.62	625.28	12.69	26.48	39.44	56.81
89	1225.01	132.354	544.0	2761.62	611.49	9.38	20.96	33.37	46.88
90	1211.56	69.347	639.3	2761.62	604.59	8.00	15.72	23.99	31.99
91	1222.52	100.265	562.1	2761.62	611.49	9.10	19.31	29.51	40.82
92	1695.50	197.217	490.2	2760.62	604.59	9.65	20.68	33.09	46.88
93	1706.22	164.618	535.1	2762.62	645.96	12.13	25.10	38.06	51.57

TABLE 3 continued

Run no	Liquid load $kg/m^2,s$	Vapor load $kg/m^2,s$	Liquid enthalpy kJ/kg	Gas enthalpy kJ/kg	P kPa	ΔP_1 kPa	ΔP_2 kPa	ΔP_3 kPa	ΔP_4 kPa
94	1751.93	132.354	562.1	2760.62	602.083	11.03	22.61	34.47	46.88
95	1791.9	66.844	562.1	2760.62	604.59	4.96	12.13	20.13	28.96
96	2282.35	64.340	606.0	2757.38	618.38	3.03	7.17	12.13	17.65
97	2244.35	132.54	575.6	2761.62	632.17	5.24	14.07	22.34	31.99
98	2171.61	164.618	548.5	2760.62	611.49	8.00	17.37	28.41	40.82
99	2137.10	197.217	580.2	2771.08	783.85	12.13	25.65	39.44	56.26
100	2142.96	164.618	611.9	2768.50	790.75	10.48	22.89	37.23	52.40
101	2210.72	100.265	655.0	2771.70	825.22	8.83	19.31	31.16	42.75
102	2175.72	132.354	639.3	2771.7	818.33	9.93	23.44	35.85	49.64
103	1678.06	197.217	593.8	2773.8	818.33	16.82	34.47	52.95	73.36
104	1708.71	164.618	611.9	2771.30	797.64	14.34	30.89	45.78	63.43
105	1737.48	132.354	632.5	2771.3	818.33	12.69	27.85	41.92	57.36
106	1039.65	213.548	584.8	2773.09	797.68	20.13	38.33	57.09	77.22
107	1112.4	132.354	662.1	2774.38	845.98	14.62	28.41	44.13	58.47
108	1189.13	100.265	657.6	2772.10	814.98	13.24	26.48	39.99	53.23
121	532.531	262.59	593.5	2775.3	825.28	22.61	45.78	68.95	93.22
122	621.722	164.63	639.3	2772.4	80.458	14.07	28.41	43.30	58.47
123	668.934	100.265	671.2	2770.80	832.18	9.93	19.58	29.51	37.51
130	305.567	262.603	620.8	2773.65	818.38	15.72	31.72	47.71	64.26
131	454.925	164.618	653.3	2771.05	804.58	11.03	22.06	31.99	45.78
138	214.756	262.603	607.4	2773.09	797.64	12.96	26.48	40.27	54.88
139	305.193	164.618	643.8	2771.70	811.43	8.83	17.93	27.30	36.40
140	366.107	100.265	657.9	2771.08	818.33	6.07	13.79	20.96	27.86
149	335.837	132.354	634.7	2774.3	811.41	7.45	15.17	22.89	30.34
150	215.255	262.603	584.8	2774.3	818.33	14.34	28.68	42.47	56.81

TABLE 4

CALCULATED INPUT CONDITIONS

Run no.	Steam quality	X	F	Flow pattern	Dimensionless vapor velocity
1	0.2524	0.1706	4.43	AF	2.994
2	0.3636	0.1050	6.84	AF	4.614
11	0.1699	0.2730	4.59	AF	3.116
18	0.2910	0.1532	9.33	AF	6.382
20	0.1063	0.4378	4.83	AF	3.266
21	0.0537	0.9709	2.36	AF	1.601
28	0.0440	1.022	2.48	AF	1.677
29	0.0660	0.6885	3.77	AF	2.545
36	-	-	-	*)	-
37	-	-	-	*)	-
38	-	-	-	*)	-
39	-	-	-	*)	-
48	0.4250	0.1015	7.43	AF	5.195
49	0.2024	0.2657	3.52	AF	2.458
66	0.1305	0.4328	4.78	AF	3.353
67	0.2229	0.2412	8.23	AF	5.767
80	0.1895	0.2875	8.86	AF	6.204
81	0.1263	0.4339	5.97	AF	4.162
82	0.0609	0.9034	2.82	AF	1.967
88	0.0561	0.9911	4.63	AF	3.244
89	0.0414	0.1308	3.37	AF	2.353
90	0.0393	1.363	3.04	AF	2.121
91	**)	1.993	2.09	BF	-
92	**)	2.187	2.69	BF	-
93	**)	2.317	2.51	BF	-
94	**)	2.683	2.15	BF	-
95	-	-	-	*)	-
96	-	-	-	*)	-
97	**)	5.682	1.19	BF	-
98	**)	3.425	2.04	BF	-
99	**)	2.500	2.93	BF	-
100	**)	2.564	2.82	BF	-
101	**)	5.633	1.20	BF	-
102	**)	3.273	2.17	BF	-

TABLE 4 continued

Run no.	Steam quality	X	F	Flow pattern	Dimensionless vapor velocity
103	0.0477	1.307	4.73	AF	3.415
104	0.0396	1.544	3.95	AF	2.845
105	**)	2.108	2.83	BF	-
106	0.1157	0.5458	7.73	AF	5.562
107	0.0763	0.8503	4.93	AF	3.570
108	0.0477	1.309	3.25	AF	2.343
121	0.2874	0.2015	11.9	AF	2.343
122	0.1776	0.3491	7.42	AF	5.342
123	0.1060	0.6083	4.27	AF	3.087
130	0.4355	0.1119	13.04	AF	9.411
131	0.2412	0.2466	7.93	AF	5.715
138	0.5265	0.0796	13.39	AF	9.633
139	0.3255	0.1702	8.08	AF	5.829
140	0.1894	0.3282	4.65	AF	3.357
149	0.2521	0.2349	6.24	AF	4.502
150	0.5197	0.08254	13.08	AF	9.445

AF - Annular Flow
BF - Bubbly Flow

*) - The vapor quality is lower than 0.5 percent and no data are calculated.

**) - The vapor quality is too low for the program to integrate the pressure drop along the pipe.

Appendix B

LISTING OF COMPUTER PROGRAMS

DOCUMENTATION OF ABBREVIATIONS USED

0010 *	KK	RUN NO. FOR HASAN'S DATA(1)
0020 *	G	TOTAL MASS FLUX
0030 *	GF	GAS PHASE MASS FLUX
0040 *	GG	LIQUID PHASE MASS FLUX
0050 *	H	DISTANCE BETWEEN EACH PRESSURE TAP
0060 *	DIST	DIST. BETWEEN EACH PRESS. GRAD. CALCULATED
0070 *	DI	INSIDE PIPE DIAMETER
0080 *	ENF	ENTHALPY OF LIQUID
0090 *	ENG	ENTHALPY OF GAS
0100 *	ENI	INLET ENTHALPY OF TWO-PHASE MIXTURE
0110 *	ENFG	ENTHALPY OF EVAPORATION
0120 *	EPD(I)	EXPERIMENTAL PRESSURE DROP
0130 *	PPD(I)	PREDICTED PRESSURE DROP
0140 *	P	INLET PRESSURE
0150 *	LMP	LOCKHART-MARTINELLI PARAMETER
0160 *	FAC	FLOW PATTERN COORDINATE F
0170 *	X	STEAM QUALITY
0180 *	BE	DIMENSIONLESS DENSITY PARAMETER BETA
0190 *	YFPL	DIMENSIONLESS DISTANCE FROM PIPE
0200 *	YF	DISTANCE FROP PIPE WALL
0210 *	DVV	DIMENSIONLESS VAPOR VELOCITY
0220 *	A1	LOCAL NAME FOR DISTANCE ALONG THE PIPE
0230 *	A2	LOCAL NAME FOR PRESSURE ALONG THE PIPE
0240 *	T	SATURATION TEMPERATURE FOR WATER
0250 *	DPDZ	FRICTIONAL PRESSURE GRADIENT
0260 *	DPDZF	(DP/DZ F) - ONLY LIQUID FLOW
0270 *	DPDZG	(DP/DZ F) _ ONLY GAL FLOW
0280 *	DADZ	ACCELERATIONAL PRESSURE GRADIENT / G**2
0285 *	A	ACCELERATIONAL PRESSURE GRADIENT
0290 *	RE	REYNOLDS NO.
0300 *	REF	REYNOLDS NO. FOR LIQUID
0310 *	REG	REYNOLDS NO. FOR GAS
0320 *	REFF	REYNOLDS NO. FOR LIQUID WITH ENTRAINMENT
0330 *	FF	FRICTION FACTOR FOR LIQUID
0340 *	FG	FRICTION FACTOR FOR GAS
0350 *	FFF	FRICTION FACTOR FOR LIQUID WITH ENTRAINMENT
0360 *	CAPX	SQUARE ROOT OF (DPDZF/DPDZG)
0370 *	SIGMA	SURFACE TENSION
0380 *	VMEWG	VISCOSITY OF THE GAS
0390 *	VMEWF	VISCOSITY OF THE LIQUID
0400 *	VF	SPECIFIC VOLUME OF THE LIQUID
0410 *	VG	SPECIFIC VOLUME OF THE GAS
0420 *	EN	ENTRAINMENT
0430 *	FIG2	TWO-PHASE GAS FRICTION MULTIPLIER

LISTING OF THE MAIN PROGRAM

```
0010 *
0020 *
0030 *       PROGRAM FOR THE CALCULATION OF PRESSURE DROP
0040 *       IN ANNULAR TWO-PHASE FLOW.
0050         REAL LMP
0060         COMMON G,GF,GG,DI,Z,I,II,H,DIST
0070         COMMON ENF,ENG,ENI,ENFG
0080         DIMENSION AK(4),EPD(4),PPD(4),DEV(4)
0090         H = 0.44
0092 *
0094 *     READING AND WRITING OF IMPUT PARAMETERS
0096 *
0100           WRITE(6,100)
0110           READ*,KK,GF,GG,ENF,ENG,P,EPD(1),EPD(2),
               EDP(3),EDP(4)
0120           WRITE(6,400)KK
0130           WRITE(6,401)GF,ENF,P
0140           WRITE(6,402)GG,ENG
0150           G = GF+GG
0160           DI = 10.11E-03
0170           ENI = (ENG*GG+ENF*GF)/G
0180           DIST = 0.0
0182 *
0184 *     CALL SUBROUTINE PPSSAW TO CALCULATE INPUT
0186 *     CONDITIONS AND FLOW PATTERN COORDINATES
0188 *
0190           CALL PPSSAW(F,P,DPDZF,DPDZ,T,X,LMP,FAC,ALPHA,
               EN,DVF,BE,YF,YFPL,DELTA)
0200           WRITE(6,510)LMP,FAC
0210           WRITE(6,520)BE,YFPL,DVV
0220           WRITE(6,530)YF,DELTA
0230           WRITE(6,200)
0240           WRITE(6,500)
0242 *
0244 *     THE RUNGE-KUTTA ITERATION PROCEDURE STARTS
0246 *     HERE. AN AVERAGE PRESSURE GRADIENT IS CALCULATED
0248 *     FOR EACH SECTION OF THE PIPE
0249 *
0250           DO 140 II = 1,4
0260           TP = P
0270           DO 107 I = 1,4
0272 *
0274 *     FOR EACH OF THE POINTS, 101, 102, 103, 104
0276 *     AN AVERAGE PRESSURE GRADIENT IS CALCULATED
0278 *
0280           GO TO (101,102,103,104),I
0290  101      A1 = Z
0300           A2 = P
0310           DIST = 0.0
0320           GO TO 105
```

```
0330  102    A1 = Z+H/2
0340         A2 = P+AK(I-1)/2
0350         DIST = H / 2.0
0360         GO TO 105
0370  103    A1 = Z+H/2
0380         A2 = P+AK(I-1)/2
0390         DIST = 0.0
0400         GO TO 105
0410  104    A1 = Z+H
0420         A2 = P+AK(I-1)
0430         DIST = H / 2.0
0440  105    CALL PPSSAW(F,A2,DPDZF,DPDZ,T,X,LMP,FAC,
             ALPHA,EN,DVV,BE,YF,YFPL,DELTA)
0450         IF(X.LE.0.005)GO TO 600
0470         AK(I) = H*F
0480  107    CONTINUE
0490         Z = Z+H
0500         P = P+(AK(1)+AK(2)*2+AK(3)*2+AK(4))/6
0510         DELP = TP-P
0520         PPD(1) = DELP
0530         PPD(2) = PPD(1)+DELP
0540         PPD(3) = PPD(2)+DELP
0550         PPD(4) = PPD(3)+DELP
0552 *
0554 *     CALCULATION OF DEVIATION BETWEEN THE
0556 *     EXPERIMENTAL AND THE PREDICTED PRESSURE DROP
0558 *
0560           DEV(II) = (EPD(II)-PPD(II))/EPD(II)
0570           ADEV = ADEV+DEV(II)/4.0
0580           AADEV = AADEV+ABS(DEV(II))/4.0
0590           SDEV = SDEV+(DEV(II)*EPD(II))**2
0600           PGRAD = F * (-1.0E+05)
0602 *
0604 *     OUTPUT OF THE PREDICTIONS OF PRESSURE DROPS
0606 *     AND DEVIATIONS.
0608 *
0610           WRITE(6,300)Z,PGRAD,PPD(II),EPD(II),
             DEV(II),T,X,ALPHA,EN
0620  140    CONTINUE
0630         WRITE(6,1300)ADEV,AADEV,SDEV
0640  100    FORMAT(15X,'GIVE THE DATA: RUN #,GF,GG,
             ENF,ENG,P,EPD(1),EPD(2),EPD(3),EPD(4)')
0650  200    FORMAT(//,1X,'L',5X,'P.GRAD',5X,'PRE.PD.',
             3X,'DEVI-',4X,'STEAM',5X,'VOID',7X,'E
0660  300    FORMAT(1X,F5.3,3X,F6.4,4X,F6.4,4X,F6.4,
             4X,F6.4,5X,F6.4,5X,E10.3)
0670  400    FORMAT(/,15X,'DATA SET #',I3,' OF DR. HASAN')
0680  401    FORMAT(/,'INPUT DATA:',3X,'LIQ.LOAD =',F7.2,'
             LIQ.ENTH.=',F7.2,J/KJ',3X,'P=',F6.4',3X,
0680  402    FORMAT(14X,'GAS=',F7.2,'KG/M2,S',3X,'ENTH.=
             ',F7.2,'J/KG')
0690  500    FORMAT(1X,'M',5X,'N/M,M2',6X,'BAR',7X,
             'ATION',4X,'C',3X,'FRAC',3X,'MENT')
0700  510    FORMAT(/,1X,'FP-COORDINATES:   L-M
```

```
                PARAMETER=',E10.5,5X,'F=',F5.2)
                =',F6.3,8X,'YF-PLUS=',F7.2,5X,'V=',E11.4)
0720            FORMAT(/,' LIQUID FILM:',11X,'DELTA  =
0725            MYF = ,'E11.4,' M')
0730            IF(X.GE.0.005)GO TO 1200
0740    600     WRITE(6,900)
0750    700     WRITE(6,1000)
0760    800     WRITE(6,1100)X,ENI,ENF,ENFG
0770    900     FORMAT(//5X,'STEAM QUALITY IS LESS THAN 0.5
                %. PRESSURE DROP IS NOT CALCULATED.')
0780   1000     FORMAT(5X,'STEAM QUALITY',5X,'SAT.
                ENTHALPY',5X,'EVAP.ENTHALPY')
0790   1100     FORMAT(5X,F10.5,8X,F13.2,5X,F13.2,5X,F13.2)
0800   1300     FORMAT(//1X,'AVER.DEV.  =  ',E10.4,5X,'AAD
                = ',E10.4,5X,'SS = ',E10.4,'BAR2')
0810   1200     CONTINUE
0820            STOP
0830            END
```

SUBROUTINE FOR THE GHOSAL MODEL

```
1100        SUBROUTINE PPSSAW(F,P,DPDZF,DPDZ,T,
1105        X,LMP,FAC,ALPHA,CAPX)
1110        REAL LMP,FA,JGC,ALFA,JG
1120        COMMON G,GF,GG,DI,Z,I,II,H,DIST
1130        COMMON ENF,ENG,ENI,ENFG
1132 *
1134 *    CALCULATION OF PHYSICAL PROPERITES
1136 *
1140        G=GF+GG
1150        VF=0.99453E-03+48.7443E-06*P**0.43503
1160        VG=1.69767*P**(-0.91215)-4.02401E-03
1170        VFG=VG-VF
1180        VMEWF=231.712E-06*P**(-0.38423)+52.7757E-06
1190        VMEWG=5.12377E-06+6.92654E-06*P**(-0.15461)
1200        ROG=1.0/VG
1210        ROF=1.0/VF
1220        ENF=545.254*P**0.21265-127.422
1230        ENFG=2474.56-217.561*P**0.32378
1240        X=(ENI-ENF)/ENFG
1250        IF(X.LE.0.005)GO TO 268
1260 *
1270      FAC = (ROG/(ROF-ROG))**0.5*3.175*VG*G*X
1280      LMP = ((1.0-X)/X)**0.9*(ROG/ROF)**
1285            0.5*(VMEWF/VMEWG)**0.1
1290 *      CALCULATION OF PHYSICAL PROPERTIES OF
1300 *      SATURATED STEAM AND WATER
1310        GG=X*G
1320        GF=(1.0-X)*G
1330        T=143.7725*P**0.19246-44.0965
1340        REN=G*DI/VMEWF
1350        RENF=G*(1-X)*DI/VMEWF
1360        FF=0.079*RENF**(-.25)
1370        DPDZF=2*FF*G**2*(1-X)**2*VF/DI
1380        RENG=G*X*DI/VMEWG
1390        FG=0.079*RENG**(-.25)
1400        DPDZG=2*FG*G**2*X**2*VG/DI
1410        CAPX=(DPDZF/DPDZG)**0.5
1412 *
1414 *    CALL SUBROUTINE NEWRAP TO CALCULATE
1416 *    THE VOID FRACTION FROM LOCKHART-MARTINELLI
1418 *    PARAMETER X.
1419 *
1420          CALL NEWRAP(CAPX,ALPHA)
1430          A2=VG*X**2/ALPHA+(1.0-X)**2 * VF/(1-ALPHA)
1440          IF(DIST.EQ.0.0) GO TO 110
1442 *
1444 *    CALCULATE THE ACCELERATIONAL PRESSURE GRAD.
1446 *
```

```
1450        DADZ = ( A2 - A1 ) / DIST
1460  110   A1 = A2
1470        A=DADZ*G**2
1480        FIFSQ=0.75/(1.0-3.0*ALPHA+2.0*ALPHA**1.5)
1490        FP = FIFSQ * DPDZF
1492 *
1494 *    CALCULATE THE TOTAL PRESSURE GRAD.
1496 *
1500        F = (FP + A) * (-1.0E-05)
1510  268   RETURN
1520        END
1530 *
1540 *
1550 *
1560        SUBROUTINE NEWRAP(X,Z)
1570        Z = ( 1.0 + X**0.8 ) ** (-0.378)
1580  108   F1=(304.0/3.0)*Z**(-2.5)-404.0*Z**(-1.5)
1590        +(608.0/3.0)*Z**(-1.0)
1600        F2 = 300.0 * Z**(-0.5) - 200.0 - X**2
1700        F = F1 + F2
1710        FD1=(-760.0/3.0)*Z**(-3.5)+606.0*Z**(-2.5)
1720        FD2=-(608.0/3.0)*Z**(-2.0)-150.0*Z**(-1.5)
1730        FD = FD1 + FD2
1740        ZI = Z - F / FD
1750        IF(ABS(Z - ZI ).LE.1.0E-04) GO TO 109
1760        Z = ZI
1770        GO TO 108
1780  109   Z = ZI
1790        RETURN
1800        END
```

SUBROUTINE FOR THE WALLIS MODEL

```
1100      SUBROUTINE PPSSAW(F,P,DPDZF,DPDZ,T,
1110      X,LMP,FAC,ALPHA,EN)
1120      REAL LMP,FA,JGC,ALFA,JG
1130      COMMON G,GF,GG,DI,Z,I,II,H,DIST
1140      COMMON ENF,ENG,ENI,ENFG
1142 *
1144 *    CALCULATION OF PHYSICAL PROPERTIES
1146 *
1150      G=GF+GG
1160      VF=0.99453E-03+48.7443E-06*P**0.43503
1170      VG=1.69767*P**(-0.91215)-4.02401E-03
1180      VFG=VG-VF
1190      VMEWF=231.712E-06*P**(-0.38423)+52.7757E-06
1200      VMEWG=5.12377E-06+6.92654E-06*P**(-0.15461)
1210      ROG=1.0/VG
1220      ROF=1.0/VF
1230      ENF=545.254*P**0.21265-127.422
1240      ENFG=2474.56-217.561*P**0.32378
1250      X=(ENI-ENF)/ENFG
1260      IF(X.LE.0.005)GO TO 268
1270 *
1280      FAC = (ROG/(ROF-ROG))**0.5*3.175*VG*G*X
1290      LMP=((1.0-X)/X)**0.9*(ROG/ROF)**
1295          0.5*(VMEWF/VMEWG)**0.1
1320      GG=X*G
1330      GF=(1.0-X)*G
1340      T=143.7725*P**0.19246-44.0965
1350      SIGMA=7.67021E-02-1.66555E-04*
1360            T-1.385948E-07*T**2
1360      REN=G*DI/VMEWF
1370      RENF=G*(1-X)*DI/VMEWF
1380      FF=0.079*RENF**(-.25)
1390      DPDZF=2*FF*G**2*(1-X)**2*VF/DI
1400      RENG=G*X*DI/VMEWG
1410      FG=0.079*RENG**(-.25)
1420      DPDZG=2*FG*G**2*X**2*VG/DI
1430      CAPX=(DPDZF/DPDZG)**0.5
1440      FIG2=1.0+20.0*CAPX+CAPX**2
1450      DPDZ=FIG2*DPDZG
1452 *
1454 *    CALCULATION OF DIMENSIONLESS VAPOR VELOCITY
1456 *    AND ENTRAINED LIQUID FRACTION IN THE VAPOR CORE.
1458 *
1460      JG=GG*VG
1470      Y=JG*VMEWG/SIGMA*(VF/VG)**0.5
1480      IF(Y.LE.0.00042) GO TO 10
1490      IF(Y.GE.0.0014) GO TO 20
1500      EN=-0.0494295+1049.794 * Y-330532.9 * Y**2
```

```
1510      GO TO 30
1520 10   EN = 0.02270985 - 596.6509 *Y + 3223134.0 *Y**2
1530      GO TO 30
1540 20   EN = 0.8
1550 30   CONTINUE
1560      REFF=RENF*(1.0-EN)
1570      FFF=0.079*(REFF)**(-0.25)
1580      DPDZFF=2.0*FFF*(G*(1.0-X)*(1.0-EN))**2*VF/DI
1582 *
1584 *   THE ITERATION PROCEDURE STARTS HERE.
1586 *
1590 101  FIFF2=DPDZ/DPDZFF
1600      ALPHA=1.0-FIFF2**(-0.5)
1610      DELTA=(1.0-ALPHA)*DI/4.0
1620      C1=1.0+75.0*(1-ALPHA)/ALPHA**2.5
1630      C2=(GG+E*GF)/GG
1640      B1=GF*((1.0-EN)/GG)*VF/VG
1650      B2=ALPHA/(1.0-ALPHA)*B1
1660      C3=(1.0-2.0*B2)**2
1670      CFIG2=C1*C2*C3
1680      IF(ABS(CFIG2-FIG2)-50.0) 103,102,102
1682 *
1684 *    ESTIMATION OF A NEW VALUE FOR THE
1686 *    TWO-PHASE FRICTIONAL MULTIPLIER FOR GAS
1688 *
1690 102  FIG2=(CFIG2+FIG2)/2.0
1700      DPDZ=DPDZG*FIG2
1710      GO TO 101
1720 103  FIG2=(CFIG2+FIG2)/2.0
1730      DPDZ=DPDZG*FIG2
1732 *
1734 *    CALCULATE THE ACCELERATIONAL PRESSURE GRAD.
1736 *
1740      A2=VG*X**2/ALPHA+(1.0-X)**2 * VF/(1-ALPHA)
1750      IF(DIST.EQ.0.0) GO TO 110
1760      DADZ=(A2-A1)/H
1770 110  A1=A2
1780      A=DADZ*G**2
1782 *
1784 *    CALCULATION OF THE TOTAL PRESSURE GRAD.
1786 *
1790      F=(DPDZ+A)*(-1.0E-05)
1800 268  RETURN
1810      END
```

SUBROUTINE FOR THE LEVY MODEL

```
0840          SUBROUTINE PPSSAW(F,P,DPDZF,DPDZ,T,X,LMP,F,
              ALPHA,EN,DVV,BE,YF,YFPL,DELTA)
0850          REAL LMP,FA,JGC,ALPHA,JG,KYR
0860          COMMON G,GF,GG,DI,Z,I,II,H,DIST
0870          COMMON ENF,ENG,ENI,ENFG
0880          RI = DI / 2.0
0882 *
0884 *    CALCULATION OF THE PHYSICAL PROPERTIES
0886 *
0890          G = GF+GG
0900          VF = 0.99453E-03+48.7443E-06*P**0.43503
0910          VG = 1.69767*P**(-0.91215)-4.02401E-03
0920          VFG = VG-VF
0930          VMEWF = 231.712E-06*P**(-0.38423)+52.7757E-06
0940          VMEWG = 5.12377E-06+6.92654E-06*P**(-0.15461)
0950          ROG = 1.0/VG
0960          ROF = 1.0/VF
0970          ENF = 545.254*P**0.21265-127.422
0980          ENFG = 2474.56-217.561*P**0.32378
0990          X = (ENI-ENF)/ENFG
1000          IF(X.LE.0.005)GO TO 268
1010 *        CALCULATION OF COORDINATES FOR FLOWPATTERN-MAP
              AFTER TAITEL AND DUKLER
1020 *
1030        FAC   =  (ROG/(ROF-ROG))**0.5*3.175*VG*G*X
1040        LMP   =  ((1.0-X)/X)**0.9*(ROG/ROF)**0.5
                  *(VMEWF/MVEWG)**0.1
1070          GG = X*G
1080          GF = (1.0-X)*G
1090          ALPHA = (1.0 +LMP**0.8) **(-0.387)
1100          DELTA = RI * (1.0 - ALPHA**0.5)
1110          T = 143.7725*P**0.19246-44.0965
1120          SIGMA = 7.67021E-02-1.66555E-04*T
              - 1.385948E-07*T**2
1130          JG = GG*VG
1140          DVV = JG*VMEWG/SIGMA*(VF/VG)**0.5
1142 *
1144 *    CALL UP THE SUBROUTINE BETAS TO CALCULATE THE
1146 *    THE DIMENSIONLESS DENSITY FUNCTION BETA.
1148 *
1150          CALL BETAS(ROF,ROG,SIGMA,RI,BE)
1160          YF = DELTA
1170          J = 0
1180   201    YFR = YF / RI
1190          FIS = 0.005 * (1.0 + 150.0 * YFR )
1200          TAUW = 0.5 * ROG * FIS * (GG/ROG)**2
1210          TAUWF = ((TAUW * ROF)**0.5) / VMEWF
1220          YFPL = YF * TAUWF
```

```
1230          RPL = RI * TAUWF
1240          IF(YFPL.GT.30.0)GO TO 202
1250          IF(J.GE.1)GO TO 202
1260          BE = 1.0 + 1.4142136 * (BE - 1.0)
1270          J = J + 1
1280   202    CONTINUE
1290          GE = GF * (1.0/BE)**0.5
1292  *
1294  *     CALL UP THE SUBROUTINE KYRS TO CALCULATE THE
1296  *     DIMENSIONLESS VELOCITY K(YF,R)
1298  *
1300          CALL KYRS(YFPL,RPL,KYR)
1310          GFF = 2.0*KYR*((TAUW*ROF)**0.5)/(RPL**2)
1320          GFFT = GF - GE
1330          DGFFT = GFF - GFFT
1340          IF(ABS(DGFFT) - 10.0)204,203,203
1342  *
1344  *      MAKE A NEW ESTIMATE OF YF
1346  *
1350   203    YFN = YF * (GFFT/GFF)
1360          YF = (YFN + YF) / 2.0
1370          GO TO 201
1380   204    CONTINUE
1390          EN = GE / GF
1400          YT = YF * (ROF/ROG) ** (1.0/BE)
1402  *
1404  *      CALCULATE THE FRICTIONAL PRESSURE GRADIENT.
1406  *
1410          DPDZ = 2.0 * TAUW / RI
1412  *
1414  *      CALCULATE THE ACCELERATIONAL PRESSURE GRAD.
1416  *
1420          A2 = VG*X**2/ALPHA+(1.0-X)**2*VF/(1-ALPHA)
1430          IF(DIST.EQ.0.0) GO TO 110
1440          DADZ = (A2-A1)/DIST
1450   110    A1 = A2
1460          A = DADZ*G**2
1470          F = (DPDZ+A)*(-1.0E-05)
1480   268    RETURN
1490          END
1500  *
1510          SUBROUTINE BETAS(ROF,ROG,SIGMA,RI,BE)
1520          COMMON G,GF,GG,DI,Z,I,II,H,DIST
1530          COMMON ENF,ENG,ENI,ENFG
1540          REAL KF,BE,BEPR,BEN,BE1,BE2,BEND
1550          REAL KYR
1550          KF = 0.4
1570          BE = 4.0
1580   301    BE1 = (ROF/ROG)**(1.0/BE) - 1.0
1590          BE2 = SIGMA * ROF / (KF * RI * GG**2)
1600          BEN = 1.0 + ( BE1 * BE2 ) ** 0.5
1610          IF(ABS(BE-BEN) - 0.01)303,302,302
1620   302    BE = (BE + BEN) / 2.0
1630          GO TO 301
```

```
1640  303    BE = BEN
1650         RETURN
1660         END
1670 *
1680         SUBROUTINE KYRS(YFPL,RPL,KYR)
1690         COMMON G,GF,GG,DI,Z,I,II,H,DIST
1700         COMMON ENF,ENG,ENI,ENFG
1710         REAL KYR
1720         YFPLN = ALOG(YFPL)
1730         IF(YFPL.GE.30.0) GO TO 502
1740         IF(YFPL.GE. 5.0) GO TO 501
1750         KYR =0.5 *RPL *YFPL**2 - (YFPL**3) / 3.0
1760         GO TO 503
1770  501    KYR = 12.51*RPL-10.45-8.05*RPL*YFPL+2.775
             *YFPL**2+5.0*RPL*YFPL*YFPLN-2.5*YFPL*YFPLN
1780         GO TO 503
1790  502    KYR=3.0*RPL*YFPL-63.9*RPL-2.125*(YFPL**2)
             -1.25*(YFPL**2)*YFPLN+2.5*RPL*YFPL*YFPLN+573.21
1800  503    RETURN
1810         END
```

Appendix C

OPTIMIZATION PRECEDURE

The correction factor for The Wallis model was obtained by using three different correction factors as reference points. Using the resulting total sum of squares of errors for these three factors, the correction factor that gave the lowest sum of squares of errors was found by curve fitting. The results from the three correction factors are listed in Table 5.

TABLE 5

WALLIS MODEL WITH THREE CORRECTION FACTORS

Correction factor	1.148	1.1715	1.950
Average Deviation (percent)	4.14	2.05	0.00
Totas Sum of Squares of Errors $(kPa)^2$	1684.97	1566.34	1588.28

From these numbers, the parameters in the fitted curve estimated a correction factor of 1.180 to give the minimum total sum of squares of errors.

Appendix D

RESULTS FROM THE PREDICTIONS

TABLE 6

RESULTS FROM GHOSAL MODEL

Run no	ΔP_1 kPa	ΔP_2 kPa	ΔP_3 kPa	ΔP_4 kPa	Average Deviation %	Absolute Average Deviation %	Sum of Squares of Errors $(kPa)^2$	Reynolds number Re_f
1	5.70	11.53	17.52	23.74	-11.39	11.39	13.37	9877
2	9.15	18.61	28.42	38.58	-16.35	16.35	58.57	8844
11	8.32	17.03	26.03	35.48	-5.83	5.83	7.04	17426
18	19.64	41.11	64.31	90.19	-49.42	49.42	2002.0	19045
20	12.98	27.15	42.59	59.63	-32.42	32.42	495.8	30737
21	6.20	12.75	19.66	26.99	-17.65	17.65	34.33	32579
28	7.90	16.52	25.90	36.18	-42.22	42.22	209.5	40390
29	12.04	25.43	40.32	57.10	-35.38	35.38	492.6	39421
48	9.62	19.52	29.26	39.75	-34.42	34.42	170.6	9775
49	4.77	9.60	14.52	19.54	-43.28	43.28	62.77	13901
66	11.62	23.80	36.49	49.84	-36.34	36.34	357.2	32693
67	20.09	41.63	64.47	89.18	-71.75	71.75	2639.0	29351
80	26.17	54.96	86.80	122.67	-59.69	59.69	4029.0	38322
81	17.60	36.63	57.19	79.56	-62.91	62.91	1599.0	40449
82	8.22	16.89	25.99	35.59	-49.50	49.50	253.7	43262
88	21.83	47.04	76.18	110.40	-84.28	84.28	4728.0	79350
89	15.78	33.72	54.03	77.28	-63.97	63.97	1555.0	78148
90	13.63	28.93	46.03	65.29	-87.59	87.59	1800.0	73687
103	27.59	59.99	97.92	143.14	-79.53	79.53	7658.0	115666
104	23.44	50.86	82.78	120.50	-74.71	74.71	5107.0	115771
106	31.61	67.05	106.75	152.00	-78.94	78.94	9015.0	71311
107	19.91	41.55	64.97	90.56	-46.15	46.15	1665.0	75101

TABLE 6 continued

Run no	ΔP_1 kPa	ΔP_2 kPa	ΔP_3 kPa	ΔP_4 kPa	Average Deviation %	Absolute Average Deviation %	Sum of Squares of Errors $(kPa)^2$	Reynolds number Re_f
108	13.88	28.91	45.12	62.68	-11.14	11.14	121.9	79438
121	33.14	68.95	108.20	151.02	-54.03	54.03	5528.0	36777
122	20.69	42.65	65.86	90.65	-51.07	51.07	1791.0	41706
123	11.72	23.93	36.60	49.81	-24.25	24.25	223.7	44730
130	26.23	54.60	83.90	115.52	-73.65	73.65	4571.0	20774
131	18.19	37.17	57.08	77.96	-70.52	70.52	1944.0	30317
138	22.39	46.54	71.09	98.01	-75.90	75.90	3301.0	14545
139	14.60	29.73	45.33	61.45	-66.52	66.52	1125.0	20480
140	8.59	17.38	26.38	35.54	-30.25	30.25	107.6	24485
149	11.44	23.24	35.38	47.71	-54.64	54.64	538.7	22631
150	22.10	44.92	68.82	93.16	-59.19	59.19	2340.0	14866

TABLE 7

RESULTS FROM WALLIS MODEL

Run no	ΔP_1 kPa	ΔP_2 kPa	ΔP_3 kPa	ΔP_4 kPa	Average Error %	Absolute Average Error %	Sum of Squares of Errors $(kPa)^2$	Reynolds number Re_{fF}	Predicted Entrainment e
1	4.03	8.14	12.32	16.58	21.61	21.61	35.87	8563	0.133
2	5.78	11.71	17.78	24.00	27.05	27.05	143.2	5620	0.365
11	5.62	11.40	17.33	23.43	29.31	29.31	183.4	14817	0.150
18	11.08	22.66	34.71	47.30	18.78	18.78	143.1	9790	0.486
20	8.31	17.05	26.23	35.88	17.83	17.83	81.89	25461	0.172
21	4.02	8.21	12.57	17.12	24.55	24.55	54.23	32260	0.010
28	5.05	10.43	16.14	22.24	10.84	10.84	14.71	39853	0.013
29	7.77	16.11	25.05	34.64	15.33	15.33	52.36	36282	0.080
48	5.78	11.66	17.62	23.68	19.49	19.49	75.14	5799	0.407
49	3.24	6.53	9.85	13.21	2.75	2.75	0.47	12917	0.071
66	7.02	14.24	21.65	29.26	18.78	18.78	74.62	26645	0.185
67	11.05	22.51	34.37	46.66	7.85	7.85	24.10	16259	0.446
80	13.95	28.62	43.98	60.14	18.22	18.22	317.2	20133	0.475
81	9.89	20.25	31.08	42.39	10.74	10.74	81.97	26991	0.333
82	4.93	10.05	15.35	20.83	11.40	11.40	14.36	41962	0.030
88	11.92	24.86	38.80	53.87	4.75	4.75	12.30	65992	0.168
89	8.72	18.17	28.36	39.38	12.82	12.82	89.53	73399	0.061
90	7.59	15.75	24.50	33.91	-0.79	3.38	4.13	70654	0.041
103	13.74	28.78	45.02	62.69	16.08	16.08	218.5	93129	0.195
104	11.73	24.56	38.45	53.58	17.56	17.56	197.6	102591	0.114
106	15.92	32.82	50.67	69.60	14.10	14.10	147.3	40490	0.432
107	10.38	21.25	32.57	44.38	26.12	26.12	401.6	58542	0.220

TABLE 7 continued

Run no	ΔP_1 kPa	ΔP_2 kPa	ΔP_3 kPa	ΔP_4 kPa	Average Error %	Absolute Average Error %	Sum of Squares of Errors $(kPa)^2$	Reynolds number Re_{fF}	Predicted Entrainment e
108	7.27	14.91	22.90	31.28	43.18	43.18	943.4	74684	0.060
121	16.27	33.20	50.72	68.92	27.01	27.01	1122.0	14265	0.612
122	10.97	22.30	33.97	46.02	21.61	21.61	289.2	24312	0.417
123	6.63	13.44	20.40	27.53	30.52	30.52	231.3	38214	0.146
130	13.19	26.79	40.73	55.06	15.14	15.14	164.0	7358	0.646
131	9.80	19.86	30.15	40.70	9.50	9.50	35.58	16900	0.443
138	11.62	23.55	35.75	48.25	11.18	11.18	74.82	5016	0.655
139	8.08	16.31	24.69	33.21	8.97	8.97	20.18	11260	0.450
140	5.17	10.42	15.74	21.13	22.06	22.06	84.66	19940	0.186
149	6.52	13.15	19.88	26.72	12.72	12.72	27.09	14570	0.356
150	11.34	22.97	34.85	47.00	19.01	19.01	195.9	5244	0.647

TABLE 8

RESULTS FROM LEVY MODEL

Run no	ΔP_1 kPa	ΔP_2 kPa	ΔP_3 kPa	ΔP_4 kPa	Average Error %	Absolute Average Error %	Sum of Squares of Errors $(kPa)^2$	Dim.less Density exponent β	Predicted Entrainment e
1	3.94	7.96	12.05	16.23	23.37	23.37	41.89	4.845	0.454
2	6.90	14.05	21.43	29.08	12.26	12.26	27.03	4.015	0.499
11	5.31	10.80	16.44	22.27	33.01	33.01	229.6	4.701	0.461
18	14.12	29.27	45.40	62.75	-5.70	8.29	91.73	3.347	0.546
20	7.75	15.99	24.71	34.00	22.73	22.73	137.5	4.643	0.465
21	3.15	6.41	9.78	13.27	41.18	41.18	156.4	6.474	0.394
28	3.88	7.99	12.30	16.85	31.89	31.89	120.6	6.448	0.395
29	6.55	13.59	21.11	29.18	28.62	28.62	207.6	5.275	0.437
48	7.45	15.09	22.89	30.87	-4.38	4.38	1.45	3.409	0.541
49	3.10	6.24	9.42	12.63	7.03	7.03	2.16	4.743	0.459
66	7.00	14.25	21.71	29.43	18.66	18.66	72.17	4.077	0.496
67	13.54	27.85	42.85	58.70	-14.45	14.45	121.6	3.244	0.555
80	17.28	35.92	55.90	77.54	-3.34	3.34	27.12	3.164	0.563
81	10.70	22.04	33.97	46.60	2.66	3.72	13.75	3.773	0.516
82	4.23	8.60	13.11	17.77	24.22	24.22	62.49	5.295	0.435
88	11.25	23.61	37.10	51.92	9.18	9.18	39.66	4.151	0.493
89	7.52	15.67	24.44	33.91	24.86	24.86	279.5	4.842	0.457
90	6.41	13.29	20.62	28.48	15.11	15.11	32.12	5.104	0.445
103	13.27	27.94	44.01	61.74	18.19	18.19	270.2	3.773	0.518
104	10.80	22.70	35.52	49.62	23.85	23.85	375.7	4.122	0.495
	18.50	38.55	60.15	83.61	-1.53	5.58	52.91	3.099	0.569
107	10.67	21.96	33.84	46.38	23.42	23.42	309.4	3.668	0.523

TABLE 8 continued

Run no	ΔP_1 kPa	ΔP_2 kPa	ΔP_3 kPa	ΔP_4 kPa	Average Error %	Absolute Average Error %	Sum of Squares of Errors $(kPa)^2$	Dim.less Density exponent β	Predicted Entrainment e
108	6.65	13.63	20.94	28.60	48.06	48.06	1178.0	4.477	0.474
121	22.99	47.61	73.78	101.86	-5.49	5.49	101.4	2.604	0.619
122	13.18	26.96	41.32	56.33	4.92	4.92	11.39	3.142	0.564
123	6.66	13.50	20.53	27.74	30.12	30.12	223.7	3.926	0.505
130	20.27	41.70	64.16	87.88	-32.90	32.90	948.8	2.534	0.628
131	12.22	24.91	38.01	51.59	-13.81	13.81	79.45	3.063	0.571
138	18.31	37.58	57.66	78.73	-42.46	42.46	1023.0	2.528	0.628
140	10.34	20.97	31.87	43.06	-17.27	17.27	76.75	3.033	0.574
140	5.40	10.90	16.48	22.15	18.44	18.44	61.40	3.798	0.513
149	7.66	15.50	23.48	31.64	-2.96	2.96	2.18	3.362	0.545
150	17.74	36.34	55.68	75.91	-28.78	28.78	609.5	2.531	0.628

TABLE 9

RESULTS FROM MODIFIED WALLIS MODEL

Run no	ΔP_1 kPa	ΔP_2 kPa	ΔP_3 kPa	ΔP_4 kPa	Average Error %	Absolute Average Error %	Sum of Squares of Errors $(kPa)^2$
1	4.77	9.64	14.61	19.68	7.14	7.14	3.26
2	6.83	13.88	21.13	28.59	13.41	13.41	33.60
11	6.65	13.52	20.60	27.92	16.10	16.10	56.61
18	13.12	26.96	41.47	56.80	3.11	6.72	14.17
20	9.97	20.63	31.99	44.13	0.13	4.34	8.93
21	4.75	9.74	14.99	20.50	10.22	10.22	8.53
28	5.98	12.42	19.36	26.84	-6.58	6.58	4.88
29	9.21	19.23	30.10	41.95	-1.46	4.58	10.64
48	6.83	13.80	20.88	28.11	4.64	4.64	7.41
49	3.83	7.72	11.66	15.65	-15.03	15.03	7.06
66	8.30	16.88	25.73	34.87	3.59	3.59	1.61
67	13.08	26.74	40.97	55.83	-9.66	9.66	54.63
80	16.53	34.08	52.64	72.38	2.35	2.35	4.70
81	11.73	24.10	37.12	50.87	-6.45	6.45	7.74
82	5.84	11.93	18.27	24.89	-5.32	5.32	2.66
88	14.15	29.77	46.83	65.59	-14.53	14.53	144.6
89	10.35	21.73	34.18	47.85	-4.63	4.63	3.13
90	8.99	18.81	29.47	41.10	-20.85	20.85	123.5
103	16.34	34.54	54.54	76.71	-1.24	2.65	13.99
104	13.94	29.44	46.52	65.44	0.68	3.06	6.82
106	18.88	39.16	60.81	84.07	-2.83	5.94	63.04
107	12.30	25.28	38.91	53.25	11.92	11.92	69.73

TABLE 9 continued

Run no	ΔP_1 kPa	ΔP_2 kPa	ΔP_3 kPa	ΔP_4 kPa	Average Error %	Absolute Average Error %	Sum of Squares of Errors $(kPa)^2$
108	8.61	17.74	27.36	37.55	32.25	32.25	503.3
121	19.27	39.48	60.54	82.61	13.03	13.03	234.2
122	12.97	26.46	40.43	54.95	6.83	6.83	25.60
123	7.84	15.92	24.22	32.76	17.57	17.57	68.26
130	15.62	31.81	48.48	65.73	-0.88	1.21	2.79
131	11.59	23.54	35.82	48.47	-7.41	7.41	24.43
138	13.75	27.95	42.52	57.53	-5.51	5.51	14.83
139	9.55	19.31	29.28	39.46	-7.87	7.87	15.71
140	6.11	12.33	18.64	25.06	7.76	8.11	15.38
149	7.77	15.56	23.56	31.72	-3.36	3.36	2.57
150	13.42	27.25	41.43	56.01	3.83	3.83	4.64

Appendix E

RESULTS FROM CURVE FITTING

The plots of error against various variables in Figures 8 to 40 were fitted to two curves by the method of least squares. The equations for the two curves were:

$$\epsilon = a + b\chi \tag{59}$$

for the two-parameter curve and

$$\epsilon = a + b\chi + c\chi^2 \tag{60}$$

for the three-parameter curve.

For each curve, the parameters and the regression coefficient R were calculated. The values of the parameters and the regression coefficient are shown in Tables 10 to 13. A small value of the regression coefficient indicates that the error is almost randomly distributed with respect to the given parameter. Hence, the model apparently accounts for the effect of this parameter properly. In Figures 8 to 37 the three parameter curve (Equation 60) is drawn to indicate any trend. To avoid crowding these figures, the straight line (Equation 59) is not plotted.

TABLE 10

CURVE FITTING FOR GHOSAL MODEL

Variable parameter	No. of parameters	a	b	c	R
π	2	-33.3040	-3.8132	-	0.143
π	3	-30.3608	-5.1562	0.1214	0.143
x	2	-48.5044	-8.69083	-	0.003
x	3	-59.5627	131.8881	-278.8843	0.066
G	2	-30.1021	-0.0256	-	0.229
G	3	-24.0147	-0.0413	0.0000	0.223
F	2	-33.511	-2.6651	-	0.132
F	3	-32.7073	-2.9253	0.0169	0.132
X	2	-46.3395	-7.4567	-	0.19
X	3	-57.4856	47.1236	-37.9856	0.088
P *)	2	-7.1666	-6.5337	-	0.212
P *)	3	177.7752	-69.9705	5.0672	0.384
Re_f	2	-36.4619	-0.0003	-	0.171
Re_f	3	-36.5584	-0.0003	-0.0000	0.171

*) - The pressure has to be given in Bar.

TABLE 11

CURVE FITTING FOR WALLIS MODEL

Variable parameter	No. of parameters	a	b	c	R
Π	2	17.5526	-0.0903	-	0.001
Π	3	16.9237	0.1966	-0.0260	0.001
x	2	17.2022	-0.2567	-	0.000
x	3	16.1554	13.0500	-26.3982	0.004
G	2	17.8645	-0.0009	-	0.002
G	3	18.2951	-0.0020	0.0000	0.002
F	2	17.5603	-0.0652	-	0.001
F	3	17.1030	0.0828	-0.0096	0.001
X	2	16.9863	0.3280	-	0.000
X	3	16.5423	2.5023	01.5132	0.001
P *)	2	14.6823	0.3757	-	0.005
P *)	3	103.9756	-30.2500	2.4465	0.278
Re_{fF}	2	17.1913	-0.0000	-	0.000
Re_{fF}	3	17.5361	-0.0000	0.0000	0.000

*) - The pressure has to be given in Bar.

TABLE 12

CURVE FITTING FOR LEVY MODEL

Variable parameter	No. of parameters	a	b	c	R
π	2	45.9232	-8.4172	-	0.806
π	3	54.1943	-12.1912	0.3413	0.814
x	2	31.7310	-121.7511	-	0.658
x	3	31.6199	-120.3392	-2.8008	0.658
G	2	-3.9235	0.0162	-	0.106
G	3	-6.5071	0.0229	-0.0000	0.107
F	2	46.8340	-6.1022	-	0.805
F	3	54.3385	-8.5309	0.1574	0.811
X	2	-6.8447	29.7806	-	0.355
X	3	-19.4582	93.4858	-44.3362	0.464
P *)	2	43.2968	-5.2521	-	0.159
P *)	3	115.6972	-30.0861	1.9837	0.190
β	2	-57.8584	16.7560	-	0.651
β	3	-155.6128	65.0792	-5.6023	0.767
e	2	157.0601	-288.4916	-	0.749
e	3	-62.9807	574.8856	-834.1401	0.781

The Levy model yielded also a correlation for entrainment vs. dimensionless vapor velocity. A curve fitting for this relationship gave the following coefficients and regression coefficients.

2	0.3977	0.0263	-	0.879
3	0.3363	0.0544	-0.0025	0.925

It has to be noted that this is not an experimental result, but rather calculated data for the experimental conditions.

*) - The pressure has to be given in Bar.

TABLE 13

CURVE FITTING FOR MODIFIED WALLIS MODEL

Variable parameter	No. of parameters	a	b	c	R
Π	2	2.1921	-0.2698	-	0.003
Π	3	-0.4992	0.9582	-0.1111	0.006
x	2	1.1662	-0.8770	-	0.000
x	3	-0.7243	23.1556	-47.6766	0.009
G	2	2.4452	-0.0018	-	0.005
G	3	3.2444	-0.0039	0.0000	0.006
F	2	2.2102	-0.1938	-	0.003
F	3	-0.3634	0.6391	-0.0540	0.006
X	2	0.9462	0.1667	-	0.000
X	3	-0.0219	4.8471	-3.2991	0.002
P *)	2	-1.4188	0.3678	-	0.003
P *)	3	102.3113	-35.2125	2.8421	0.251
Re_{fF}	2	1.3054	-0.0000	-	0.000
Re_{fF}	3	1.3805	-0.0000	0.0000	0.001

*) - The pressure has to be given in Bar.

Appendix F

PLOTS OF THE PREDICTIONS

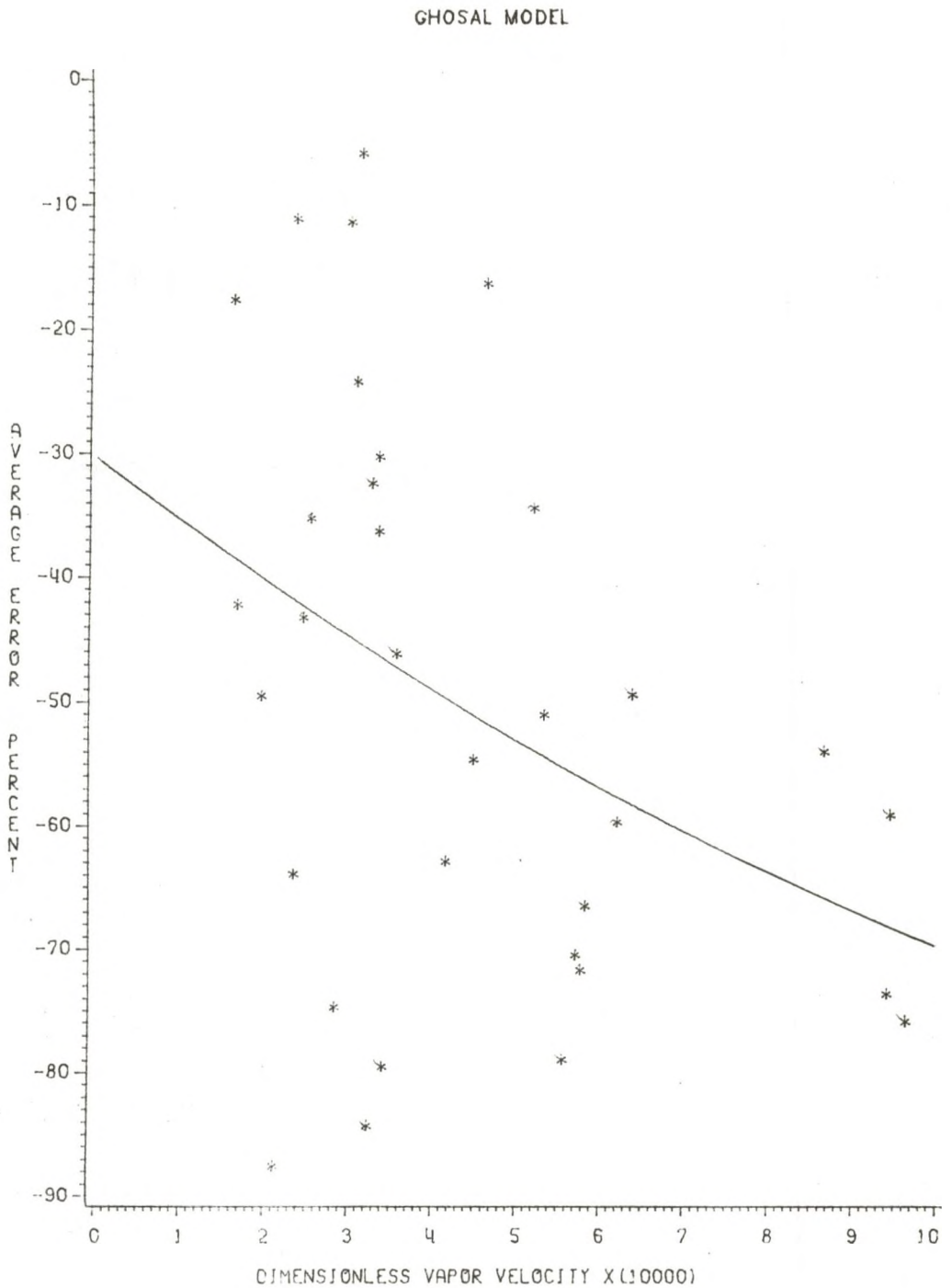

Figure 8: Average error vs. dimensionless vapor velocity.

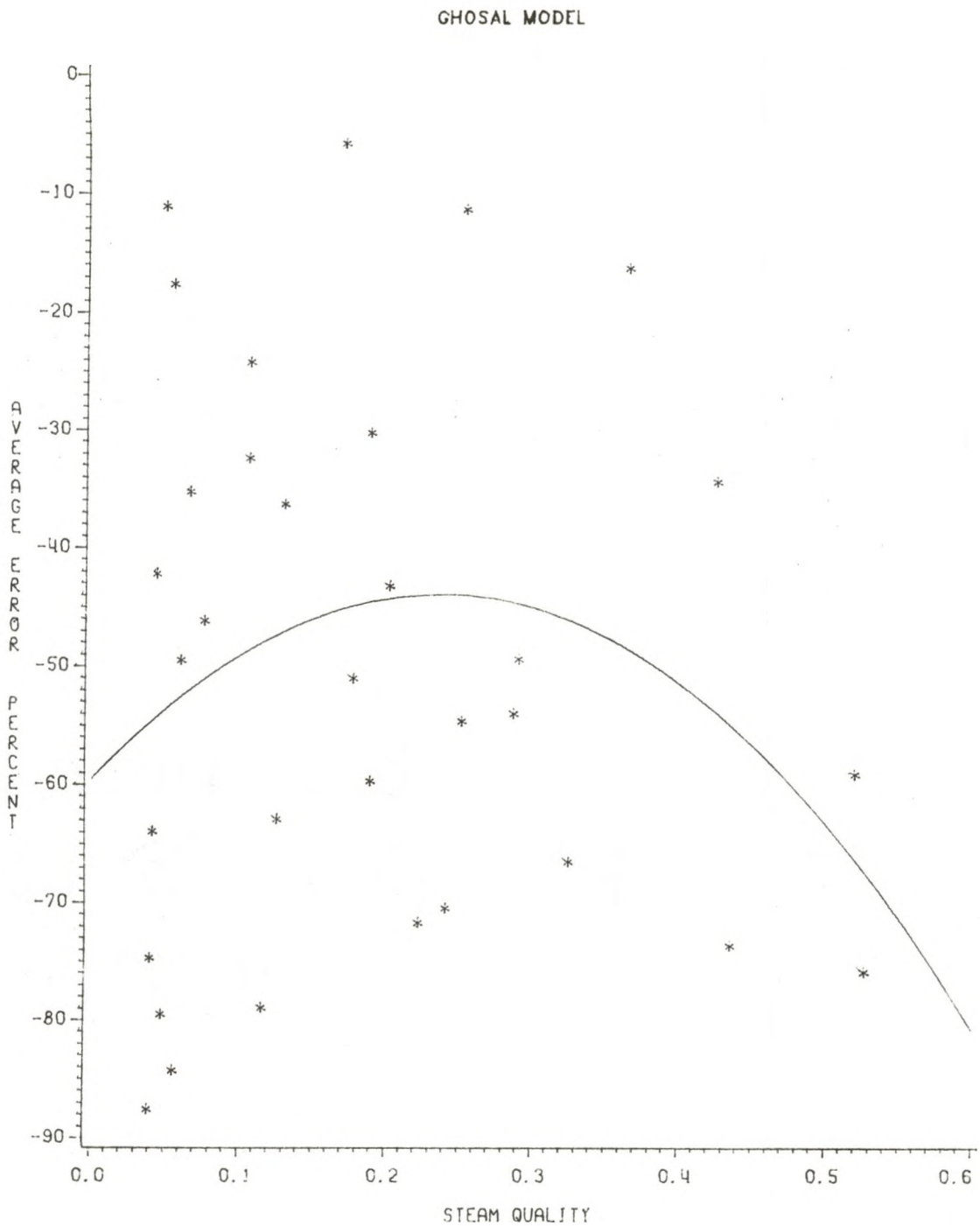

Figure 9: Average error vs. steam quality.

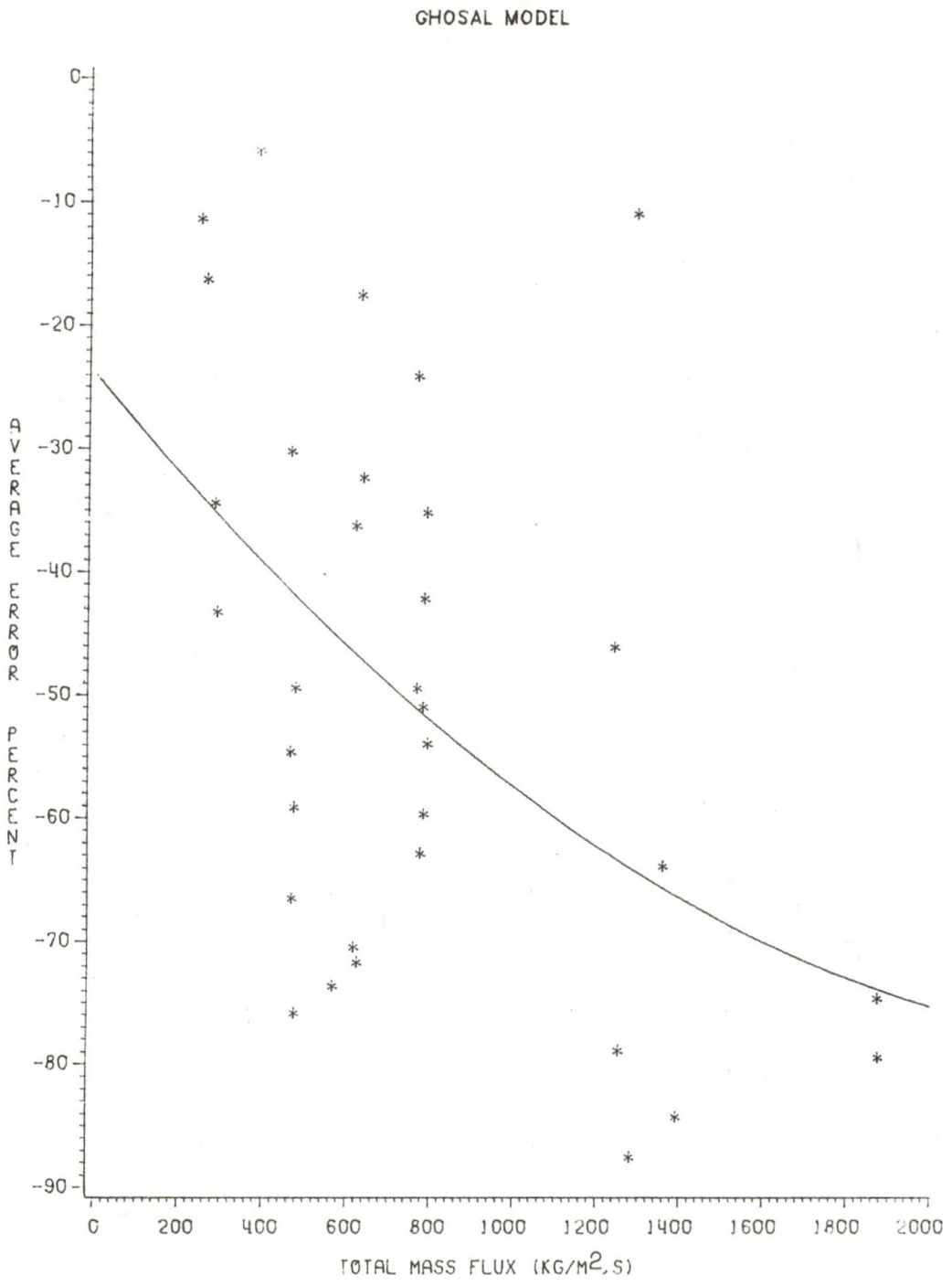

Figure 10: Average error vs. total mass flux.

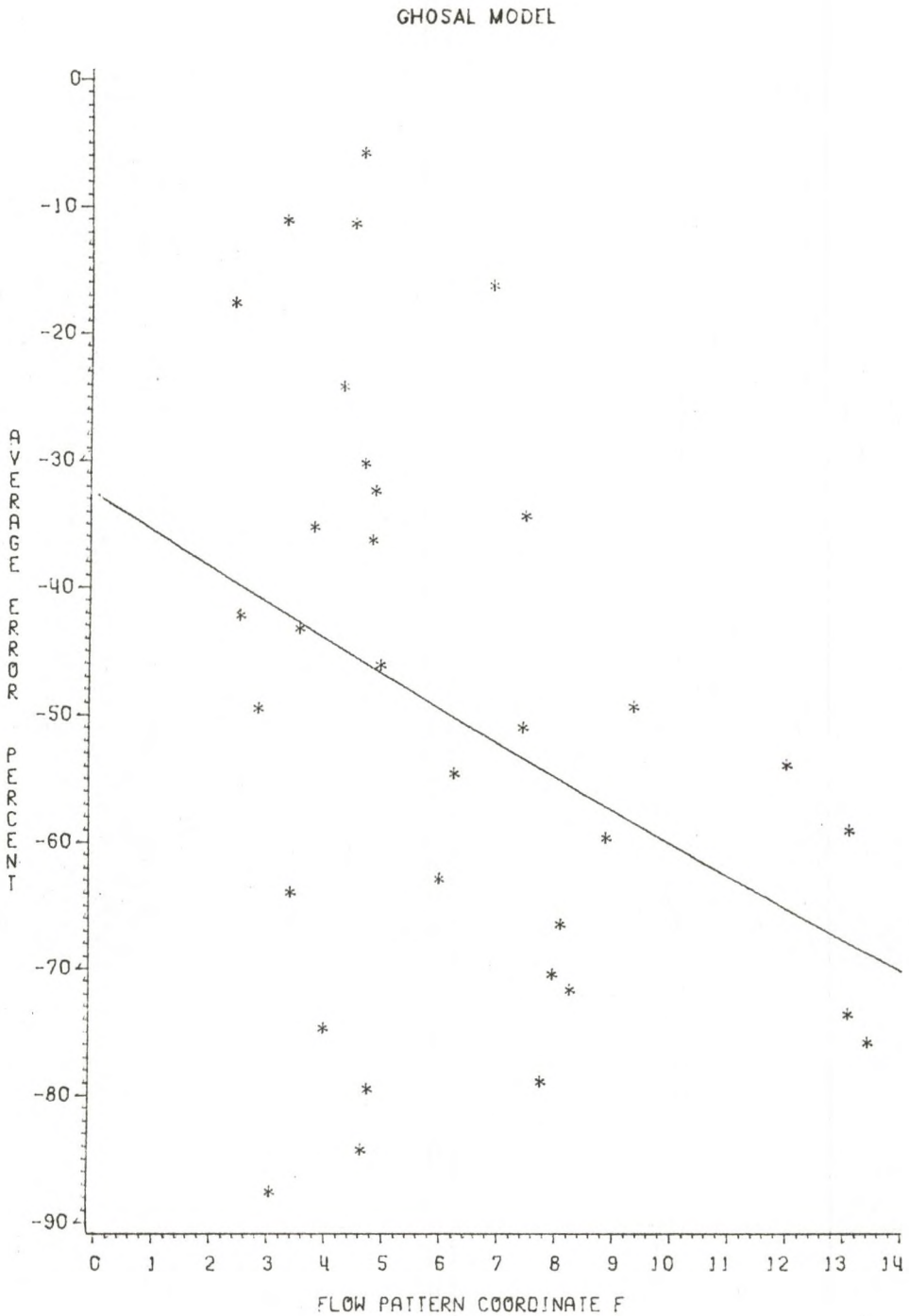

Figure 11: Average error vs. flow pattern coordinate F.

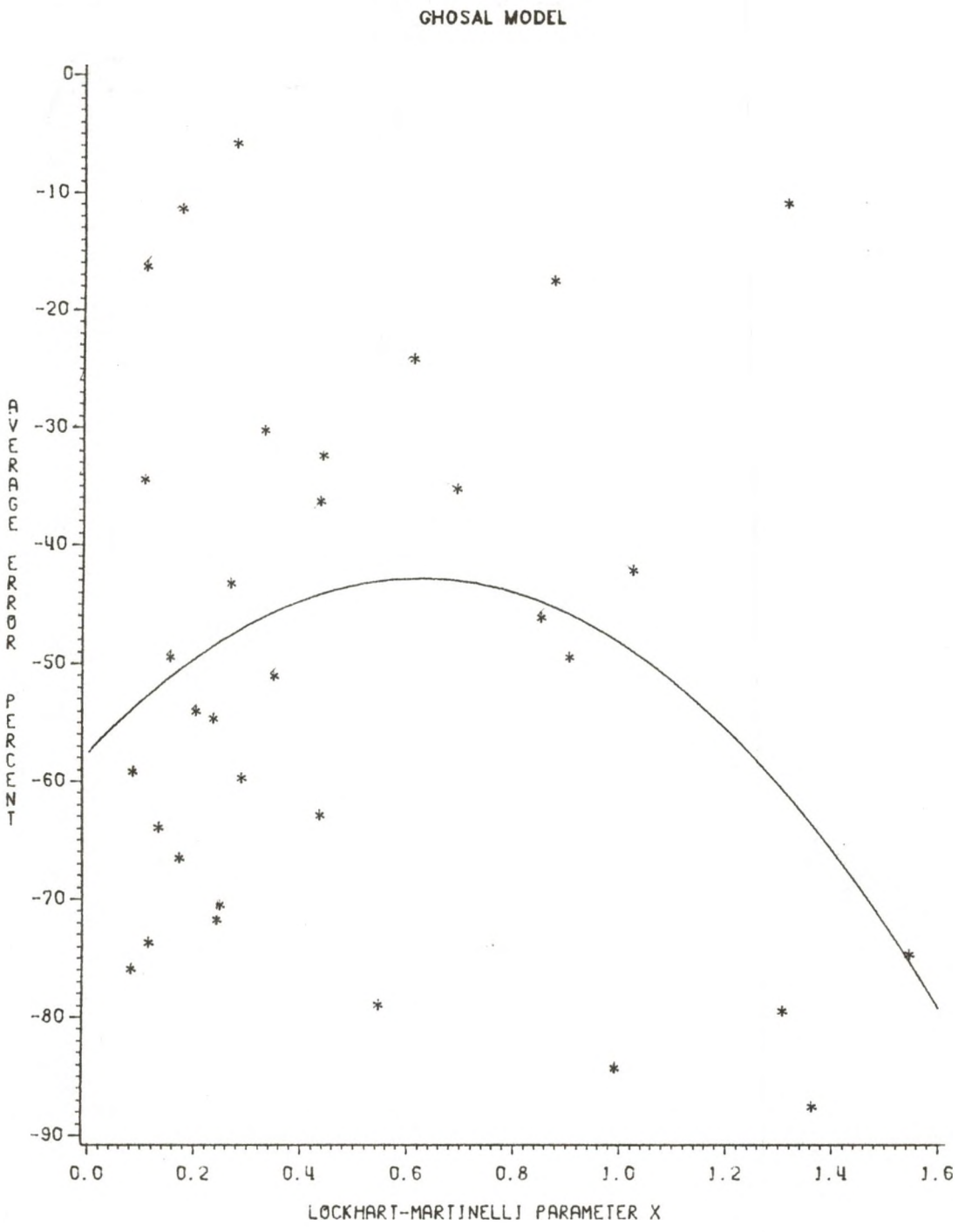

Figure 12: Average error vs.
Lockhart-Martinelli parameter X.

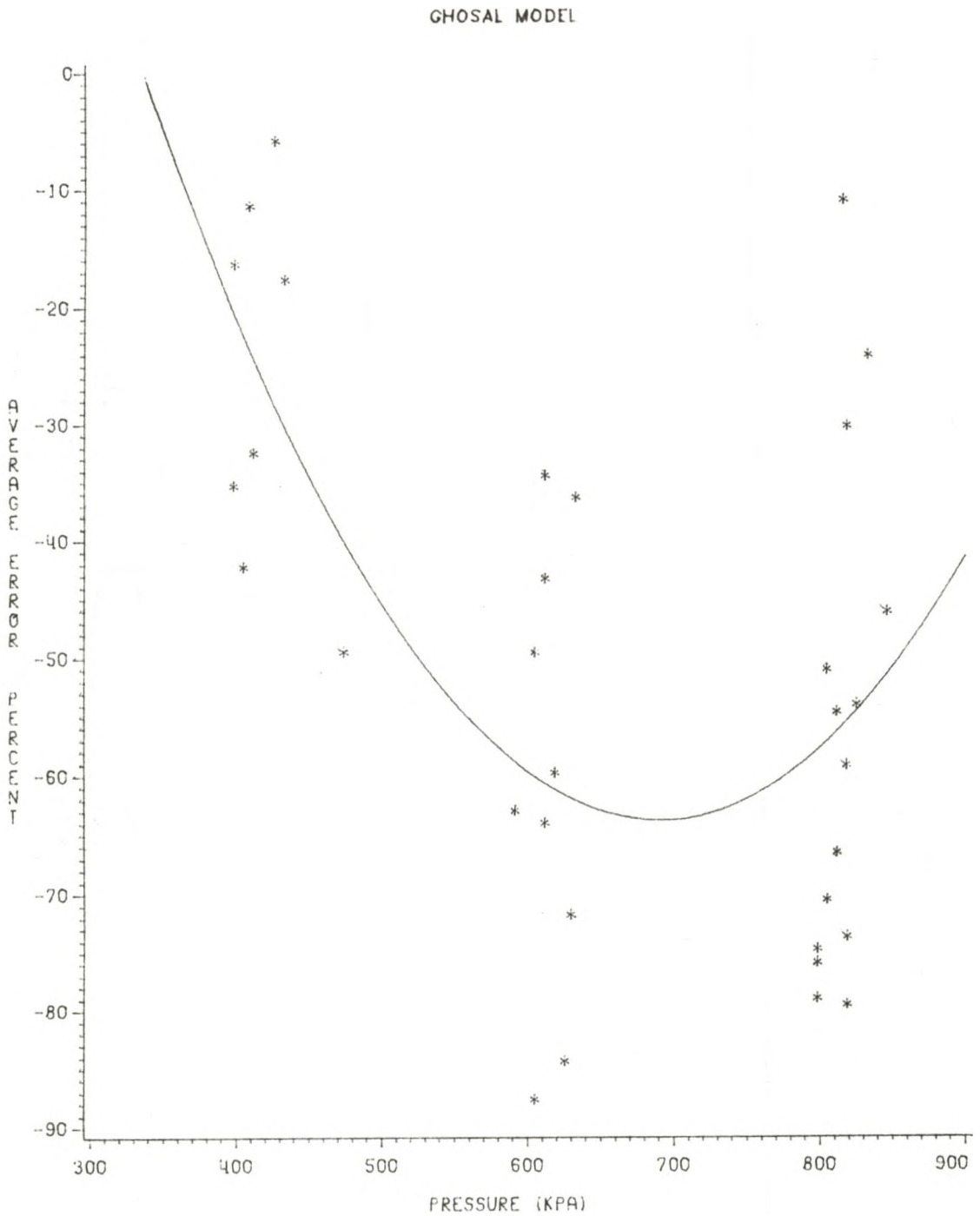

Figure 13: Average error vs. pressure.

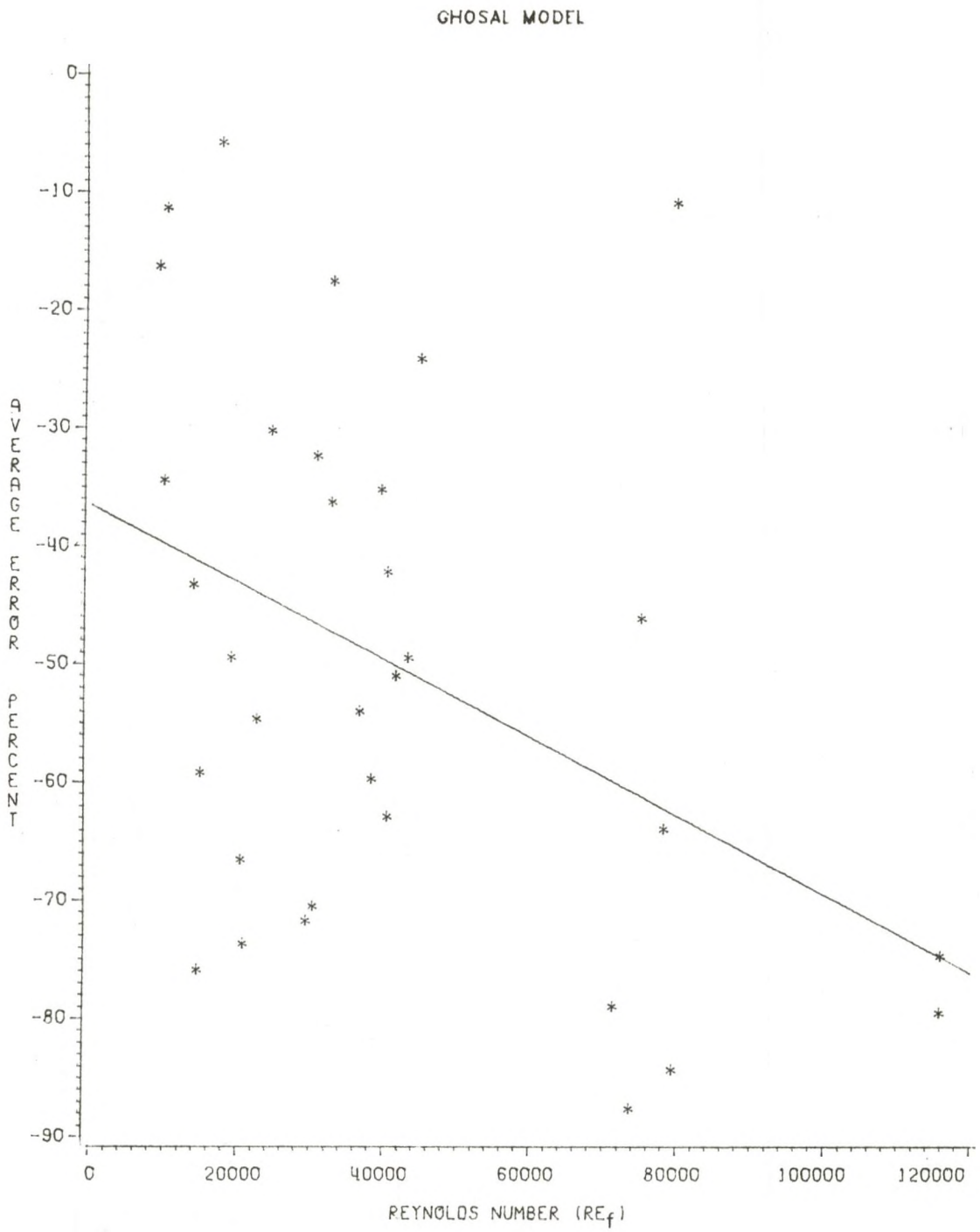

Figure 14: Average error vs. Reynolds number.

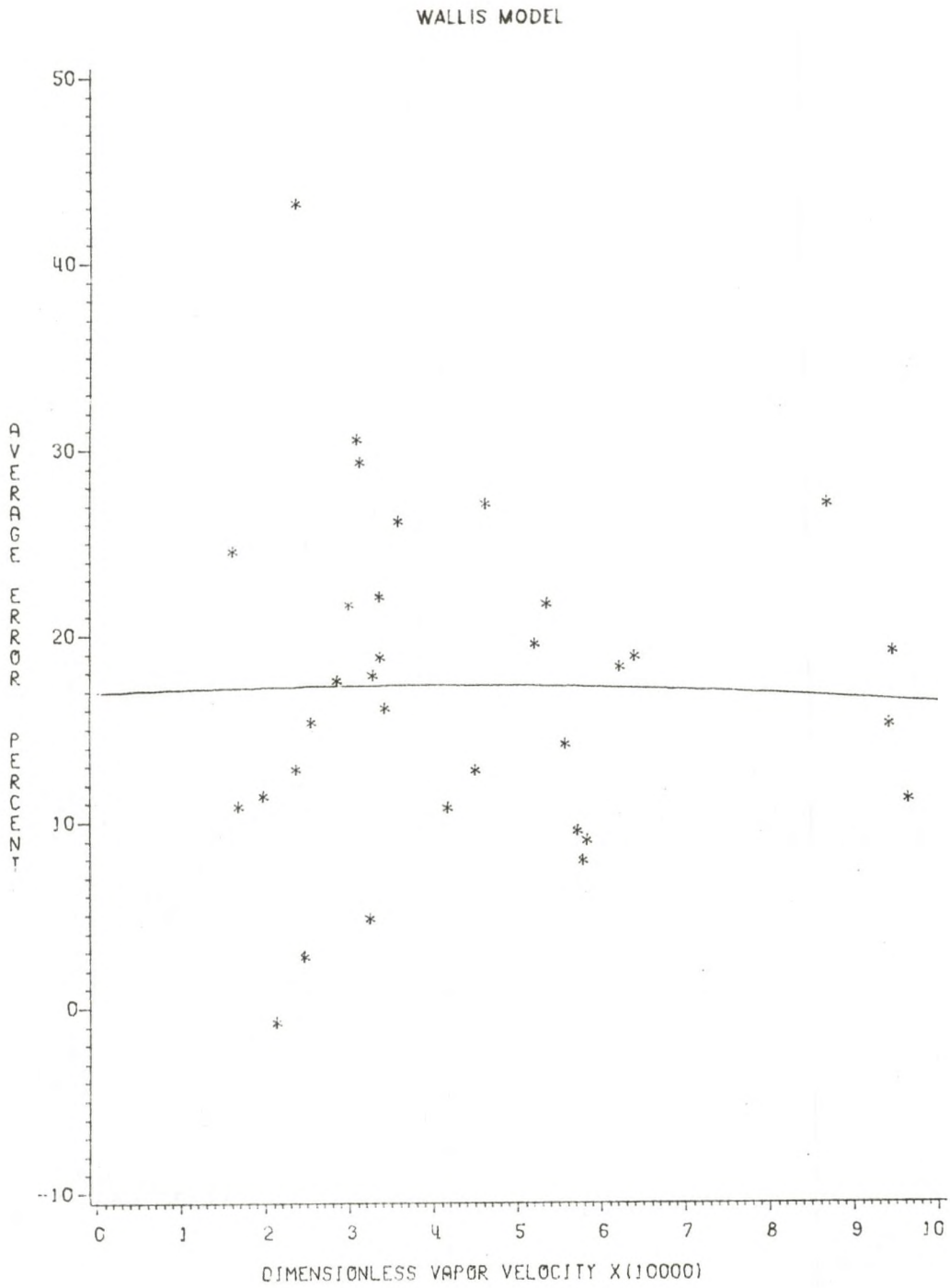

Figure 15: Average error vs. dimensionless vapor velocity.

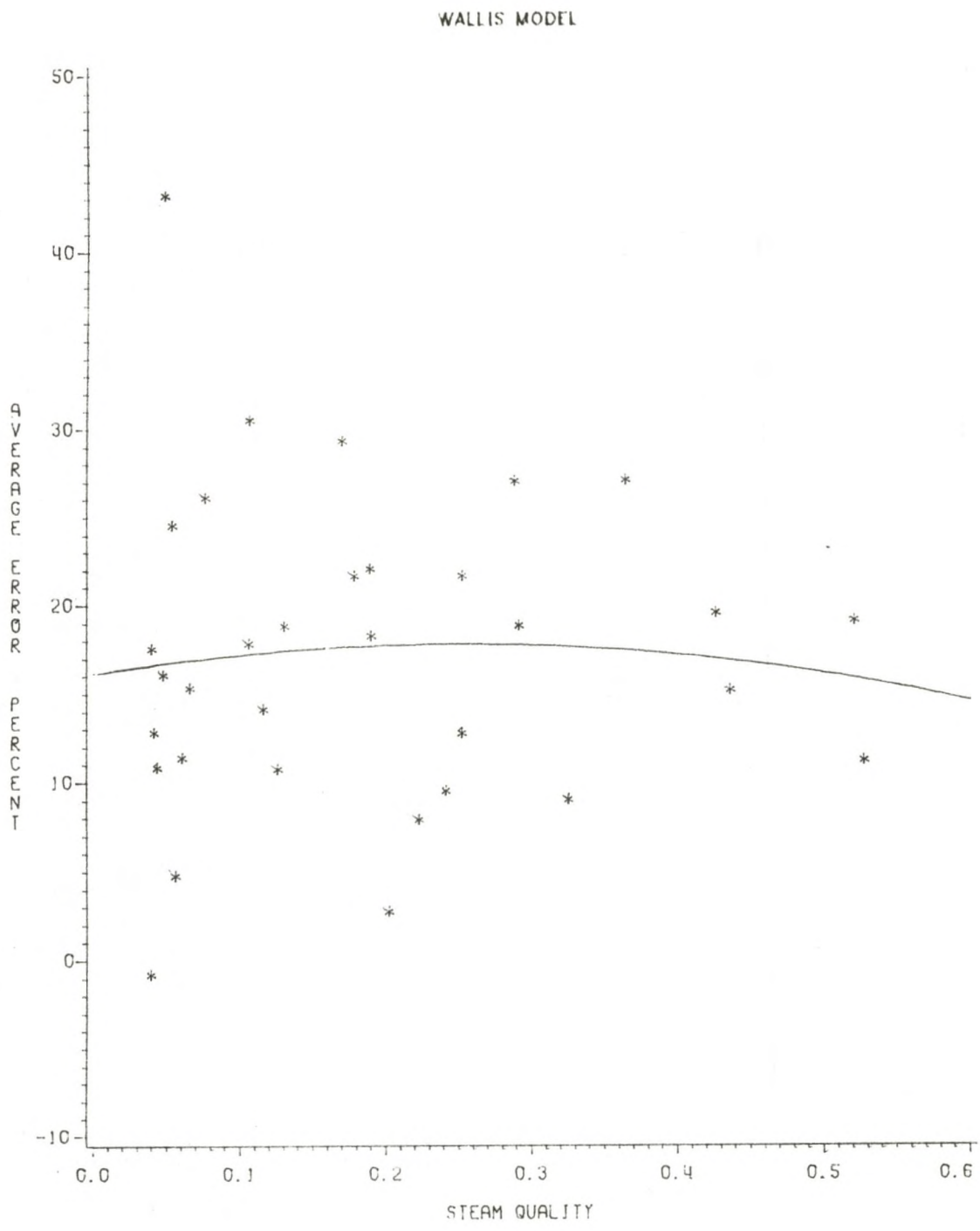

Figure 16: Average error vs. steam quality.

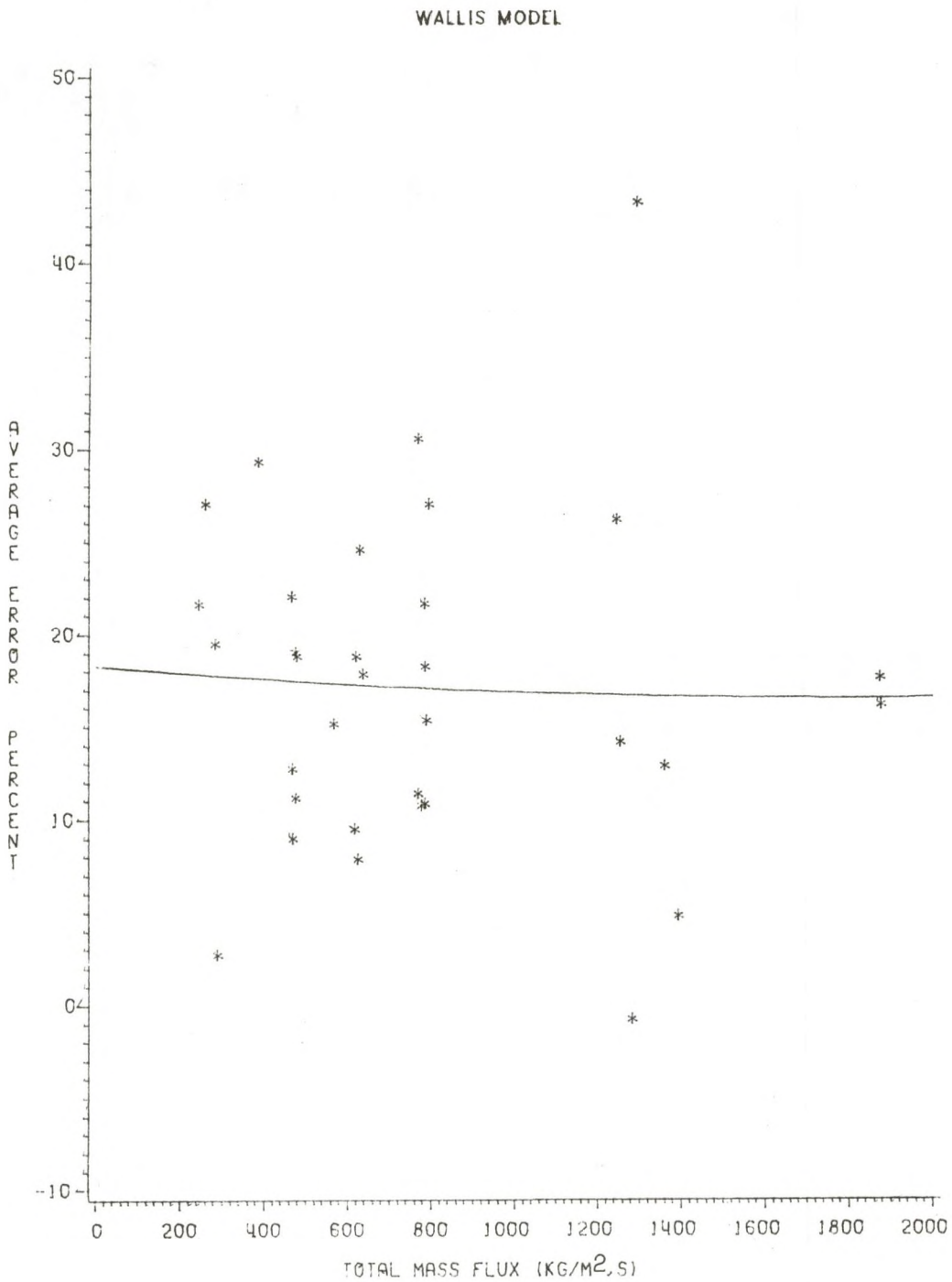

Figure 17: Average error vs. total mass flux.

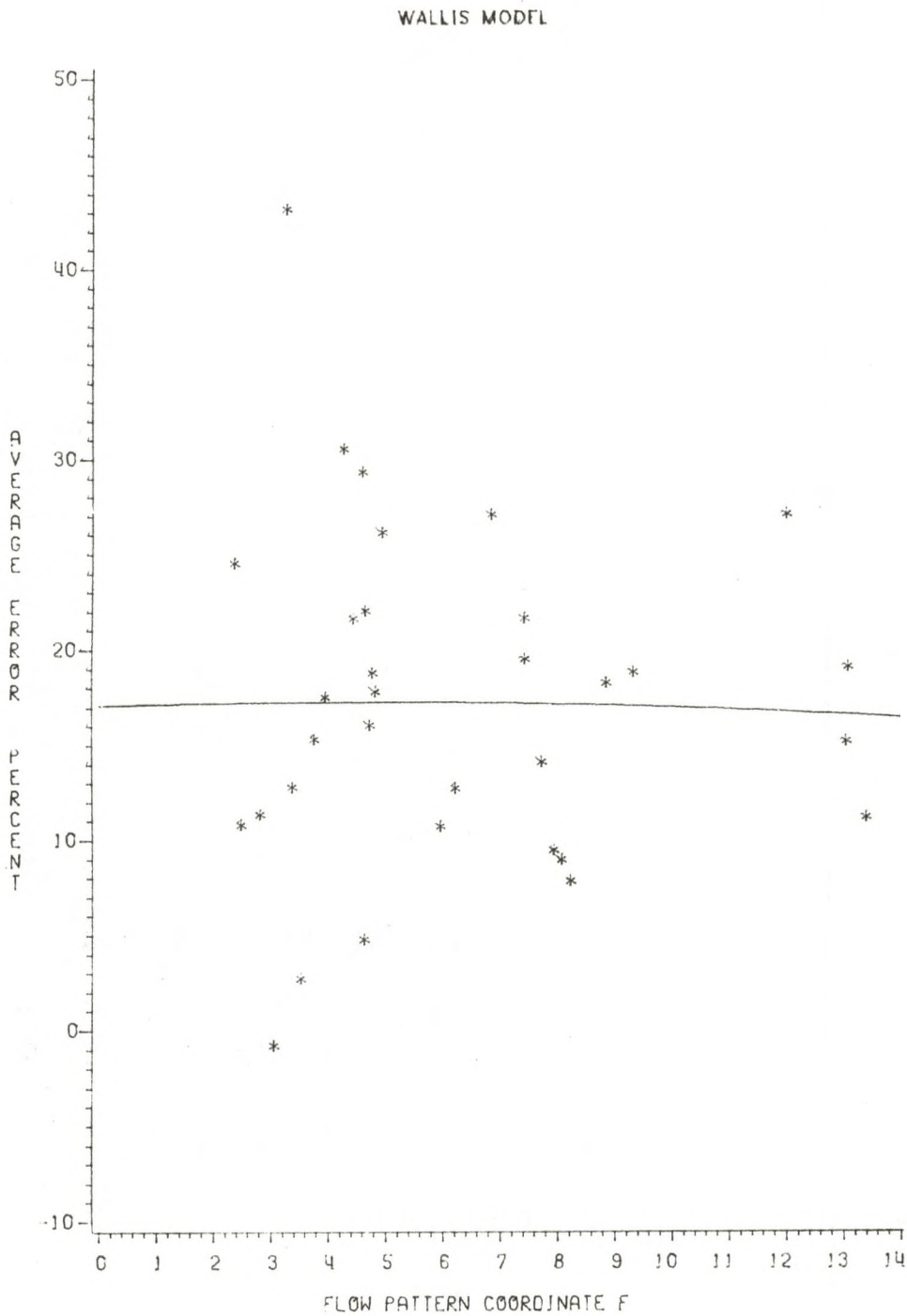

Figure 18: Average error vs. flow pattern coordinate F.

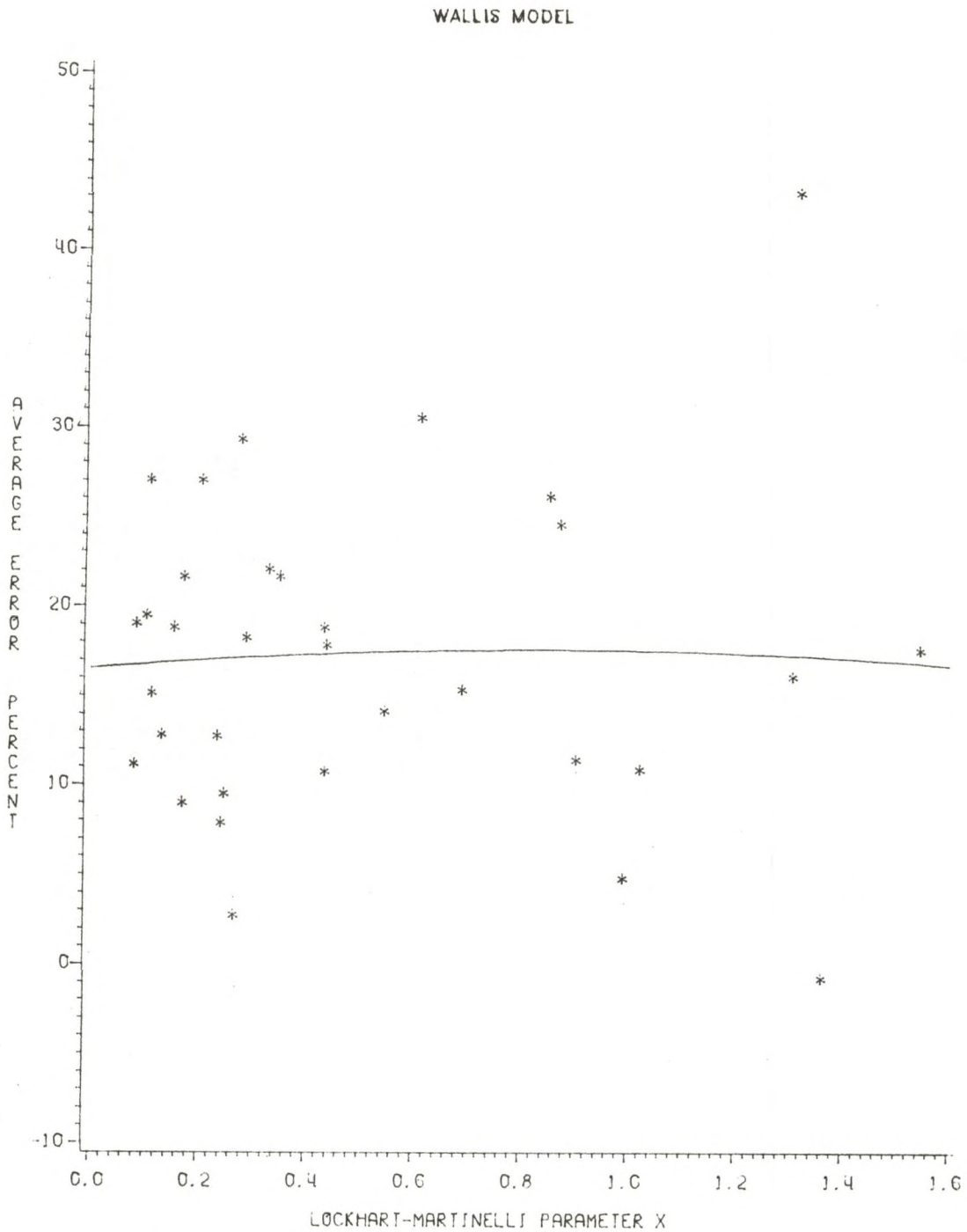

Figure 19: Average error vs.
Lockhart-Martinelli parameter X.

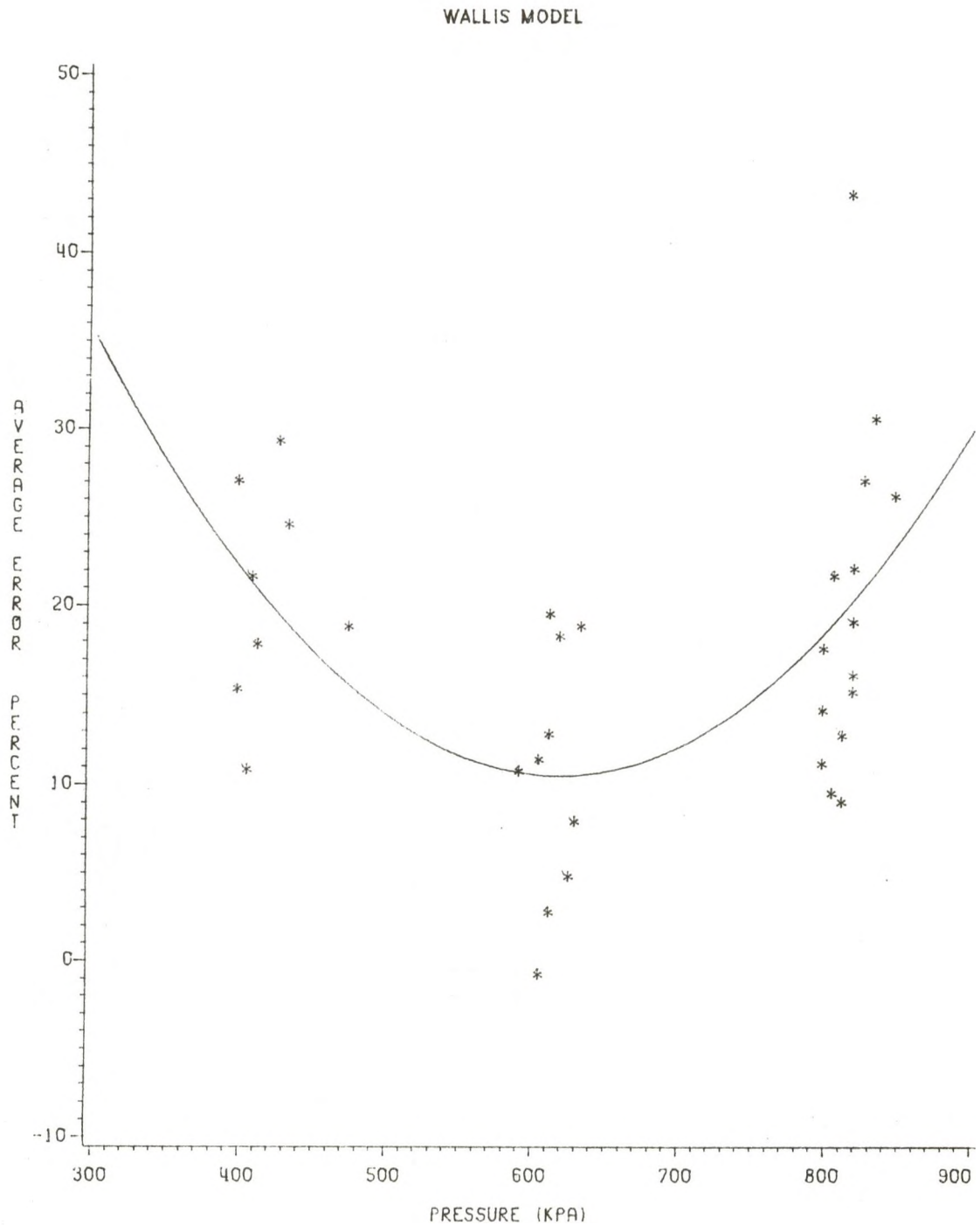

Figure 20: Average error vs. pressure.

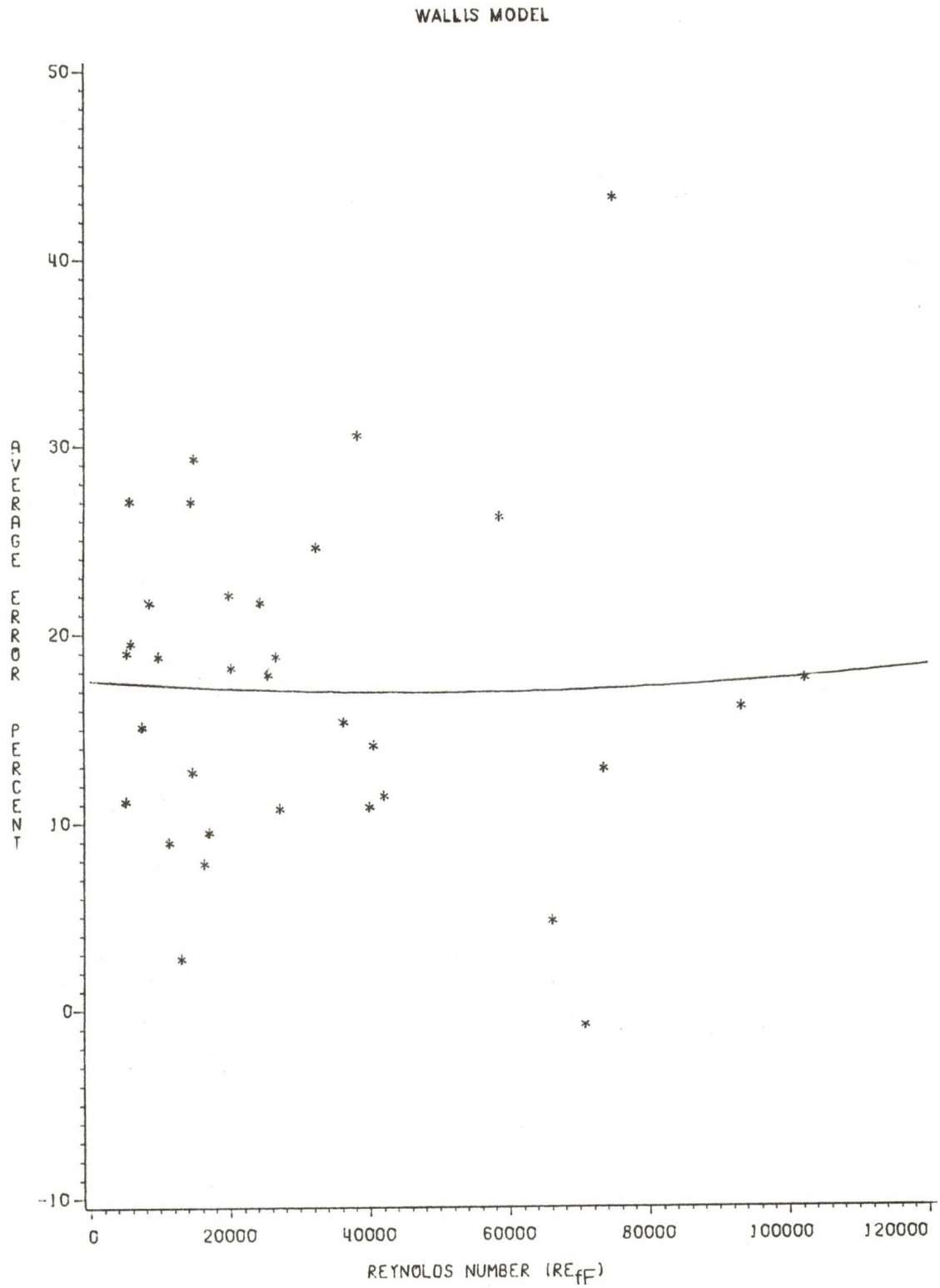

Figure 21: Average error vs. Reynolds number.

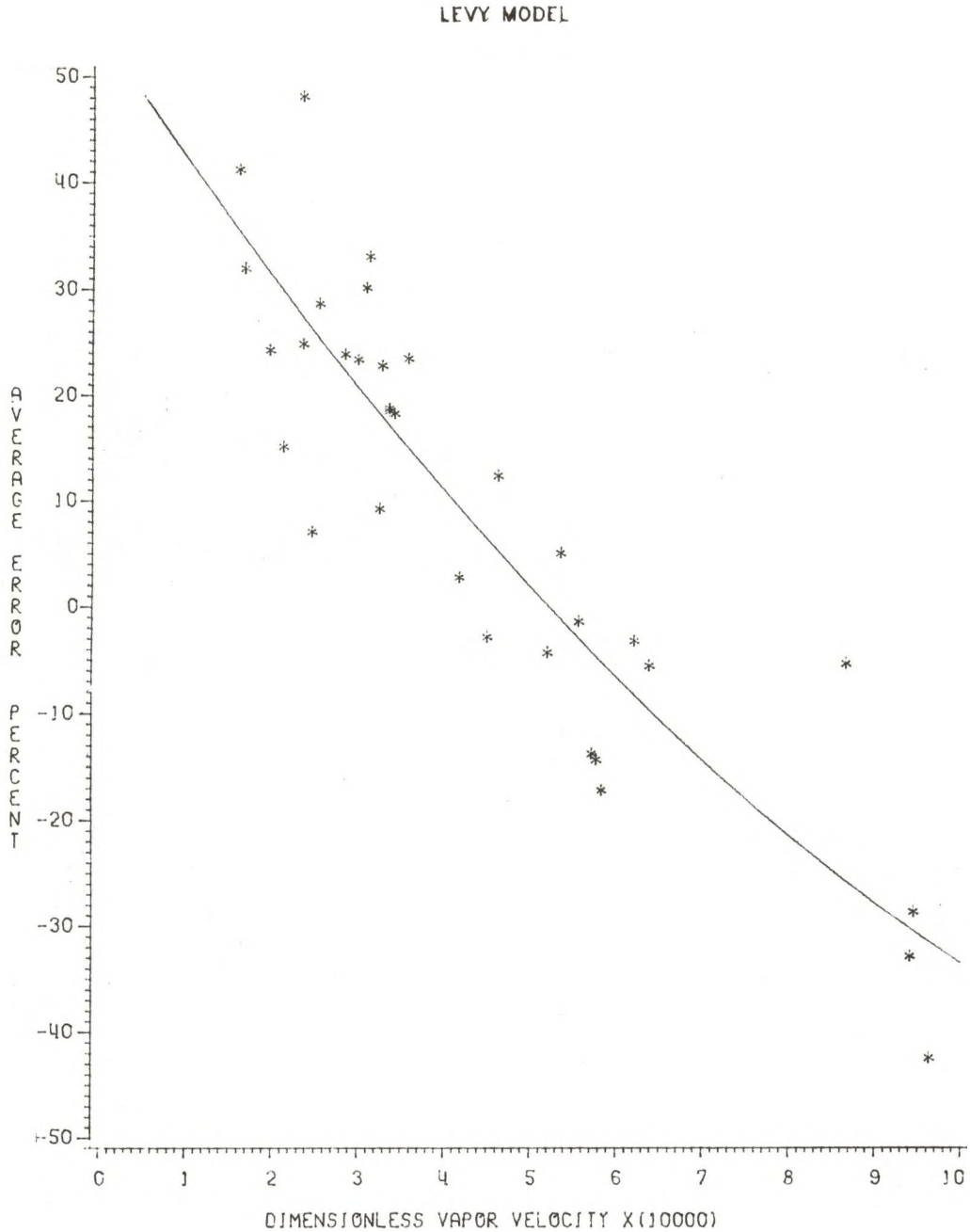

Figure 22: Average error vs. dimensionless vapor velocity.

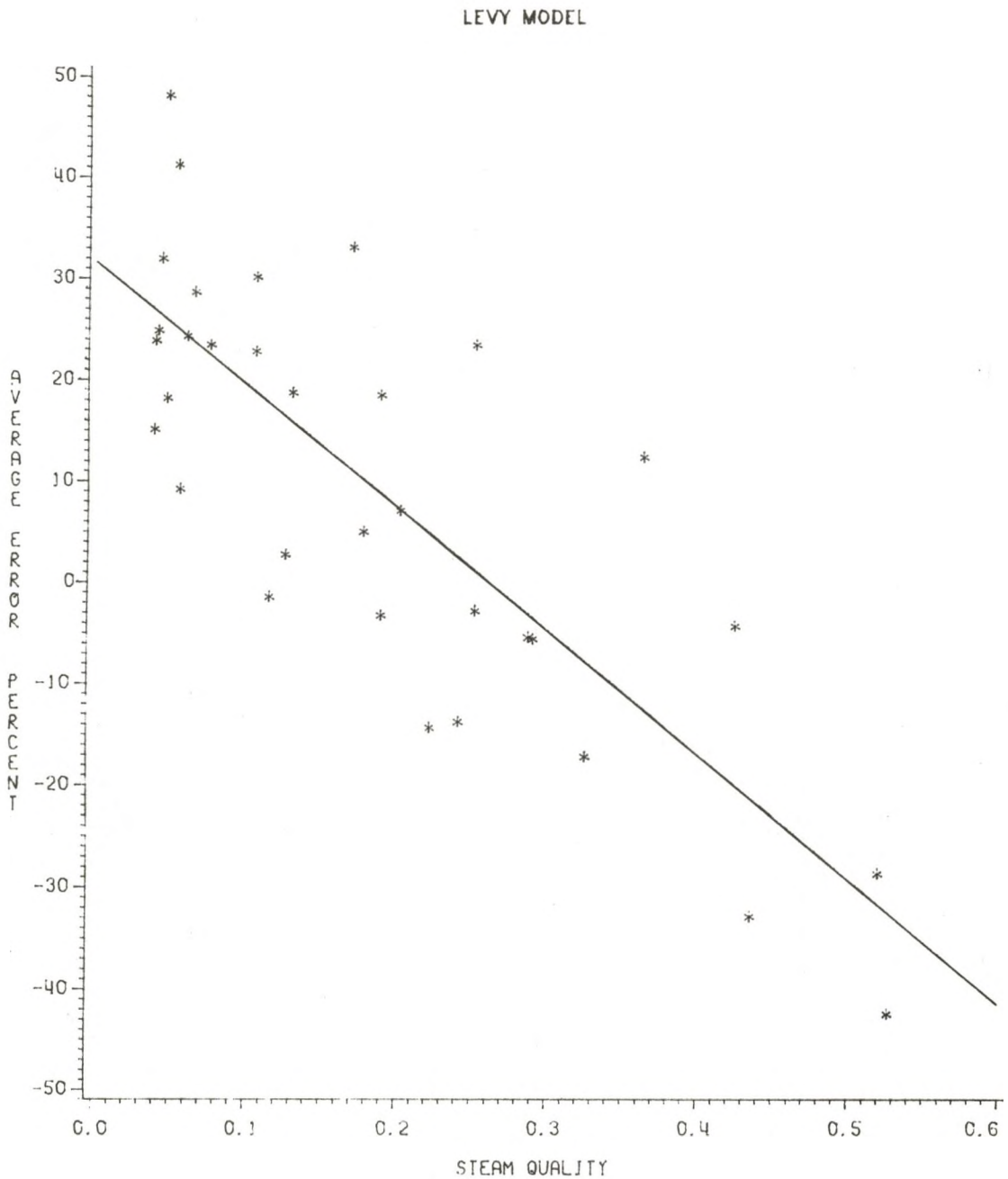

Figure 23: Average error vs. steam quality.

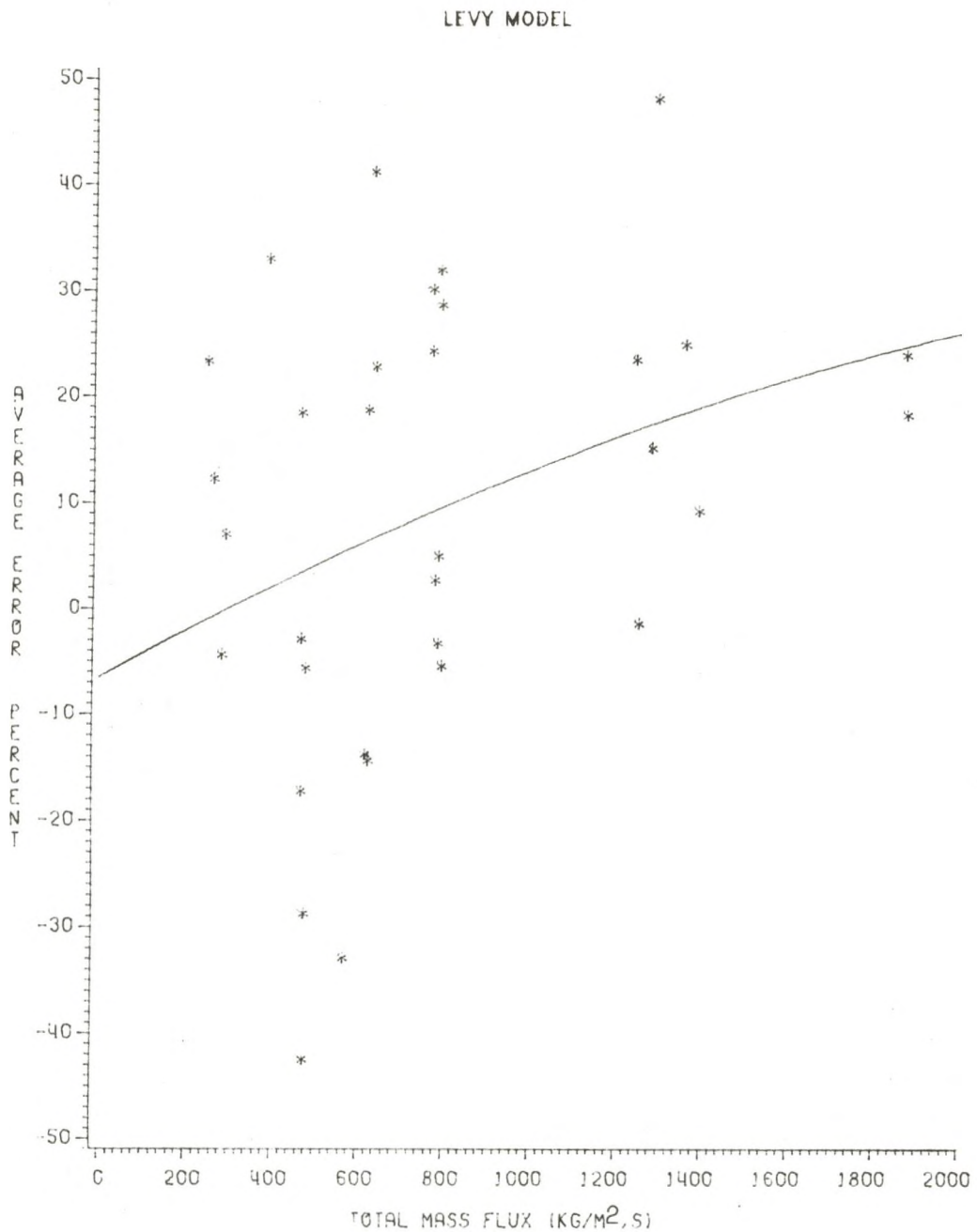

Figure 24: Average error vs. total mass flux.

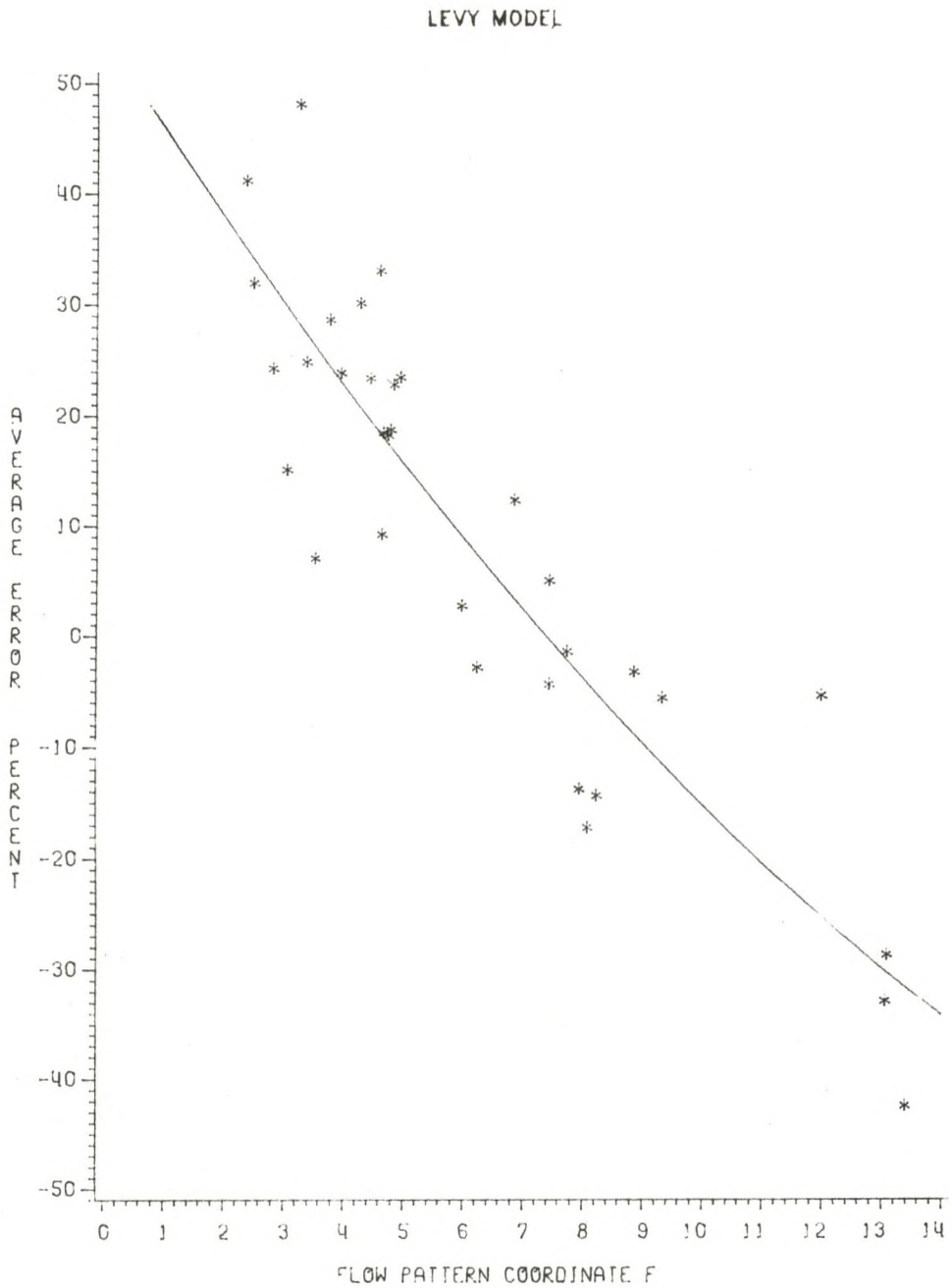

Figure 25: Average error vs. flow pattern coordinate F.

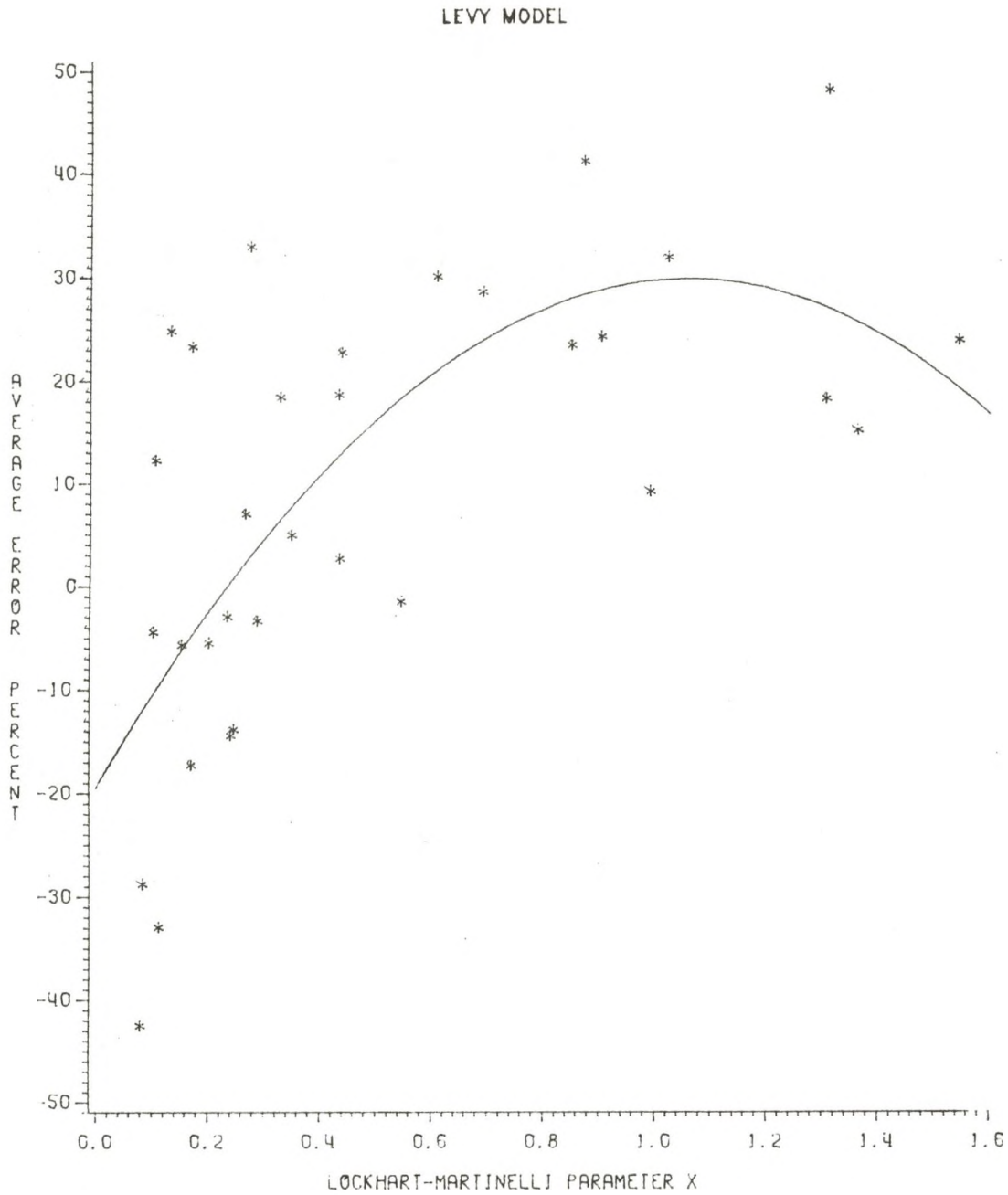

Figure 26: Average error vs.
Lockhart-Martinelli parameter X.

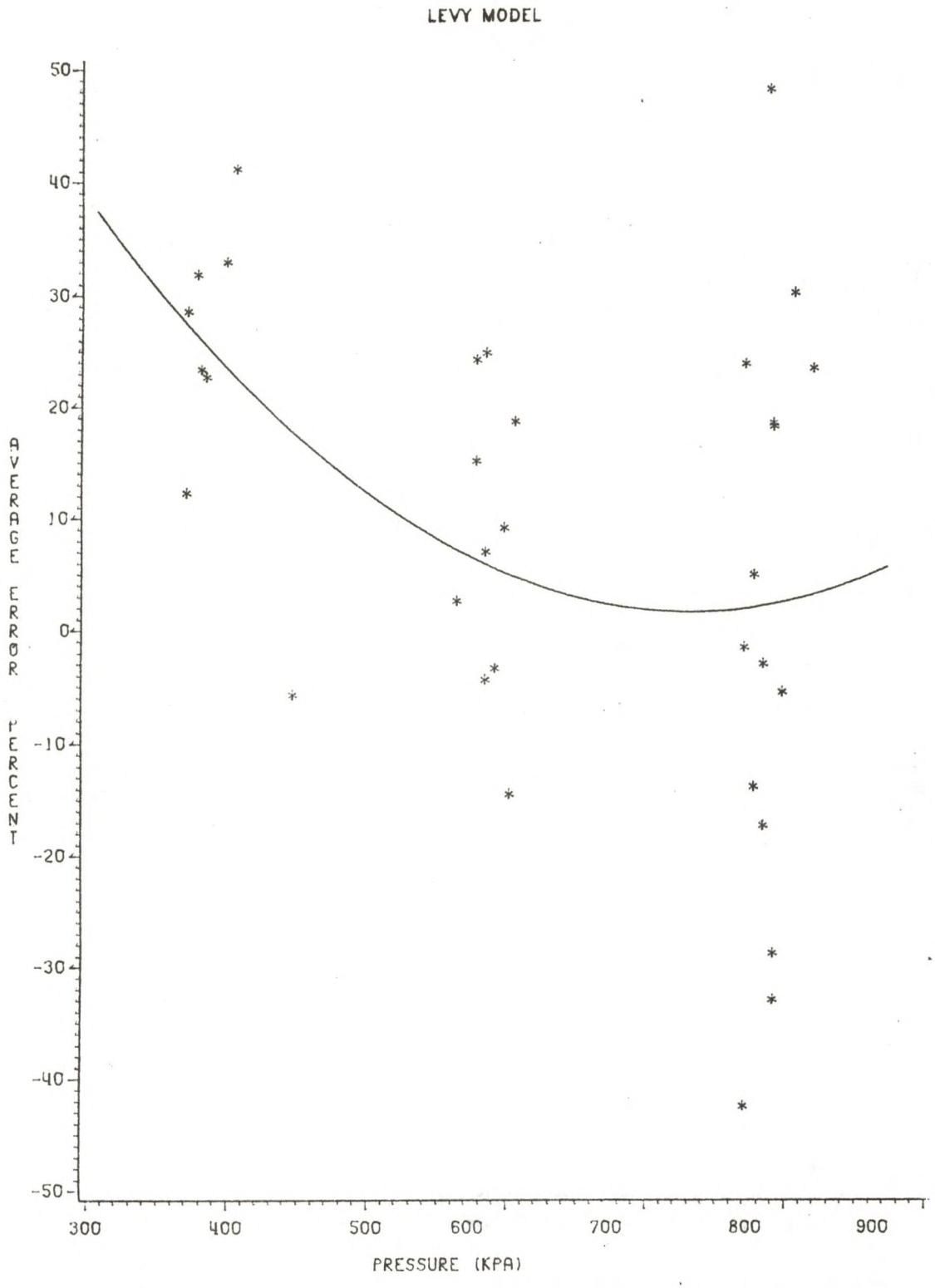

Figure 27: Average error vs. pressure.

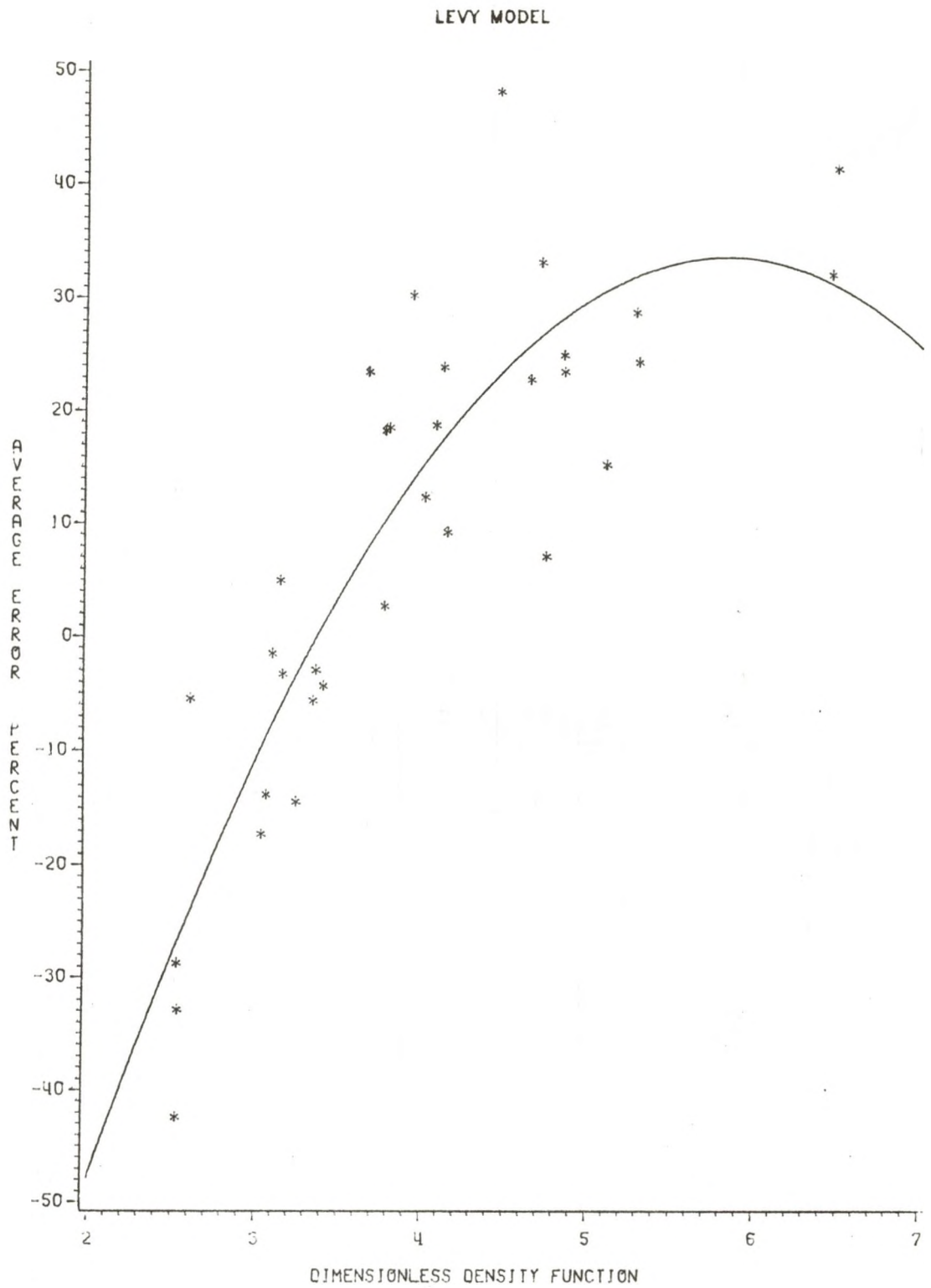

Figure 28: Average error vs. dimensionless density function.

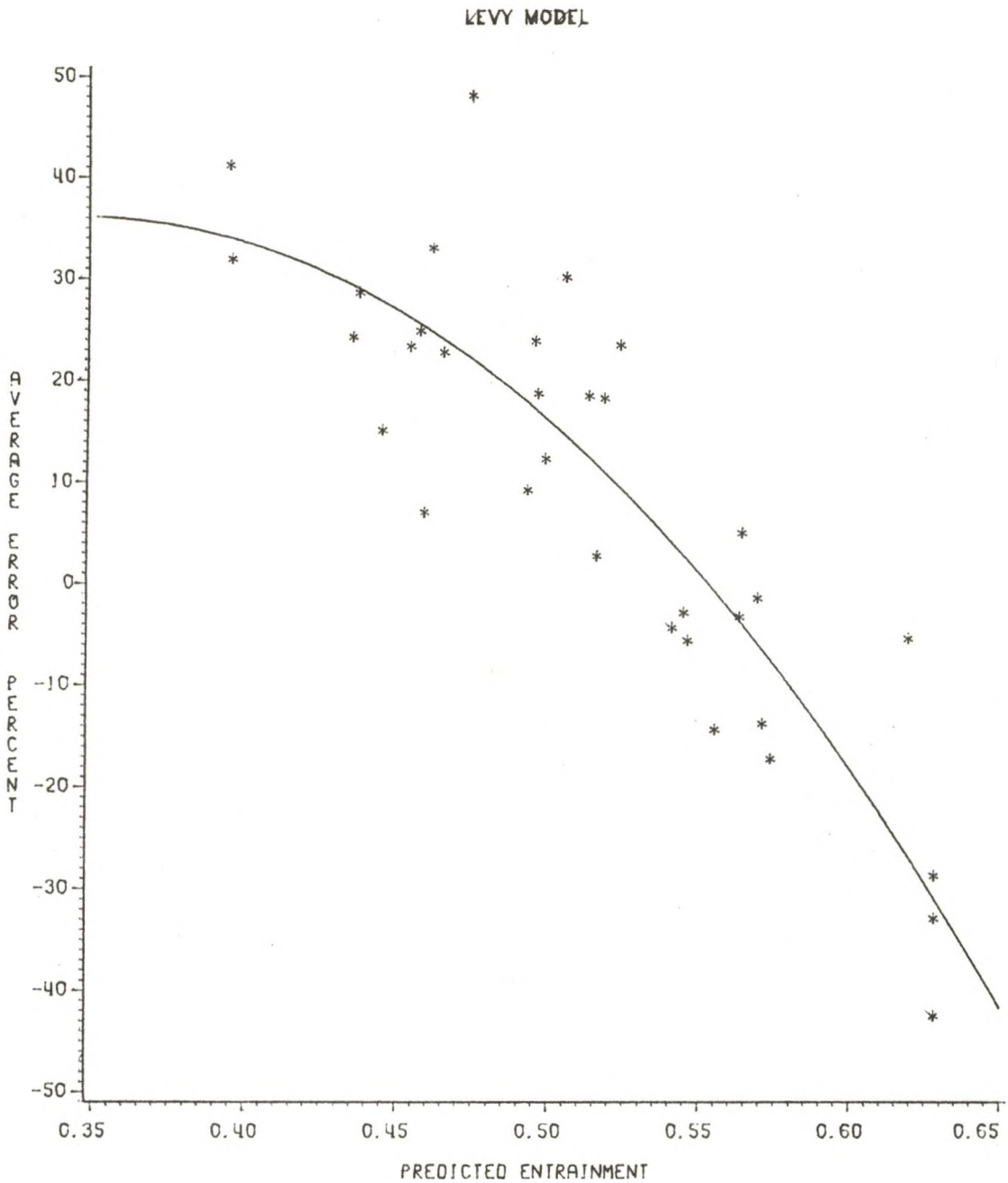

Figure 29: Average error vs. predicted entrainment.

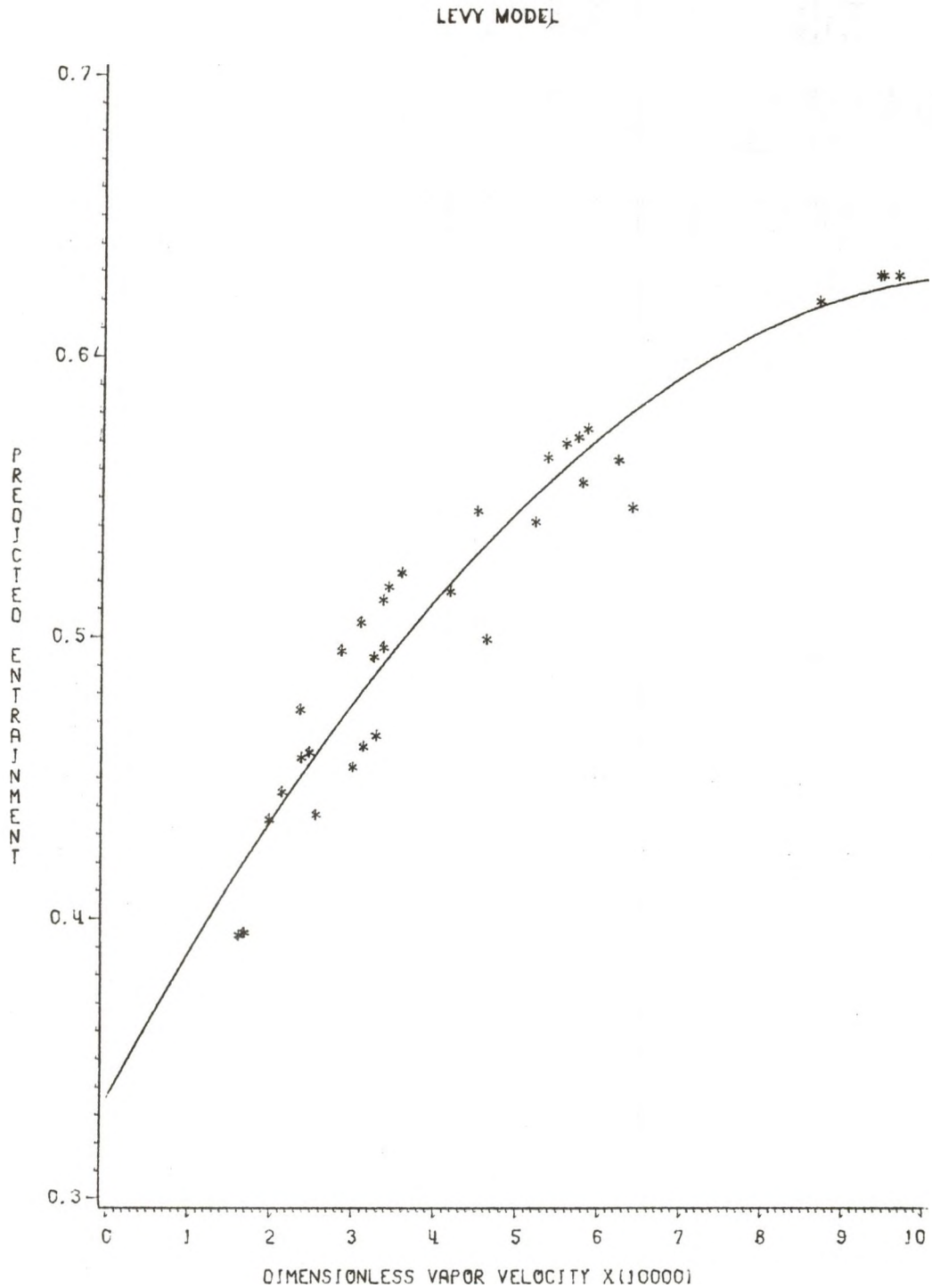

Figure 30: Predicted entrainment vs. dimensionless vapor velocity.

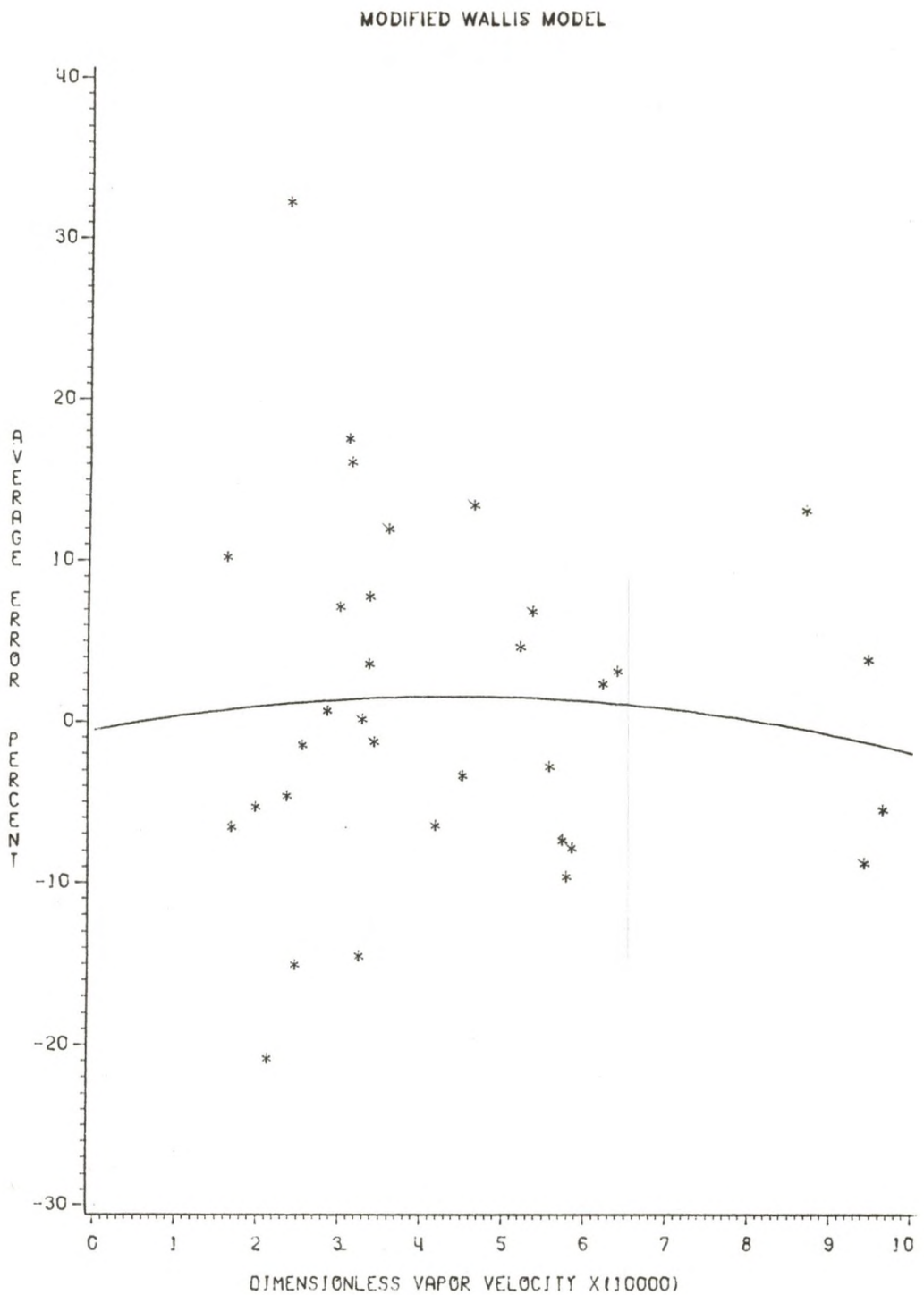

Figure 31: Average error vs. dimensionless vapor velocity.

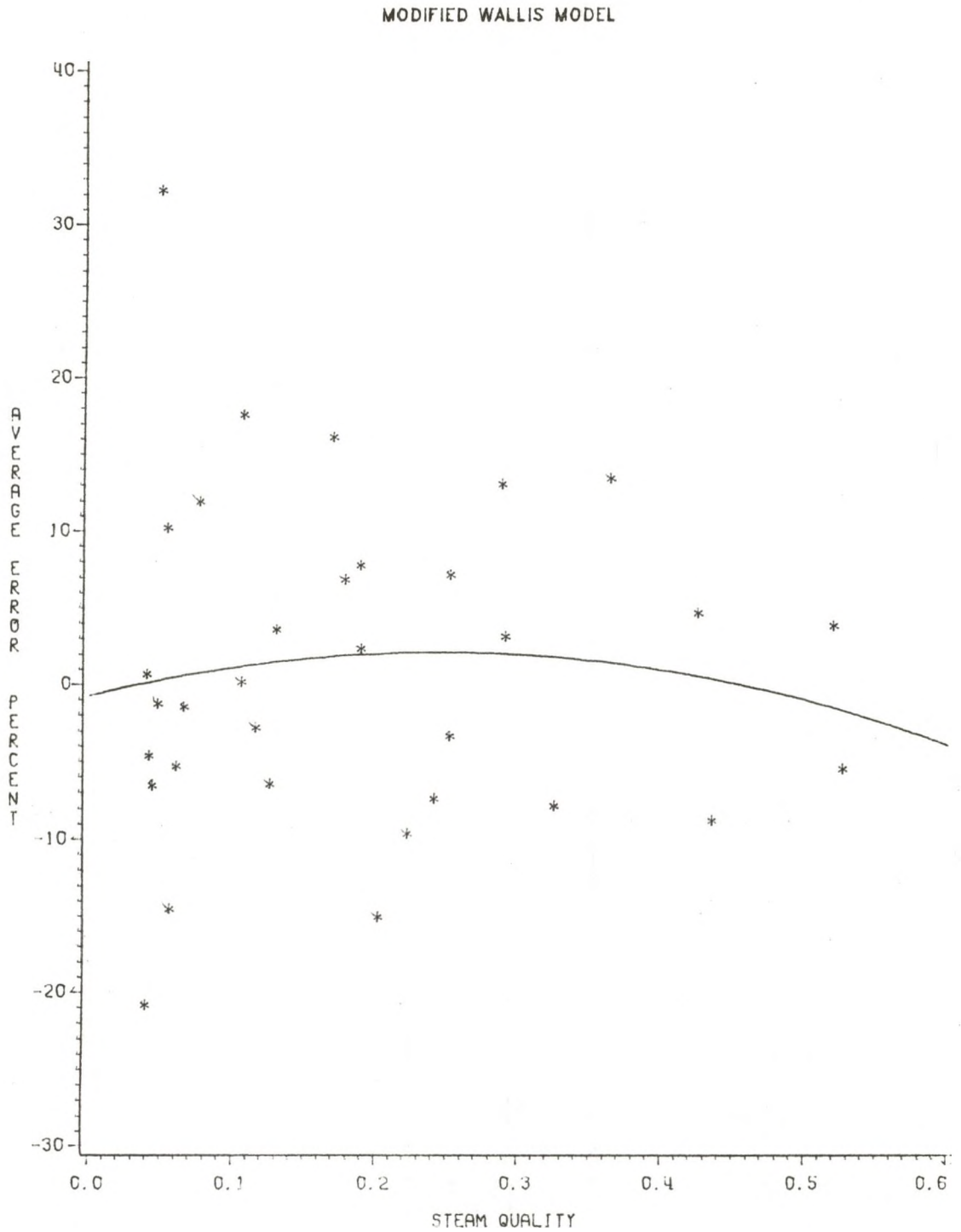

Figure 32: Average error vs. steam quality.

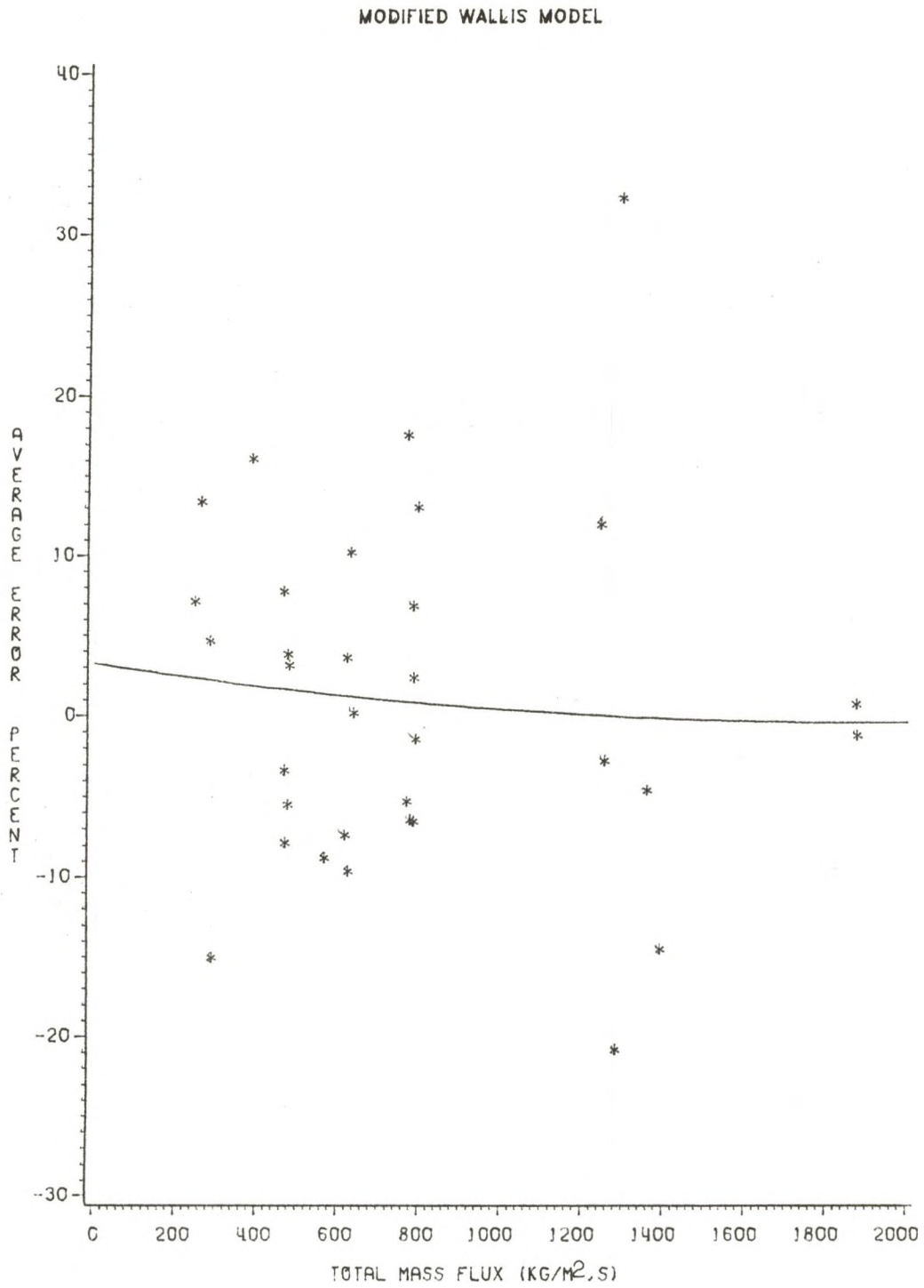

Figure 33: Average error vs. total mass flux.

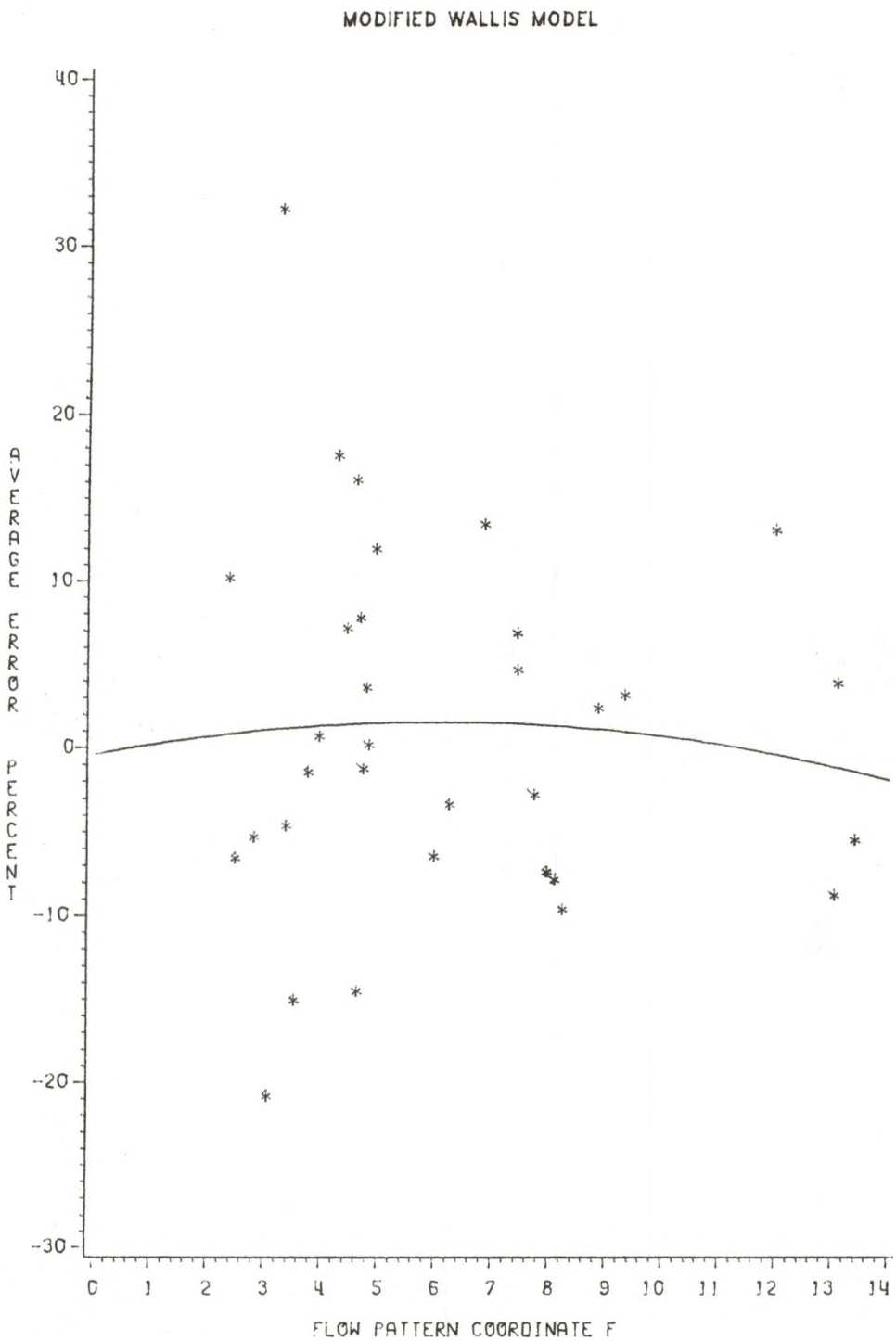

Figure 34: Average error vs. flow pattern coordinate F.

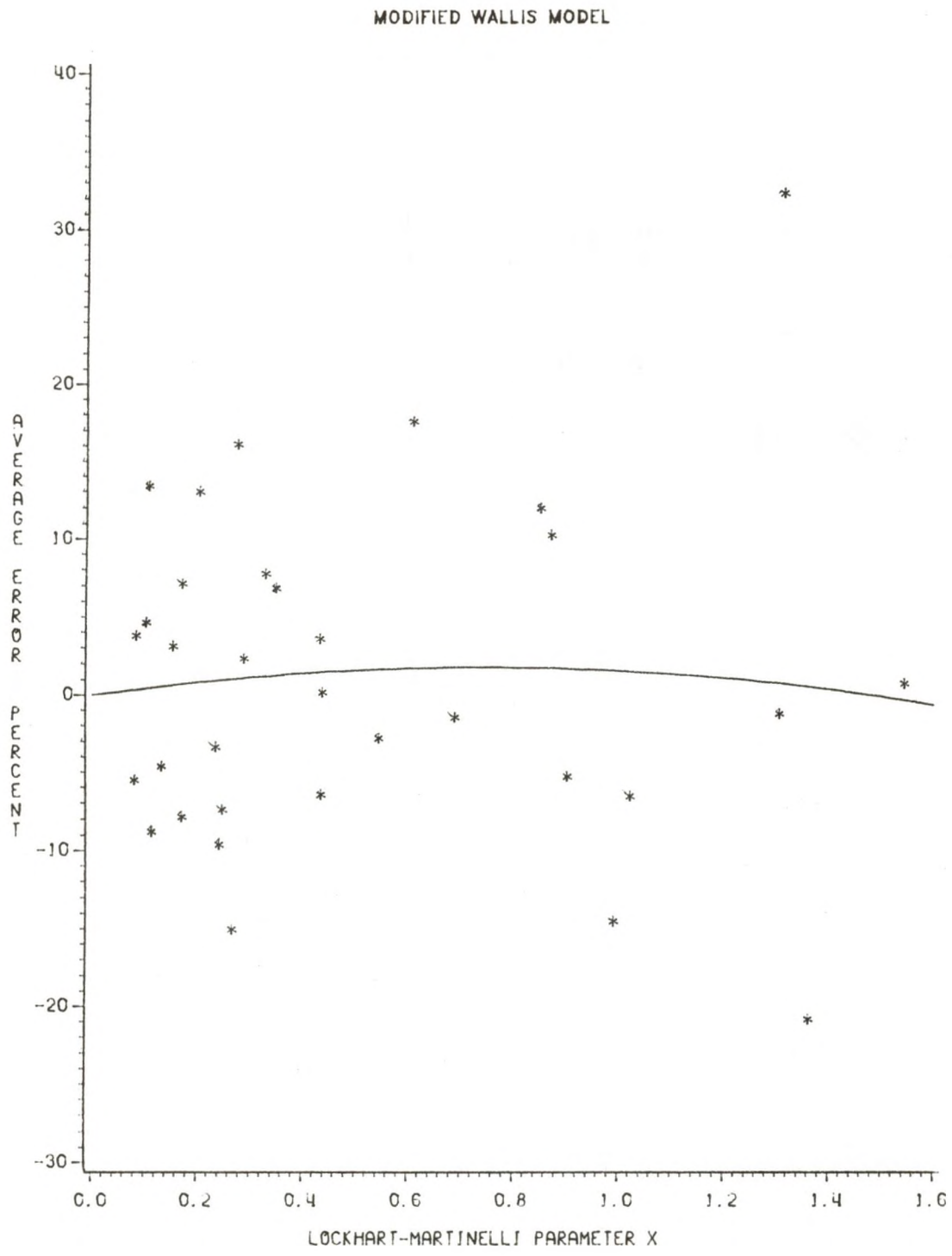

Figure 35: Average error vs.
Lockhart-Martinelli parameter X.

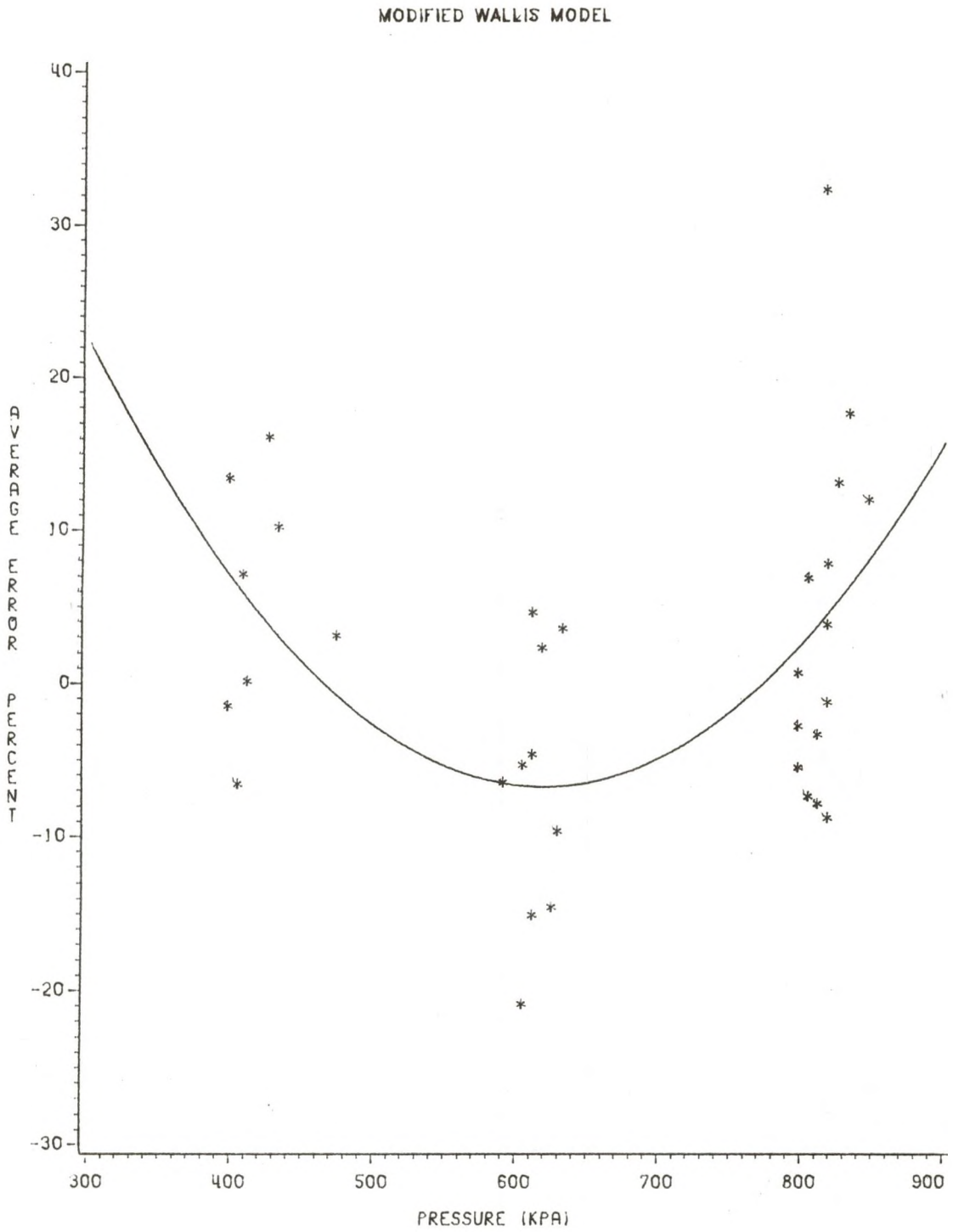

Figure 36: Average error vs. pressure.

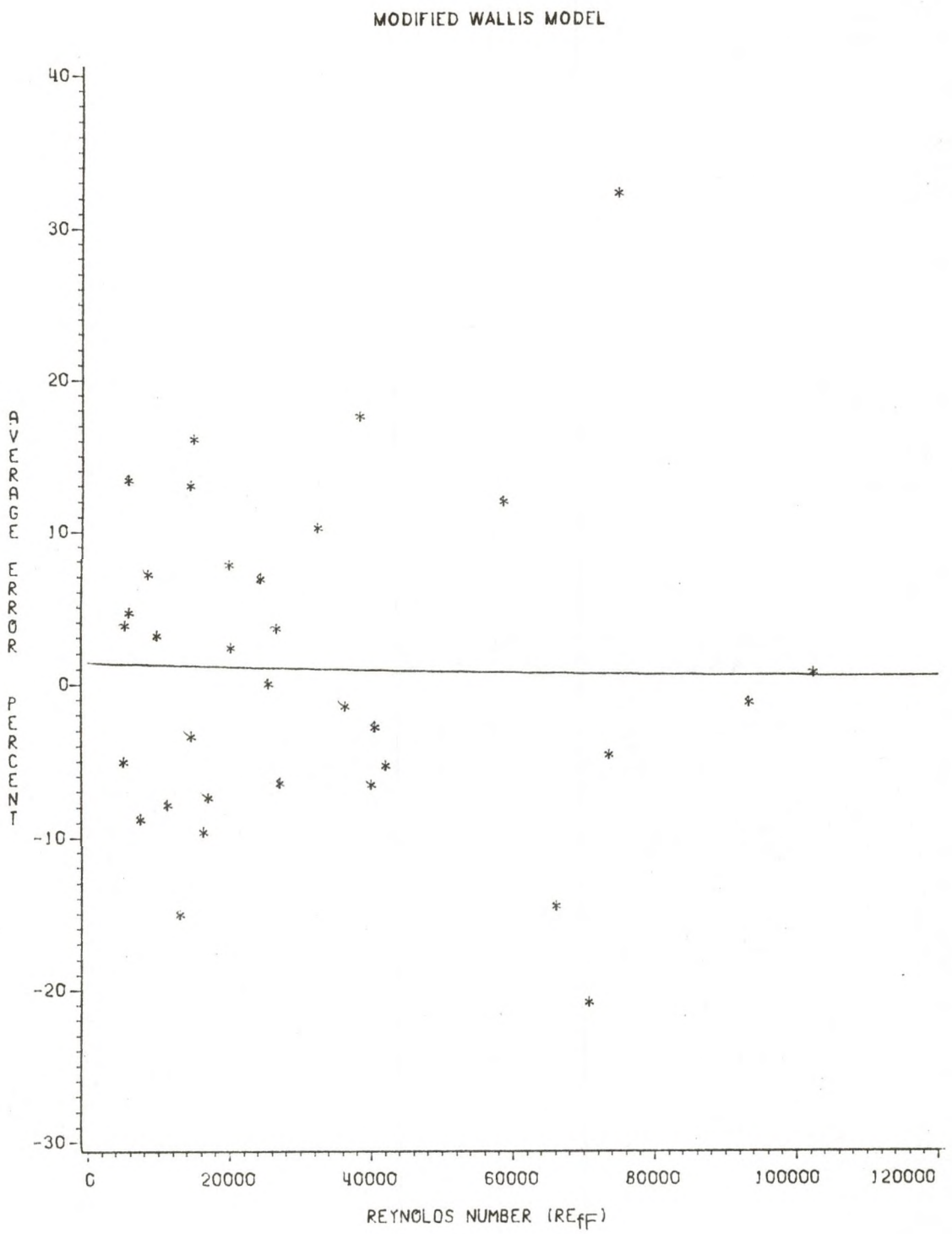

Figure 37: Average error vs. Reynolds number.

Appendix G

SYMBOLS USED

A	Cross sectional area for fluid flow	m
a	Parameter used in Equation 60 and 61	-
b	Parameter used in Equation 60 and 61	-
C	Parameter used in Equation 10	-
c	Parameter used in Equation 61	-
D	Tube diameter	m
e	Fraction of liquid entrained in the vapor	-
F	Flow pattern coordinate defined by Equation 1	-
f_{TP}	Two-phase friction factor	-
f_f	Friction factor for liquid phase flowing alone	-
f_{fF}	Friction factor for liquid phase flowing alone with entrainment taken into consideration	-
f_g	Friction factor for gas phase flowing alone	-
f_i	Interfacial friction factor	-
G	Total mass flux	$kg/m^2,s$
G_f	Liquid mass flux	$kg/m^2,s$
G_g	Gas mass flux	$kg/m^2,s$
g	Acceleration due to gravity	m/s^2
i_g	Enthalpy of the gas	J/kg
i_{fg}	Heat of evaporation	J/kg
i_f	Enthalpy of liquid	J/kg
i_{in}	Enthalpy of gas and liquid at inlet condition	J/kg
i_{sat}	Saturation enthalpy of liquid	J/kg
j_g	Superficial velocity of gas phase	m/s
L	Tube length	m
P	Pressure at inlet conditions	kPa
ΔP_i	Pressure drop at pressure tap no. i	kPa

R	Pipe radius	m
R^+	Dimensionless pipe radius	-
Re	Reynolds number	-
Re_f	Reynolds number for the liquid phase	-
Re_{fF}	Reynolds number for the liquid phase with entrainment taken into consideration	-
Re_g	Reynolds number for the gas phase	-
SS	Sum of squares of errors	$(kPa)^2$
T_{sat}	Saturation temperature	^oC
u_f	Actual velocity of liquid phase	m/s
u_g	Actual velocity of gas phase	m/s
$\bar{v}$	Average specific volume of gas and liquid	m/kg
v_f	Specific volume of liquid	m^3/kg
v_g	Specific volume of gas	m^3/kg
W_f	Mass flow rate of liquid phase	kg/s
W_g	Mass flow rate fo gas phase	kg/s
X	Lockhart-Martinelli parameter defined by Equation 2	-
x	Mass fraction of gas / steam quality	-
Y_f	Thickness of liquid film	m
Y_f^+	Dimensionless film thickness	-
Y_t	Thickness of the liquid film and transition layer	m

Greek symbols

α	Void fraction	-
β	Dimensionless density function defined by Equation 45	-
δ	Liquid film thickness used in Equation 11 and 12	m
ϵ_i	Percent error in prediction of pressure drop as defined by Equation 26	-
ρ_c	Density of the gas core	kg/m^3
ρ_f	Density of the liquid	kg/m^3
ρ_g	Density of the gas	kg/m^3
μ_f	Viscosity of the liquid	Ns/m^2
μ_g	Viscosity of the gas	Ns/m^2
ϕ_f^2	Two-phase frictional multiplier based on pressure gradient for liquid flow alone	-
ϕ_{fF}^2	Two-phase frictional multiplier based on pressure gradient for liquid flow alone and entrainment taken into consideration	-
ϕ_g^2	Two-phase frictional multiplier based on pressure gradient for gas flow alone	-
σ	Surface tension	N/m
τ_w	Shear stress at the pipe wall	N/m^2
τ_i	Shear stress at the gas-liquid interface	N/m^2
θ	Inclination of the pipe	deg.
χ	Variable in Equation 61 and 62	-

Differentials

(dp/dz)	Pressure gradient	kPa/m
(dp/dz A)	Accelerational pressure gradient	kPa/m
(dp/dz F)	Frictional pressure gradient	kPa/m
$(dp/dz\ F)_f$	Frictional pressure gradient assuming total flow to be liquid	kPa/m

$(dp/dz\ F)_{fF}$	Frictional pressure gradient assuming total flow to be liquid and with entrainment taken into consideration	kPa/m
$(dp/dz\ F)_{g}$	Frictional pressure gradient assuming total flow to be gas	kPa/m
$(dp/dz\ Z)$	Pressure gradient due to static head	kPa/m

REFERENCES

1. Hasan A.T.M.R. Low Pressure Boiling in Straight Tubes and a Bend. Ph.D. Dissertation, University of Waterloo, Ontario, Canada, 1979, 242 pp

2. Alves, G.E. Cocurrent Liquid-gas Flow in a Pipeline Contactor. Chem. Eng. Progr., 4 (8) 449-456 (1954)

3. Baker, O. Design of Pipelines for Simultaneous Flow of Oil and Gas. Oil and Gas Journal, 26, July (1954)

4. Bell, K.J., J. Tabordek, and F. Fenoglio. Interpretation of Horizontal Intube Condensation Heat Transfer Correlations with a Two-phase Flow Regime Map. Chem. Engng. Prog. Symp. Series, 66,No 102, 1970, pp 150-163

5. Mandhane, J.M., G.A. Gregory, and K. Aziz. A Flow Pattern Map for Gas-liquid Flow in Horizontal Pipes. Int. J. Multiphase Flow, 1 537-553 (1974)

6. Taitel, Y. and A.E. Dukler. A Model for Predicting Flow Regime Transitions in Horizontal and Near Horizontal Gas-liquid Flow. AIChE Journal, 22 45-47 (1976)

7. Collier, J.G. Convective Boiling and Condensation. McGraw-Hill, New York, N.Y., 2nd Ed. 1981 435 pp

8. McAdams, W.H. Vaporization Inside Horizontal Tubes - II - BenzeneOil Mixtures. Trans, ASME, 64 193 (1942)

9. Cicchitti, A. Two-phase Cooling Experiments Pressure Drop, Heat Transfer and Burnout Measurements. Energia Nucleare, 7 (6) 407-425 (1960)

10. Dukler, A.E. Pressure Drop and Hold-up in Two-phase flow Part A - A Comparison of Existing Correlations and Part B - An Approach Through Similarity Analysis. AIChE Journal, 10 (1) 38-51 (1964)

11. Lockhart, R.W. and Martinelli, R.C. Proposed Correlation of Data for Isothermal Two-phase Two-component Flow in Pipes. Chem.Eng.Prog., (45) 39 (1949)

12. Wallis, G.B. One-dimensional Two-phase Flow. McGraw-Hill, New York, N.Y., 1969 p 51

13. Johannessen, T. A Theoretical Solution to the Lockhart and Martinelli Flow Model for Calculating Two-phase Flow Pressure Drop and Hold Up. Int. J. Heat Mass Transfer, 15 1443-1449 (1972)

14. Friedel, L. Momentum Exchange and Pressure Drop in Two-phase Flow. Advanced Studies in Two-phase Flow, NATO Seminar, Istanbul, Turkey, 1977 p 263

15. Chisholm, D. The Influence of Mass Velocity on Friction Pressure Gradients During Steam-water Flow. Paper 35 presented at 1968 Thermodynamics and Fluid Mechanics Convention, Institute of Mechanical Engineers, Bristol, March 1968

16. Hasan, A.T.M.R. and E. Rhodes. Effect of Mass Flux and System Pressure on Two-phase Friction Multiplier. Chem. Eng. Comm. In press.

17. Shubri, M., R.J. Yandis and E. Rhodes. Effect of Heat Flux on Pressure Drop in Low-pressure Flow Boiling in a Horizontal Tube. The Can. J. of Chem. Engng., 59 April 149-154 (1981)

18. Baroczy, C.J. A Systematic Correlation for Two-phase Pressure Drop. AIChE reprint 37 represented at 8th National Heat Transfer Conference, Los Angeles, August 1965

19. Wallis, G.B. One-dimensional Two-phase Flow. McGraw-Hill, New York,N.Y., 1969, p 262

20. Marchaterre, J.F. and B.W. Hoglund. Correlation for Two-phase Flow. Nucleonics, August 142 (1962)

21. Collier, J.G. Convective Boiling and Condensation, McGraw-Hill, New York, N.Y.,2nd Ed. 1981, p 77

22. Wallis, G.B. One-dimensional Two-phase Flow. McGraw-Hill, New York, N.Y., 1969, pp 282-314

23. Ellis,S.R.M. and B. Gay The Parallel Flow of Two Fluid Streams - Interfacial Shear and Fluid - Fluid Interaction. Trans. Inst. Chem. Eng. (37) 206 (1959)

24. Krasiakova,L.Y. Some Characteristics of Movements of Two-phase Mixtures in a Horizontal Pipe. AERE-lib / Trans., 695 (1957)

25. Hewitt,G.F. and P.M.C.Lacey. The breakdown of the Liquid Film in Annular Flow. Int. J. Heat Mass Transfer, (8) 781-791 (1965)

26. Wallis, G.B. Vertical Annular Flow: I, A Simple Theory. II, Additional Effects. Papers presented at the annual meeting of the AIChE, Tampa, Florida, May 1968

27. Shearer, C.J. and R.M. Nedderman. Pressure Gradient and Liquid Film Thickness in Co-current Upwards Flow of Gas-liquid Mixtures: Application to Film-cooler Design. Chem. Eng. Sci., 20 671-683 (1965)

28. Levy, S. Prediction of Two-phase Critical Flowrate. J. Heat Trans., Series C, (87) 53 (1965)

29. Ghosal, S.K. and N. Sen. Prediction of Frictional Pressure Drop in Gas-liquid Annular Two-phase Flow. IE(I) Journal-CH (India), 61, 44-47 Feb. (1981)

30. Wallis, G.B. One-dimensional Two-phase Flow. McGraw-Hill, New York, N.Y., 1969, pp 320-321

31. Wallis, G.B. One-dimensional Two-phase Flow. McGraw-Hill, New York, N.Y., 1969, p 326

32. Wallis, G.B. Discussion of Ref. 44. Intern. J. Heat Mass Transfer, (11) 783-785 (1968)

33. Steen, D.A. and G.B. Wallis. AEC Report NYO-3114-2, 1964

34. Levy, S. and J.M. Healzer. Application of Mixing Length Theory to Wavy Turbulent Liquid-gas Interface. Journal of Heat Transfer Transactions of the ASME, 103 Aug. 492-500 (1981)

35. U.K. Steam Tables in S.I. Units Edward Arnold Ltd. London, 1970

36. Wallis, G.B. One-dimensional Two-phase Flow.New York, N.Y., 1969 pp 49-55

37. Hasan, A.T.M.R. Low Pressure Boiling in Straight Tubes and a Bend. Ph.D. Dissertation, University of Waterloo, Ontario, Canada, 1979, p 86

38. Levy, S. and J.M. Healzer. Prediction of Annular Liquid-gas Flow with Entrainment. NP-1581, EPRI Research Project 1380-1, 1979